IMPACT OF CASPASE-6 MODULATION ON HUNTINGTON DISEASE PHENOTYPES IN THE YAC128 MOUSE MODEL

by

Safia Ladha

B.Sc., University of Waterloo, 2009

A THESIS SUBMITTED IN PARTIAL FULFILLMENT OF THE REQUIREMENTS FOR THE DEGREE OF

DOCTOR OF PHILOSOPHY

in

THE FACULTY OF GRADUATE AND POSTDOCTORAL STUDIES

(Medical Genetics)

THE UNIVERSITY OF BRITISH COLUMBIA

(Vancouver)

April 2016

ABSTRACT

Huntington disease (HD) is an autosomal dominant neurodegenerative disorder characterized by motor, cognitive, and psychiatric symptoms. HD is caused by a CAG repeat expansion in the *huntingtin* (*HTT*) gene leading to the production of the mutant huntingtin protein (mHTT). Caspase-6 (C6) is a cysteine aspartyl protease that plays a central role in apoptosis and has been postulated to play a role in inflammation. Increased C6 activation is observed in human HD brains and mouse models and the inhibition of C6-mediated cleavage of mHTT protects against neuropathology and behavioural deficits in the YAC128 mouse model of HD. Additionally, alterations in inflammation are a feature of many neurodegenerative diseases, including HD. Hyperactive inflammatory responses are observed in both HD patients and mouse models and C6 has been postulated to play a role in mediating inflammation. Constitutive deletion of the *Casp6* gene (denoted as *C6*) in YAC128 mice results in a partial rescue of some features of HD; however, the continued presence of the 586 cleavage fragment in the absence of C6 suggests possible compensation by other proteases. The goal of this thesis was to investigate the impact of modulating C6 in the adult YAC128 mouse and to further characterize the role of C6 in inflammation. To that end, the *C6* gene was partially deleted in the adult YAC128 mouse and characterization of these mice reveals no amelioration in motor or cognitive phenotypes but a modest improvement in certain psychiatric behaviours. Neuropathological assessment shows no attenuation in canonical brain pathology but peripherally, the loss of C6 attenuates the overactive inflammatory response observed in YAC128 mice. These data suggest that partial loss of C6 in the brain is not sufficient to improve most behavioural and neuropathological phenotypes but implicate C6 in the regulation of inflammation. Furthermore, loss of C6 results in a blunted inflammatory response characterized by reduced cytokine release. As the presence of elevated cytokine levels have been suspected to cause psychiatric behaviours such as depression, this finding provides a possible mechanistic link between C6 activity and the onset of affective behaviours.

PREFACE

For data presented in chapter 3, I was responsible for the design of all experiments and carried out all biochemical experiments. Subcutaneous pellet implantation surgeries were assisted by Robert Xie and tamoxifen injections were conducted by myself, Mark Wang, Jason Yao, Robert Xie and Piers Ruddle.

For data presented in chapter 4 and 5, Amber Southwell and Shaun Sanders advised on the design of behaviour experiments. Shaun Sanders and Dagmar Ehrnhoefer assisted with data interpretation. Behaviour testing was assisted by Bobby Felczak, Robert Xie and Yun Ko. Sonia Franciosi and Erika Villanueva conducted neuropathological experiments. Yu Deng and Qingwen Xia assisted with western blots and RT-qPCR experiments and Piers Ruddle carried out perfusions, and assisted with dissections and cell culture. Galen Wright and David Arenillas conducted the bioinformatic analysis of caspase-6 transcription factor binding sites. I was responsible for the design and data analysis of all other experiments.

Chapter 6 is in preparation to be submitted (Ladha S, Casal L, Caron N, Qiu X, Connolly C, Leavitt BL, Ehrnhoefer DE, Hayden MR. A role for caspase-6 in mediating the inflammatory response in Huntington disease). Dagmar Ehrnhoefer assisted with the design and interpretation of experiments. Enzo Casal assisted with biochemical experiments and video scoring. Nicholas Caron conducted the microglial culture. I was responsible for the design and data analysis of all other experiments.

The studies described in this thesis have been approved by the Animal Care Committee at the University of British Columbia. All mice were handled according to institutional guidelines. Approval certificates numbers include A12-0063 and A12-0121.

TABLE OF CONTENTS

LIST OF TABLES

LIST OF FIGURES

LIST OF SYMBOLS AND ABBREVIATIONS

4-OHT	4-hydroxytamoxifen
Aβ	amyloid-β
AD	Alzheimer's disease
APP	amyloid precursor protein
ATP	adenosine triphosphate
ANOVA	analysis of variance
BACHD	bacterial artificial chromosome transgenic mouse model of Huntington disease carrying full-length human *HTT* with 97 CAG repeats
C57BL/6J	black coat-coloured inbred mouse strain
C6	caspase-6
C6R	caspase-6 resistant mutant huntingtin
CAG	cytosine-adenine-guanine
cKO	conditional deletion region of *C6*
CNS	central nervous system
COS	cell CV-1 (simian) in Origin and carrying the SV40 genetic material (COS-7)
Cre	cyclization recombination
CSE	control standard endotoxin
CSF	cerebrospinal fluid
DRPLA	dentatorubral pallidoluysian atrophy
DTA	diptheria toxin A
ELISA	enzyme-linked immunosorbent assay
EPM	elevated plus maze
FITC	fluorescein isothiocyanate
FRET	fluorescence resonance energy transfer
FVB/NJ	friend virus B NIH Jackson white coat-coloured inbred mouse strain
G418	Geneticin, an aminoglycoside antibiotic
GABA	γ-aminobutyric acid
HD	Huntington disease
Hip14	huntingtin-interacting protein 14
HPLC	high performance liquid chromatography
HTT	huntingtin
IAP	inhibitor of apoptosis protein
IFN-γ	interferon gamma
IGF-1	insulin-like growth factor 1
IL	interleukin
IP	intraperitoneal
JHD	juvenile Huntington disease
KC	keratinocyte chemoattractant
LDH	lactate dehydrogenase
LoxP	locus of X-over P1, 34 bp Cre recombinase sequence from P1 bacteriophage

mHTT	mutant HTT, >35 poly glutamines
MRI	magnetic resonance imaging
MSNs	medium spiny neurons
MTT	3-(4,5-dimethylthiazol-2-yl)-2,5-diphenyltetrazolium bromide dye
NF-κB	nuclear factor kappa-light-chain-enhancer of activated B cells
PBS	phosphate buffered saline
PD	Parkinson's disease
PET	positron emission tomography
polyQ	poly glutamine
PSEN1/2	presinilin 1/2
PTMs	post-translational modifications
R6/2	transgenic mouse model of HD carrying exon 1 of human HTT with 148-153 CAG repeats
RM	repeated measures
RT-qPCR	reverse transcriptase quantitative polymerase chain reaction
SBMA/SMAX1	spinal and bulbar muscular atrophy, X-linked 1
SCA	spinocerebellar ataxia
TAT	trans-activator of transcription, derived from human immunodeficiency virus 1
TF	transcription factor
TM	tamoxifen
TNF-α	tumour necrosis factor alpha
UBC	ubiquitin C
WT	wild type
XIAP	X-linked inhibitor of apoptosis protein
YAC128	yeast artificial chromosome transgenic mouse model of HD carrying full-length human *HTT* with 128 CAG repeats

ACKNOWLEDGEMENTS

There are a number of people who have played pivotal roles throughout this journey. Firstly, I must acknowledge my supervisor, Dr. Michael Hayden, for providing me with an incredible opportunity and enabling unique experiences that have allowed me to grow as a person and scientist. Thank you for accepting nothing but excellence and for helping me achieve my goals.

To my advisory committee – Dr. Sharon Gorski, Dr. Blair Leavitt, and Dr. Michel Roberge – thank you for sharing your time and wisdom with me. Your unwavering support and continuous guidance has been instrumental in my success and for that I express my profound appreciation.

The Hayden lab is full of exceptional people and the support I have received from its members have carried me through the last six years. To Dagmar Ehrnhoefer and Shaun Sanders – your advice, mentorship and friendship have been invaluable to me and I most certainly could not have completed this without you. I greatly appreciate our enlightening scientific discussions and the encouragement you both provided at the most trying times during this journey. You both set the bar high and act as incredible role models both in and out of the lab. You inspire me to become an exceptional scientist and for that I am grateful.

This work could not have been possible without the immense help of a number of technicians whose contributions, big and small, have helped shape this work. Thank you Yu Deng, Piers Ruddle, Qingwen Xia and Enzo Casal for your dedication and hard work. Thank you to Mark Wang and Bobby Felczak for being instrumental in facilitating the animal studies and to Sonia Franciosi, Erika Villanueva and the rest of the team for all the neuropathological analysis. Thank you to Dr. Mahmoud Pouladi, Dr. Jeff Carroll and Dr. Liza Sutton for being sources of inspiration and good friends. Thank you to Katherine Mui, Mandi Schmidt and Erika Villanueva for the countless games of Sequence and sushi lunches – these kept me sane and provided much-needed relief from the trials and tribulations of being a graduate student.

There are certain individuals I had the great fortune of meeting during my undergraduate years and to whom I owe much of my success thus far. Thank you to Colleen Phillips-Davis for initially seeing something in me that at the time I did not see in myself. Thank you to Dr. Robert G Bristow and Carla Coackley who welcomed me as a co-op student and gave me my first exposure to scientific research. Thank you to Professor Roland Hall – your unflinching support and encouragement since BIOL 361 has undoubtedly contributed to my academic success.

Thank you to Kaveesh Padiachy who provided the initial spark and helped realize I was capable of achieving anything. Thank you to Pierce Mellors-Selman for being an immense pillar of support, source of strength and incredible friend throughout the years. To Hanif Shariff – thank you for helping me see this thesis through to the end and for inspiring me to become the best possible version of myself.

Lastly, to my family – Zul, Shemin and Zain. Your unwavering positive reinforcement and faith in me have meant the world. I am who I am today because of you and I owe the realization of my dreams to you.

DEDICATION

TO SHEMIN, ZAIN AND ZUL – THE CONSTANTS IN MY LIFE WITHOUT WHOM THIS WOULD NOT HAVE BEEN POSSIBLE.

1 INTRODUCTION

1.1 HUNTINGTON DISEASE

Huntington disease (HD) is an inherited, adult-onset neurodegenerative disease affecting approximately 4-14 in 100,000 individuals in Western populations (Kay et al., 2014). Recent prevalence reports conducted in British Columbia, Canada since the availability of genetic diagnostics estimate prevalence rates in this region to be 13.7 per 100,000 individuals (corresponding to 1 in 7,299), with 17.2 per 100,000, or 1 in 5,814 affected among individuals of Caucasian ancestry (E. R. Fisher and Hayden, 2014). The past two decades have seen great advances in our understanding of the pathogenic mechanisms underlying this devastating disease; however, despite the discovery of its causative genetic mutation in 1993 (Group, 1993), no disease-modifying therapies exist today.

1.1.1 History

Huntington disease is named after physician George Huntington, who aptly described the hereditary, motor and psychiatric features of the disease in a paper published in 1872 (Huntington, 1872). Though not the first recorded mention of the disease, George Huntington's paper was the first holistic and clear description of the condition drawing upon the observations of three generations of family doctors. This pioneering work sparked scientific interest in the disease and led to a gradual increase in HD research in the century that followed, with a dramatic rise in attention and publications in the latter decades of the twentieth century (Harper, 2014). This was in part due to the development of collaborative groups initiated by HD sufferers and their families, which enabled significant fundraising, improved services for affected individuals and increased public awareness.

In 1983, work by Gusella and colleagues mapped the disease-causing gene to the short arm of chromosome 4 through the discovery of a polymorphic DNA marker genetically linked to the disease (Gusella et al., 1983). Several additional polymorphic DNA markers linked to HD were also discovered that enabled

predictive testing (Gilliam et al., 1987; Hayden et al., 1988a; 1988b; Skraastad et al., 1992; Wasmuth et al., 1988). During this time, the first case of prenatal diagnosis was achieved using polymorphic DNA probes *in utero* and enabled diagnosis of an at-risk fetus with 96% accuracy (Hayden et al., 1987). Early clinical ascertainment of neurodegeneration in HD patients was enabled by the application of positron emission tomography (PET) technology as a sensitive marker to identify and quantify dopamine receptors in affected regions of the brain, in which a marked reduction in both D1 and D2 dopamine receptors was observed (Filloux et al., 1990; Hägglund et al., 1987; Richfield et al., 1991; Sedvall et al., 1994).

The discovery and further mapping of a large founder population in Venezuela confirmed the presence of HD-linked polymorphic markers (Wexler et al., 2004) and the systematic study of this population acted as a catalyst for the formation of the Huntington's Disease Collaborative Research Group in 1983, whose goal was to map and isolate the gene responsible for HD (Harper, 2014). A decade of coordinated efforts among multiple international groups culminated in the discovery of the causal mutation, a cytosine-adenine-guanine (CAG) trinucleotide repeat expansion equal to or greater than 36 repeats encoding a polyglutamine (polyQ) tract in exon 1 of the *huntingtin (HTT)* gene on chromosome 4 (Group, 1993). With the causal gene and mutation identified, a new era of HD research was born, focused on unraveling the molecular mechanisms underlying pathogenesis and establishing long-term studies that would form the basis of future therapeutic clinical trials.

1.1.2 Genetics

HD follows a pattern of autosomal dominant inheritance where offspring of an affected parent have a 50% chance of inheriting the disease. This risk is based on the fact that the majority of individuals affected with HD are heterozygotes, though rare homozygotes have been identified (Wexler et al., 1987). There exists a strong inverse correlation between the number of CAG repeats and age at onset, with longer CAG tracts conferring symptoms at an earlier age (Andrew et

al., 1993). The number of CAG repeats in unaffected control individuals ranges from 9 to 35, with a median of 18, while expanded alleles 36 and greater have a median of 44 CAG repeats (Kremer et al., 1994). Reduced penetrance has been observed with alleles containing 36 to 39 repeats, where such individuals may or may not develop the disease (McNeil et al., 1997; Semaka et al., 2013). Within the non-disease range exists a class termed intermediate alleles, ranging from 27 to 35 CAG, which typically do not confer symptoms of the disease but have a greater propensity to expand into the disease-causing range, particularly if inherited from the paternal chromosome (Semaka et al., 2013; Telenius et al., 1993). This instability of the *HTT* CAG tract expansion results in a phenomenon known as genetic anticipation, whereby individuals in subsequent generations display an earlier age of onset due to CAG tract expansion and often a more severe phenotype (Ridley et al., 1988).

A subset of HD cases can be classified as juvenile HD (JHD), defined as individuals with onset before 20 years of age (Quarrell, 2014). JHD cases make up between 1 to 10% of all HD cases and individuals with JHD typically have longer CAG sizes ranging from 60-250, often as a result of expansion of the CAG tract through paternal transmission (Telenius et al., 1993). Individuals presenting with onset earlier than 20 years of age and with less than 60 CAG repeats have also been documented (Andrew et al., 1993). While JHD and adult-onset HD share many clinical features, symptoms of rigidity, bradykinesia, epilepsy and dystonia are more prominent features in those affected with JHD (van Dijk et al., 1986).

HD is one of nine diseases belonging to a larger group of polyQ disorders, all of which contain an expanded polyglutamine tract in their respective genes. Other members include dentatorubral pallidoluysian atrophy (DRPLA); spinal and bulbar muscular atrophy, X-linked 1 (SMAX1/SBMA); and six spinocerebellar ataxias (SCA) types 1, 2, 3, 6, 7, 17 (Gatchel and Zoghbi, 2005). Despite the fact that these conditions share common features such as adult-onset symptomology, accumulation of mutant protein as insoluble aggregates and slow disease progression, each of the diseases is subject to profound degeneration of a

specific neuronal population, resulting in a unique presentation of clinical features and neuropathology.

1.1.3 Clinical features

HD is characterized by a triad of motor, cognitive and psychiatric deficits. The prevailing and often diagnostic motor symptom is chorea, a Greek word referring to the ‘dance’-like involuntary movements of the trunk, face and extremities exhibited by affected individuals (Huntington, 1872). Other motor disturbances include hypokinesia, seen particularly in juvenile HD patients (van Vugt et al., 1996), dystonia (Louis et al., 1999), myoclonus (Vogel et al., 1991) and tics (Becker et al., 2007).

Cognitive and psychiatric deficits in affected individuals typically precedes motor symptom onset by several years and are reported to be the most debilitating aspects of the disease, placing a great burden on HD families (Paulsen, 2011). Cognitive deficits can include impaired sensorimotor gating (Swerdlow et al., 1995), as well as executive function (Lawrence et al., 1996), memory (Butters et al., 1986; Caine et al., 1977), attention and awareness deficits (Couette et al., 2008; Finke et al., 2006). Psychiatrically, individuals affected with HD have been found to exhibit anxiety, depression, anhedonia, irritability, apathy and sometimes suicidal tendencies (Paulsen et al., 2001). Interestingly, these neuropsychiatric features can occur independently of motor or cognitive symptoms (Paulsen et al., 2001), suggesting that different molecular mechanisms may govern these symptoms.

1.1.4 Huntingtin structure and function

HTT is a large, 348-kDa protein containing 3144 amino acids and 67 exons and is highly conserved among vertebrates, with 80% conservation between its most divergent species (Zuccato et al., 2010). The HTT protein contains several distinctive features, notable among which are the polyQ tract followed by a proline-rich region. In addition, within HTT exists several domains termed huntingtin, elongation factor 3, protein phosphatase 2A and TOR 1 (HEAT) repeats important for protein-protein interactions (Andrade and Bork, 1995;

Neuwald and Hirano, 2000). Interestingly, conservation studies have revealed that the polyQ region was anciently acquired by HTT and mediates its binding to interactors (Harjes and Wanker, 2003). Dispersed between the HEAT repeats are regions of proteolytic susceptibility, which are rich in the amino acids proline, glutamic acid, serine and threonine thus termed PEST sites – sites of extensive proteolysis by caspases, calpains and cathepsins (Rogers et al., 1986; Warby et al., 2008; B. K. Y. Wong et al., 2015). HTT is also subject to numerous posttranslational modifications (PTMs), including ubiquitination, phosphorylation, palmitoylation, SUMOlaytion, acetylation and proteolytic cleavage, all of which can influence successive PTMs and the functions of HTT (Ehrnhoefer et al., 2011b; D. D. O. Martin and Hayden, 2015; D. D. O. Martin et al., 2014). A simplified schematic of HTT structure and sites of proteolytic cleavage is illustrated in Figure 1.1.

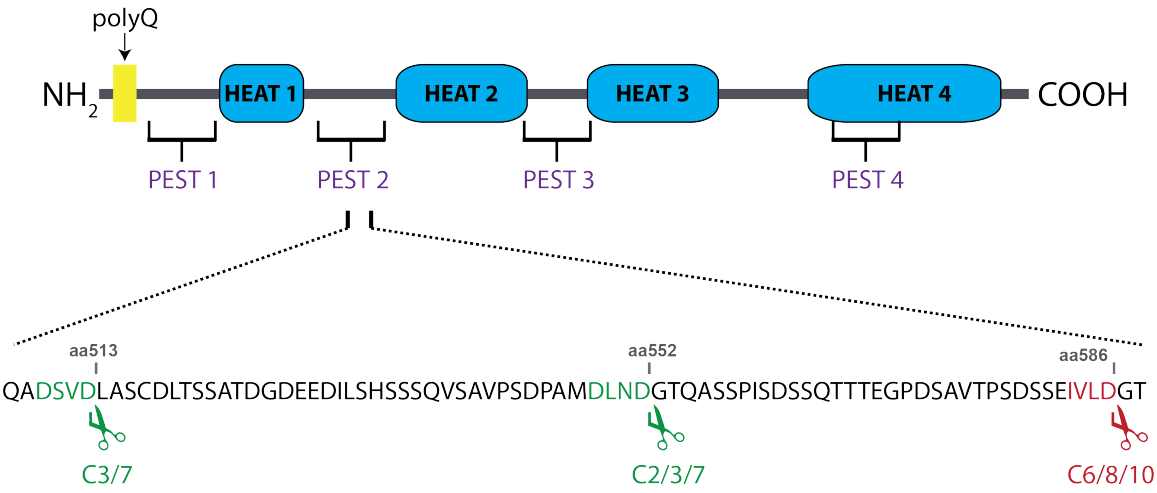

Figure 1.1: Huntingtin structure and proteolytic cleavage sites. A schematic diagram of HTT. The putative huntingtin, elongation factor 3, protein phosphatase 2A and TOR 1 (HEAT) domains are indicated along with the proteolytically active PEST sequences rich in proline, glutamic acid, serine and threonine and the polyQ tract. Sites within the PEST 2 region subject to cleavage by caspases-2, -3, -6, -7, -8 and -10 are also noted.

HTT is expressed ubiquitously throughout tissues, with the highest expression found in the brain and testes (Trottier et al., 1995). The absence of both copies of murine huntingtin (*Hdh*$^{-/-}$) is embryonic lethal in mice, suggesting that HTT is

essential for embryonic development and its normal function is critically important in mice (Duyao et al., 1995; Nasir et al., 1995; Zeitlin et al., 1995). Functions of WT HTT have been discovered through HTT interaction studies and diverse roles for HTT have been proposed in intracellular transport (Y. C. Wong and Holzbaur, 2015), cytoskeleton assembly and cilia function (Karam et al., 2015; Metzler et al., 2007), endocytosis (Kegel et al., 2000), synaptic activity (R. Smith et al., 2005), autophagy (D. D. O. Martin et al., 2015; Ochaba et al., 2014; Rui et al., 2015), transcriptional regulation (Cha, 2007), regulation of brain-derived neurotrophic factor (BDNF) production (Zuccato et al., 2001) and apoptosis (Leavitt et al., 2006; Rigamonti et al., 2000; Zeitlin et al., 1995). Studies investigating the normal functions of HTT in patients and mouse models of HD have revealed that the pathogenesis is characterized by a dual impairment of the WT function of HTT and a toxic gain of function of mHTT (Cattaneo, 2003; Cattaneo et al., 2005; Van Raamsdonk et al., 2005b). Moreover, the presence of WT HTT is protective against apoptotic stimuli (Rigamonti et al., 2000), excitotoxicity (Leavitt et al., 2006), mHTT-induced cellular toxicity (Ho et al., 2001; Leavitt et al., 2001) and striatal neuronal atrophy (Van Raamsdonk et al., 2006b).

1.1.5 Proteolysis in Huntington disease

The HTT protein is subject to extensive proteolysis by several classes of proteases, including caspases, calpains, cathepsins and matrix metalloproteinases (Gafni and Ellerby, 2002; Goldberg et al., 1996; Miller et al., 2010; Nicholson et al., 1995; Wellington et al., 2002; 1998; 2003). Early hints that HTT was a substrate for proteases came when purified recombinant caspase-3 (C3) enzyme, endogenous active C3 and/or cellular lysates subject to apoptotic stimuli were capable of generating specific HTT fragments (Goldberg et al., 1996; Nicholson et al., 1995). It was later confirmed that HTT is also a substrate for caspases-1, -2, -3, -6, -7, -8 and -10 (Hermel et al., 2004; Wellington et al., 1998; B. K. Y. Wong et al., 2015) and that amino acid sites 513, 552 and 586 within the PEST 2 region were particularly susceptible to proteolysis (Wellington et al., 1998) (Figure 1.1).

While the 513 cleavage site is shared amongst C2, C3, and C7 (Hermel et al., 2004), the 586 site was originally thought to be uniquely cleaved by C6 (Wellington, 2000). However, recent *in vitro* work suggests that although C6 is the protease that preferentially cleaves HTT at 586 to generate the greatest proportion of the N-terminal 586 fragment, C8 and C10 are also capable of cleaving at the 586 site albeit to a lesser extent (B. K. Y. Wong et al., 2015).

While C6 is basally expressed at low levels in the brain, increased C6 activity has been observed in mouse models of HD as well as presymptomatic and symptomatic post-mortem human HD brains (Godefroy et al., 2013; Graham et al., 2010; Warby et al., 2008). Interestingly, the levels of active C6 positively correlate with CAG size and inversely with age of onset (Graham et al., 2010). Increased C6 activity has also been observed in skeletal muscle tissue from human HD patients as well as mouse models of HD and has been shown to play a role in mediating muscle cell death and atrophy (Ehrnhoefer et al., 2014).

N-terminal fragments generated by proteolysis have been detected in tissues of both humans and mouse models with HD (Goldberg et al., 1996; Nicholson et al., 1995; Wellington et al., 1998) and their detection *in vivo* has been facilitated by using neo-epitope antibodies that bind to newly exposed regions of HTT resulting from proteolysis (Kim et al., 2001; Mende-Mueller et al., 2001; Wellington, 2000). The pathogenic role played by N-terminal fragments was emphasized in the characterization of the R6/1 and R6/2 mouse models in which the N-terminal portion of mHTT was sufficient to cause HD-like neurodegeneration in mice (Mangiarini et al., 1996). These findings, along with similar results obtained in other polyQ diseases led to the ‘toxic fragment hypothesis’, which posited that N-terminal fragments containing the polyQ expansion generated by proteolytic events are the primary toxic species in disease pathogenesis (Wellington et al., 1998). Evidence that these N-terminal fragments play a central role in mediating pathogenesis arose from the expression of mHTT resistant to C6-mediated cleavage at the 586 site (C6R), which completely prevented the development of behavioural deficits and neuropathology in the YAC128 mouse (Graham et al., 2006). Furthermore, the characterization of a mouse solely expressing N-terminal

586 mHTT fragment demonstrated that this fragment is sufficient to initiate the onset of HD-related phenotypes such as progressive motor dysfunction and neuropathology (Tebbenkamp et al., 2011; Waldron-Roby et al., 2012).

Follow-up studies on the C6R mice revealed that the presence of mHTT resistant to cleavage at the 586 site also attenuated C6 activation in neurons *in vitro* (Graham et al., 2010), implying the existence of a positive feedback loop between C6 activation and the generation of the 586 mHTT fragment (Graham et al., 2010; 2011). Furthermore, these C6R mice have reduced nuclear accumulation of mHTT (Warby et al., 2008) and are protected from neurodegeneration. Interestingly, the characterization of the serendipitously established 'shortstop' YAC mouse, which carries exons 1 and 2 of mHTT including an expanded polyQ tract, revealed no neurodegeneration or behavioural abnormalities despite the presence of widespread inclusions containing N-terminal fragments (Slow et al., 2005), thereby calling into question the association between inclusions and disease phenotype.

These observations fueled an existing debate regarding the pathogenicity of inclusions. The identification of polyQ-positive intranuclear neuronal inclusions in both human and mouse HD brains and their presence prior to and correlating with symptom onset in mice was suggestive of an early and central role for inclusions in the pathogenesis of HD (Davies et al., 1997; DiFiglia et al., 1997). By contrast, other studies revealed that neurodegeneration could occur in the absence of aggregates (Hodgson et al., 1999) and that the presence of aggregates was not always required in the manifestation of neurodegenerative phenotypes (Slow et al., 2005). Furthermore, studies at the single-neuron level demonstrated that neuronal cell death did not directly occur as a result of the presence of aggregates; rather, the presence of diffuse mHTT predicted neuronal survival with neurons lacking visible aggregates at a greater risk of neuronal apoptosis (Arrasate et al., 2004). Taken together, these data proposed that insoluble inclusions are non-toxic and may be neuroprotective, while soluble oligomers of mHTT mediate toxicity.

While much research has been dedicated to elucidating the potential toxicity associated with N-terminal fragments containing the polyQ tract, recent work has highlighted that the C-terminal fragments generated by the same proteolytic events may also play a role in mediating HD pathogenesis (El-Daher et al., 2015). C-terminal fragments corresponding to known cleavage events have been identified in post-mortem HD brains (Landles et al., 2010; Mende-Mueller et al., 2001) but their contribution to disease has not been extensively studied. Elegant experiments using the tobacco etch virus protease and engineered HTT constructs allowing for temporally controlled proteolysis revealed that C-terminal fragments also induce toxicity through endoplasmic reticulum dilation and stress, leading to cell death (El-Daher et al., 2015).

1.1.6 Neuropathology

The tissue most profoundly affected in HD is the striatum, a subcortical structure that serves as primary input to the basal ganglia at the base of the forebrain. The basal ganglia are a collection of large nuclei responsible for movement and mood and are comprised of the striatum, globus pallidus, subthalamic nucleus and substantia nigra (Waldvogel et al., 2014). The striatum is structurally composed of the caudate nucleus, which rostrally forms a head and extends posteriorly into a tail; and the putamen, which is connected to the caudate via lateral ridges of grey matter extending through the internal capsule and confers the characteristic striated appearance of this structure (Albin et al., 1989).

Two classes of neurons are resident to the striatum – projection medium spiny neurons (MSNs), which constitute the majority of striatal neurons, and the supporting interneurons. MSNs receive significant excitatory input from the cortex, constituting the cortico-striatal pathway, and then transmit these signals via inhibitory output onto the internal and external segments of the globus pallidus through one of two opposing pathways. In the direct pathway, inhibitory γ-aminobutyric acid (GABA)-ergic signals from the striatum synapse onto tonically active inhibitory neurons of the internal segment of the globus pallidus, resulting in disinhibition and a net excitatory effect, ultimately resulting in initiation

of volitional movement. In the indirect pathway, GABAergic signals project to the external segment of the globus pallidus for a net inhibitory effect, resulting in the suppression of movement (Albin et al., 1989). Thus, these two pathways work in an antagonistic manner, with a balance between the two necessary for suppressing competing motor programs and enabling the selection of action.

In HD, the selective loss of striatal MSNs projecting onto the external segment of the globus pallidus and subsequent dysfunction of the indirect pathway results in an absence of normal inhibitory input and ultimately leads to overactivation of the motor cortex, which manifests in chorea (Waldvogel et al., 2014).

Neuropathologically, brains of individuals affected with HD examined post-mortem display significant bilateral atrophy of the striatum with concomitant enlargement of ventricles (Waldvogel et al., 2014). As striatal loss follows a distinctive pattern of caudo-rostral and dorso-ventral/medial-lateral degeneration, a 5-level grading scale was established by Vonsattel and colleagues in 1985 in order to classify the extent of degeneration. The neuropathological classification for HD begins with Grade 0, in which the striatum is macroscopically indistinguishable from a normal brain but microscopically reveals 30-40% loss of MSNs, and ends with Grade 4, in which significant and macroscopically-evident striatal atrophy is present, with 95% loss of MSNs (Vonsattel et al., 1985). While striatal atrophy is the hallmark of HD and can be seen by magnetic resonance imaging (MRI) as much as 15 years prior to symptom onset (Aylward et al., 2004), volume loss in other brain tissues have also been observed as the disease progresses, most notably white matter loss and a significant reduction in cortical volume (Carroll et al., 2011a; Lerch et al., 2008; Rosas et al., 2003).

1.1.7 Peripheral pathology

Historically, HD research has primarily focused on deciphering the pathogenic mechanisms governing brain pathology, with reason – the distinctive motor, cognitive and psychiatric features are rooted in neuronal dysfunction. However, a growing body of evidence points to significant peripheral pathology that cannot necessarily be simply explained as secondary effects of brain dysfunction. It is

now clear that non-central nervous system (CNS) tissues are also affected in HD, as we know that huntingtin is widely expressed throughout the body (Hoogeveen et al., 1993; Trottier et al., 1995) and that the presence of mutant huntingtin in isolated peripheral cells exerts toxic affects. Together, these observations suggest that pathogenicity may arise as a direct result of mutant huntingtin in the periphery rather than secondary sequelae of neuronal dysfunction. Clinical signs of peripheral pathology have long been noted in HD patients, including weight loss (Sassone et al., 2009; van der Burg et al., 2009), muscle wasting (Ribchester et al., 2004; Zielonka et al., 2014), cardiac dysfunction (Bär et al., 2008; E. Chiu and Alexander, 1982; Melik et al., 2012), testicular atrophy (Van Raamsdonk et al., 2007a; 2007b) and enhanced inflammation (Björkqvist et al., 2008; Wild et al., 2011) among others.

It is noteworthy that several peripheral changes are detectable prior to symptom onset (Björkqvist et al., 2008), lending further support to the notion that peripheral dysfunction can occur prior to CNS dysfunction. While it has been suggested that changes in the HD brain, particularly in the hypothalamus, can lead to subsequent alterations in peripheral tissues (Aziz et al., 2007; Petersén and Björkqvist, 2006), it is likely that the flow of cause-and-effect is not unidirectional. Indeed, the impact of peripheral modulation on CNS outcomes is becoming increasingly appreciated and points to bilateral communication between systems (Carroll et al., 2015). Further, recent studies suggest that peripheral interventions can have direct consequences on the CNS outcomes in HD (Kwan et al., 2012a; Träger et al., 2014a) and thus merit further therapeutic investigation.

1.1.8 Inflammation

Over the last decade, much research has been dedicated to uncovering the role of inflammation in HD. Central to this work has been the investigation of whether the observed alterations of inflammation in HD are due to cell autonomous processes of dysfunctional immune cells or due to immune reactions as a consequence of neuronal degeneration. Activation of microglia, the resident immune cells of the CNS, along with elevated plasma levels of proinflammatory

cytokine interleukin-6 (IL-6) have been detected in presymptomatic HD patients as well as in those in low-grade and advanced stages of the disease (Björkqvist et al., 2008; Tai et al., 2007). Moreover, these increased levels of plasma IL-6 also correlate with disease severity (Björkqvist et al., 2008). Evidence of immune activation in the CNS also comes from analyses of the cerebrospinal fluid (CSF) where elevated levels of cytokines IL-6, IL-8 and tumor necrosis factor alpha (TNF-α) have been found (Björkqvist et al., 2008).

Another study found that presymptomatic HD patients possessed elevated levels of interleukin-1 beta (IL-1β) in blood plasma, which correlated with a concomitant increase in IL-1β in the patients' basal ganglia (Politis et al., 2015), suggesting an association between central and peripheral immune activation. Furthermore, transcriptional analyses conducted in human control and HD brains revealed a significant enrichment of differentially expressed genes belonging to the immune and inflammatory pathways (Labadorf et al., 2015). Peripherally, immune system changes can be seen at both the mRNA and protein levels, where expression changes of genes and proteins produced by innate immune cells are elevated in human HD patients and correlate with disease severity (Dalrymple et al., 2007; Runne et al., 2007).

Interestingly, monocytes and macrophages cultured from HD patients do not demonstrate above-normal secretion of inflammatory cytokines under basal conditions; however, a significant increase in cytokine secretion from these cells has been observed following inflammatory stimulation, suggesting these cells are hyperactive in their response to external stimuli (Björkqvist et al., 2008; Franciosi et al., 2012; Träger et al., 2014a). Additionally, monocytes expressing mHTT also demonstrate impaired migration to an inflammatory stimulus (Kwan et al., 2012b).

In mice, studies have shown that mHTT-expressing astrocytes, the most abundant glial cell in the brain, are defective in their abilities to support neuronal function. Exclusive expression of mHTT in astrocytes in transgenic mice resulted in body weight loss, motor deficits and reduced survival (Bradford et al., 2009).

Astrocytes cultured from a transgenic mouse model of HD ubiquitously expressing expanded exon 1 mHTT display enhanced activation of the nuclear factor kappa-light-chain-enhancer of activated B cells (NF-κB) pathway and amplified cytokine production (Hsiao et al., 2013). Further, treatment of these mice with a TNF-α inhibitor conferred protection against motor dysfunction and caspase activation (Hsiao et al., 2014). This data suggests that both non cell-autonomous and cell-autonomous changes resulting from mHTT expression in CNS and peripheral immune cells are sufficient to cause an exacerbated inflammatory state in HD.

Lastly, several studies have shown a link between inflammation and psychiatric function, where increased levels of proinflammatory cytokines are associated with the onset of depression, apathy and anhedonia in humans and mice (Anisman and Merali, 1999; Dantzer et al., 1999; Meyers, 1999; Walker et al., 1997; Yirmiya, 1996). Thus, it is plausible that the enhanced inflammatory state observed in HD patients and mouse models contributes to the development of psychiatric phenotypes that also accompany the disease.

1.1.9 Excitotoxicity

Excitotoxicity is a well-characterized feature of HD (Beal, 2004; DiFiglia, 1990; Fan and Raymond, 2007; Sepers and Raymond, 2014; Tabrizi et al., 1999; Zeron et al., 2001; 2002). MSNs resident to the striatum receive glutamatergic input from the cortex and the presence of mHTT results in enhanced striatal excitatory activity through reduced glutamate uptake in the synaptic cleft and overactive signaling to N-methyl-D-aspartate (NMDA) receptors (Faideau et al., 2010; Sepers and Raymond, 2014). This excessive signaling results in increased calcium influx in the post-synaptic cell and subsequent caspase activation, mitochondrial dysfunction and neuronal cell death (Bezprozvanny, 2007; Bezprozvanny and Hayden, 2004; Graham et al., 2010; Milnerwood et al., 2010; Shehadeh et al., 2006; H. Wang et al., 2004). Indeed, abnormal calcium homeostasis has been observed in both HD patient lymphoblasts and HD mouse models (Bezprozvanny and Hayden, 2004; Panov et al., 2002) and mHTT has

been shown to directly influence calcium signaling through binding and sensitization of the inositol 1,4,5-trisphosphate receptor (Bezprozvanny, 2007; Bezprozvanny and Hayden, 2004).

Targeting NMDA receptor signaling has proven to be a suboptimal therapeutic strategy, given that basal NMDA receptor signaling is important for maintaining cell survival and neuroplasticity (Hardingham and Bading, 2010; 2003). Work over the last decade has identified the pathogenic role of extrasynaptic NMDA receptors, receptors localized outside the synaptic cleft whose activation promotes cell death signaling and whose blockade ameliorates synaptic dysfunction in HD (Dau et al., 2014; Hardingham et al., 2002; Milnerwood et al., 2010; Parsons and Raymond, 2014). Interestingly, modulation of C6 is protective against excitotoxicity – the genetic ablation of C6 or expression of C6-resistant mHTT in YAC128 mice confers resistance against excitotoxic insults (Graham et al., 2006; Uribe et al., 2012).

1.1.10 Mouse models of HD

Numerous mouse models of HD have been characterized and fall into 3 general classes: N-terminal fragment transgenic models, knock-in models and full-length transgenic models.

The R6/1 and R6/2 fragment transgenic models express exon 1 of mutant human HTT and were generated with 116 and 144 CAG repeats, respectively (Mangiarini et al., 1996). These mice have an accelerated phenotype compared to other transgenic models and develop motor coordination deficits, severe weight loss and muscle wasting, hypokinesis and reduced survival (Menalled et al., 2009). These studies demonstrated that the presence of an N-terminal mHTT fragment was sufficient to cause neurological phenotypes resembling HD in mice.

Knock-in models have also been created by inserting the expanded exon 1 of human *HTT* into the endogenous mouse *Hdh* gene. Knock-in models are advantageous in that they possess spatially and temporally appropriate levels of HTT expression, unlike transgenic lines that overexpress HTT (Pouladi et al.,

2013). Phenotypically, knock-in mouse models display a progressive development of neurodegenerative phenotypes, which are milder than transgenic models during the early stages of the disease but eventually progress to more robust phenotypes (Hickey et al., 2008; Lerner et al., 2012; Menalled et al., 2014; Menalled and Chesselet, 2002).

Both fragment and knock-in models lack human genomic and corresponding protein context of the disease-causing expansion, an important feature which undeniably influences toxicity through regulatory mechanisms, interactions and post-translational modifications (Ehrnhoefer et al., 2009). In an attempt to circumvent this, full-length mHTT transgenic models were developed using yeast artificial chromosome (YAC) and bacterial artificial chromosome (BAC) technology. These transgenes contain human full length *HTT* with the endogenous genomic regulatory elements and expanded CAG tracts and have randomly integrated into the mouse genome at variable copy numbers (Gray et al., 2008; Menalled et al., 2014; Pouladi et al., 2012). The well-characterized YAC128 mouse model expresses full-length human *mHTT* with 128 CAG repeats, while the BACHD mice expressed full-length human *mHTT* with 97 CAG repeats. Both models develop selective striatal and cortical neuropathology as well as progressive motor, cognitive and psychiatric deficits (Gray et al., 2008; Pouladi et al., 2012; Slow et al., 2003; Van Raamsdonk et al., 2007a). Interestingly, both models also display significant body weight gain, a feature in contrast to the manifestation of the disease in humans. This weight gain has been attributed to the overexpression of HTT through the modulation of the insulin-like growth factor-1 (IGF-1) pathway (Pouladi et al., 2010). These mouse models demonstrate a slower and more gradual onset of phenotypes and mirror the time course of human pathology more accurately, thus making them particularly suitable for pre-clinical therapeutic testing.

While both full-length transgenic models display similar behavioural and neuropathological features, there are also distinct differences between the YAC128 and BACHD models. YAC128 mice display an accumulation of striatal mHTT aggregates and a reduction in the expression of striatally enriched genes,

both of which are absent in BACHD mice (Pouladi et al., 2012) and should be taken into consideration when designing pre-clinical therapeutic trials. A summary of phenotypes observed in the YAC128 model on the FVB/NJ background is listed in Table 1.1.

Table 1.1: Summary of phenotypes in the YAC128 mouse model of HD.

Neuropathological Phenotypes	**Effect/Age**	**Reference**
Brain weight	Decreased - 9 months	Slow et al., 2003
Striatal volume	Decreased - 3 months	Slow et al., 2003; Carroll et al., 2011
Cortical volume	Decreased - 12 months	Slow et al., 2003; Carroll et al., 2011
Corpus callosum volume	Decreased - 3 months	Lerch et al., 2008; Carroll et al., 2011
Striatal neuronal counts	Decreased - 12 months	Slow et al., 2003
Axonal degeneration	Susceptible	Shehadeh et al., 2005
Behavioural Phenotypes	**Effect/Age**	**Reference**
Motor learning	Decreased - 2 months	Van Raamsdonk et al., 2007
Motor function - rotarod performance	Decreased - 3 months	Slow et al., 2003
Spontaneous activity	Increased - 2 months Decreased - 8 months	Slow et al., 2003; Van Raamsdonk et al., 2005
Motor function - climbing	Decreased - 7 months	Southwell et al., 2009
Cognitive function - object learning	Decreased - 6-7 months	Southwell et al., 2009
Cognitive function - spontaneous alternation	Decreased - 7 months	Carroll et al., 2011
Cognitive function - sensorimotor gating by pre-pulse inhibition	Decreased - 12 months	Carroll et al., 2011
Cognitive function - swimming T-maze with reversal	Decreased - 2 months	Van Raamsdonk et al., 2005
Psychiatric behaviour - anxiety in open field	Increased - 6-7 months	Southwell et al., 2009
Psychiatric behaviour - anxiety in elevated plus maze	Increased - 6-7 months	Unpublished
Psychiatric behaviour - depression	Increased - 3 months	Pouladi et al., 2009
Psychiatric behaviour - anhedonia	Increased - 3 months	Pouladi et al., 2009
Peripheral Phenotypes	**Effect/Age**	**Reference**
Body weight	Increased - 2-3 months	Slow et al., 2003; Pouladi et al., 2010
Plasma IGF-1 levels	Increased - 3 months	Pouladi et al., 2010
Testes weight	Decreased - 12 months	Van Raamsdonk et al., 2007
Inflammatory responses	Increased - 3 months	Tråger et al., 2014; Bjorkqvist et al., 2008
C6 activation in muscle	Increased - 12 months	Ehrnhoefer et al., 2014
Motor function - grip strength	Decreased - 14 months	Xie et al., 2010

The polyQ expansion in these full-length transgenic mice occur on distinct haplotypes and the absence of specific HD mutation-linked single nucleotide polymorphisms negate the possibility of testing certain gene silencing compounds (Southwell et al., 2013). These challenges were overcome with the creation of a fully humanized mouse model of HD termed the Hu97/18 model, which involved cross-breeding the BACHD and YAC18 mice (containing mHTT with 97 CAG repeats and WT HTT with 18 CAG repeats, respectively) on the *Hdh* null background (Southwell et al., 2013). This line was the first mouse model to accurately recapitulate human HD genetics by having no endogenous mouse HTT, two human *HTT* genes and heterozygosity of the CAG expansion (Southwell et al., 2013), making it particularly amenable to pre-clinical gene silencing trials. Similar to full-length transgenic mice, Hu97/18 mice also develop motor, cognitive and psychiatric deficits and neuropathological alterations (Southwell et al., 2013).

1.2 CASPASES

Caspases are a conserved family of endoproteases that play a central role in regulating cell death and inflammation. Their name is derived from the observation that they are *c*ysteine-dependent, *asp*artate-specific prote*ases*; that is, there is an obligate requirement for the presence of a catalytic cysteine residue in the caspase active site as well as an aspartic acid residue preceding the cleavage site in the substrate (McIlwain et al., 2015; Troy and Jean, 2015).

1.2.1 Classification of caspases

Mammalian caspases can be grouped according to various features – their structure and whether they possess a long or short pro-domain or their predominant function in regulating inflammatory and cell death pathways. These classifications are not mutually exclusive as members from different structural categories often function within shared cellular pathways.

Structurally, caspases can be categorized based on possession of a short pro-domain (caspase-3, -6, -7 and -14) or a long pro-domain (caspase-1, -2, -4, -5, -8 and -12). They can be further sub-classified based on function – caspase-3, -6

and -7 are considered effectors of programmed cell death, known as apoptosis, and caspase-14 plays a role in keratinocyte differentiation (Eckhart et al., 2000). Among the caspases with a long pro-domain, caspase-2, -8, -9, and -10 are initiators of apoptosis while caspase-1, -4, -5, -11 and -12 play a role in regulating the inflammatory response (McIlwain et al., 2015; Shalini et al., 2014; Shi et al., 2014; Troy and Jean, 2015).

1.2.2 Structure and activation of caspases

Caspases are initially produced as inactive zymogens linearly consisting of an N-terminal pro-domain (Pro), a linker (L), a large subunit (~20 kDa, termed 'p20'), an inter-subunit linker followed by a small subunit (~10 kDa, termed 'p10') (Alnemri et al., 1996; Pop and Salvesen, 2009; Troy and Jean, 2015) (Figure 1.2A). The structural classification of caspases also provides insight to their activation mechanisms – caspases with short pro-domains (effectors) typically exists as dimers and require cleavage by an initiator caspase to become active, while those with longer pro-domains (initiators) typically exists as monomers and become active through proximity-induced dimerization (Boatright and Salvesen, 2003; Mace et al., 2014). This dimerization occurs via binding of adaptor proteins to one of two motifs found in the pro-domain, the caspase activation and recruitment domain (CARD) or the death-effector domain (DED) (Bouchier-Hayes and S. J. Martin, 2002; Valmiki and Ramos, 2009) (Figure 1.2B).

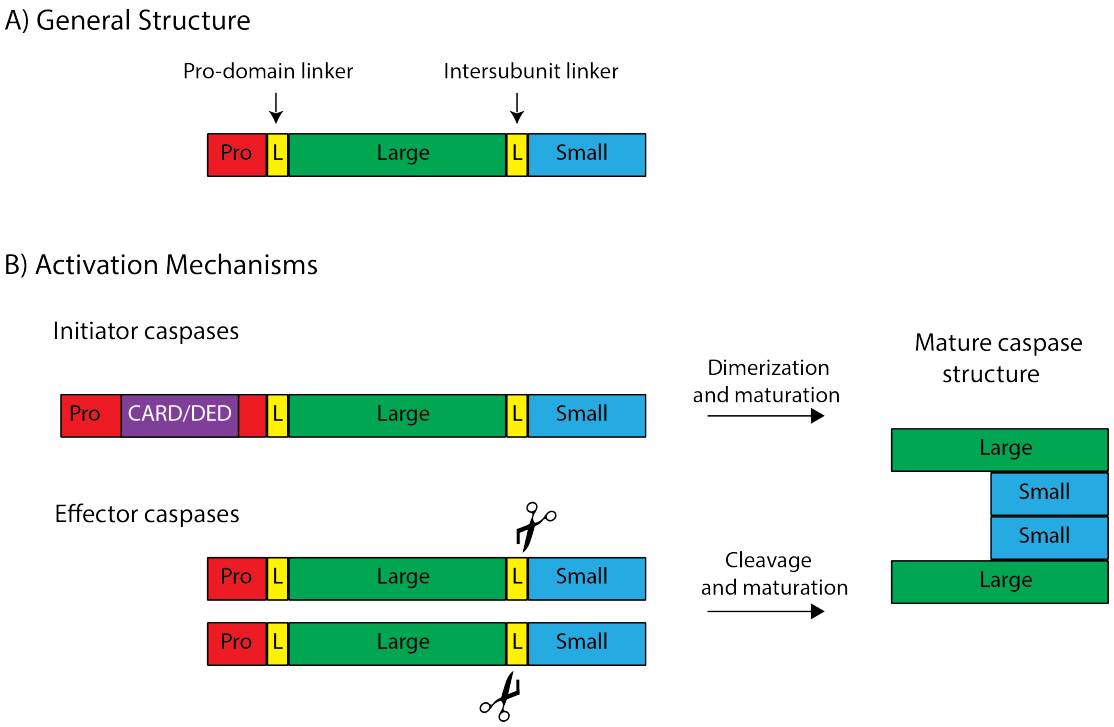

Figure 1.2: Caspase structure and activation. The general caspase structure consists of a long or short pro-domain, a pro-domain linker, a large subunit, an inter-subunit linker followed by a small subunit (A). Initiator caspases exist as monomers and become activated through proximity-induced dimerization while effector caspases exist as dimers and are activated through inter-subunit cleavage (B).

1.2.3 Functions and regulation of caspases

Caspases are central to the execution of apoptosis, the systemic and controlled demolition of the cell. This pathway follows a hierarchical structure, with apical initiator caspases being activated by dimerization and subsequently activating downstream effector caspases through proteolytic processing (McIlwain et al., 2015; Pop and Salvesen, 2009; Troy and Jean, 2015). This cascade ultimately results in cleavage and destruction of intracellular components and the occurrence of characteristic apoptotic features such as DNA fragmentation and membrane blebbing (McIlwain et al., 2015).

Apoptosis can proceed through one of two pathways, the extrinsic or intrinsic pathway. The extrinsic pathway is initiated by an extracellular ligand binding to a transmembrane death receptor, resulting in the recruitment of adaptor proteins

and caspase-8 (C8) monomers followed by subsequent dimerization and activation of C8. C8 can then cleave and activate downstream effector caspases-3, -6 or -7 ultimately resulting in apoptosis (McIlwain et al., 2015; Pop and Salvesen, 2009; Troy and Jean, 2015). Alternatively, the intrinsic pathway is initiated by external mutagens or cellular stresses leading to cytochrome C release, which binds the adaptor protein APAF1 (Slee et al., 1999). The assembly of several APAF1 monomers into an oligomeric complex then leads to the recruitment and activation of caspase-9 (C9); these components along with cytochrome c have been termed to apoptosome (Cain et al., 2002). C9 can then activate downstream effector caspases to complete the apoptotic cascade.

A second well-known role for caspases is in mediating inflammation. Activation of inflammatory caspases occurs through the formation of the inflammasome, analogous to the apoptosome. Various cellular stimuli trigger pattern-recognition receptors, which lead to adaptor protein binding and subsequent recruitment and activation of pro-inflammatory caspases such as caspase-1 (C1). Activated pro-inflammatory caspases subsequently cleave the proform of cytokines, thereby activating them and leading to inflammatory cytokine release and inflammation (Davis et al., 2011; Martinon et al., 2002; McIlwain et al., 2015). Interestingly, expression of C1 is increased in humans and mouse models of HD as a direct result of intranuclear mHTT (S. H. Li et al., 2000) and inhibition of C1 activity has been shown to slow the progression of disease symptoms in R6/2 mice (Ona et al., 1999). Furthermore, C1 activity is also associated with C6 activity and the modulation of C1 activity has been shown to mitigate C6 activation (Guo et al., 2006; Kaushal et al., 2015), a relationship further discussed in section 1.3.1. These data highlight the benefits of mitigating the inflammatory phenotypes observed in HD.

Several alternate forms of cell death have been identified that are characterized by distinctive features and the involvement of specific caspases. Overactivation of caspase-1 can result in a phenomenon known as pyroptosis, the non-apoptotic, uncontrolled rupture of the cell and release of its inflammatory contents (Cookson and Brennan, 2001; Fink and Cookson, 2006). Furthermore,

recent work has identified inflammatory caspases as receptors that can directly bind external stimuli such as lipopolysaccharides (LPS) via their CARD domain, resulting in inflammatory cell death (Shi et al., 2014).

C8 has been affiliated with necroptosis, a form of cell death characterized by swelling of cellular contents, increased cell volume and eventual cell rupture (Vandenabeele et al., 2010). Necroptosis occurs when the cell encounters genotoxic stress and the ripoptosome is formed by assembly of proteins RIP1, FADD, $FLIP_L$, and C8, leading to pore formation and necroptotic cell death (Shalini et al., 2014; Ye et al., 2013).

Caspases-3, -6 and -8 have also been shown to play a role in modulating cell proliferation and differentiation (N. J. Kennedy et al., 1999; Lens et al., 2002; Olson et al., 2003; Watanabe et al., 2008; Woo et al., 2003). Treatment of T-cells with a caspase inhibitor resulted in an inhibition of cell expansion, a pro-proliferative role that was later attributed to C8 (N. J. Kennedy et al., 1999; Lens et al., 2002) . C8 and C6 have been implicated in positively regulating B-cell activation and differentiation (Olson et al., 2003; Watanabe et al., 2008) while an anti-proliferative role in B-cells has been demonstrated for C3 (Woo et al., 2003). Interestingly, effector caspases-3 and 6 play crucial non-apoptotic roles in the CNS where they are responsible for selective axonal, dendritic and synaptic pruning and plasticity (Bingol and Sheng, 2011; Hyman and Yuan, 2012; Z. Li and Sheng, 2012; Nikolaev et al., 2009; C. Shen et al., 2014; Uribe et al., 2012). C3 was found to play a role in memory and learning of songs in zebra finches (Huesmann and Clayton, 2006) and its activation is essential for long-term depression (Z. Li et al., 2010).

Numerous studies in recent years have uncovered the delicate crosstalk between two major cellular systems, apoptosis and autophagy, which is the orderly degradation system for long-lived proteins and organelles (Hou et al., 2009; Maiuri et al., 2007). It has been shown that several key proteins involved in the regulation of autophagy are caspase substrates and that the cleavage and subsequent inactivation of autophagy proteins inhibits autophagic function

(Norman et al., 2010; Wirawan et al., 2010; Yu et al., 2004). This hypothesis is strengthened by studies of caspase deletion mice or caspase inhibition, which have demonstrated an upregulation of autophagic activity in the absence of certain caspases (Aharony et al., 2015; Tiwari et al., 2014; B. K. Y. Wong et al., 2015).

Caspases are regulated by a family of intracellular inhibitor of apoptosis proteins (IAPs), which are so classified based on the presence of a baculoviral inhibitor repeat domain (Eckelman et al., 2006). Of the IAP members, only X-linked IAP (XIAP) has been found to directly inhibit caspase activity, specifically caspases-3, -7, and -9, while others indirectly modulate caspase function and cell death (Eckelman et al., 2006; Eckelman and Salvesen, 2006). Caspase-8 activity is regulated by the endogenous inhibitor c-FLIP, which dimerizes the zymogen and inhibits its activation (Irmler et al., 1997). IAPs themselves are also subject to regulation by endogenous inhibitors of IAPs, which are released and bind to IAPs upon mitochondrial permeabilization, enabling caspase activity and subsequent cell death (Du et al., 2000; Hegde et al., 2002; Verhagen et al., 2000).

1.3 CASPASE-6

Altered C6 activity is observed in several pathological conditions, including neurodegeneration (Graham et al., 2011; LeBlanc et al., 1999), ischemic stroke (Akpan et al., 2011; Shabanzadeh et al., 2015), memory and aging (Albrecht et al., 2007; Ramcharitar et al., 2013a), epilepsy (Narkilahti and Pitkänen, 2005) as well as colon and gastric cancers (J. W. Lee et al., 2006; Yoo et al., 2004). Caspase-6 is of particular interest in HD due to the observation that levels of active C6 are significantly increased in post-mortem brains of both low- and high-grade HD patients, as well as in presymptomatic brains (Graham et al., 2010). Furthermore, the prevention of C6-mediated cleavage of mHTT protects YAC128 mice against behavioural and neuropathological dysfunction (Graham et al., 2006), highlighting the validity of C6 as a potential therapeutic target.

1.3.1 Caspase-6 structure, activation and regulation

Caspase-6 (C6), encoded by the gene *Casp6* (also known as mammalian ced-3 homologue *(Mch-2))*, is traditionally classified as an effector caspase with a short pro-domain and shares approximately a third of its sequence identity with fellow effector caspases-3 and -7 (X.-J. Wang et al., 2015). The dimeric structure of the C6 zymogen follows the canonical effector caspase form and cleavage at one or both of the inter-subunit linkers by caspase-3 (C3) during the apoptotic cascade is sufficient for activation (Hirata et al., 1998; Klaiman et al., 2009; Slee et al., 1999) (Figure 1.3).

C6 activation has been observed in the absence of C3 and was discovered to undergo intramolecular self-processing and autoactivation *in vitro* and *in vivo* (Klaiman et al., 2009; X.-J. Wang et al., 2010). However, this pattern of activation is distinctly different than C3-mediated activation. During autoactivation, the first cleavage event to occur is at the junction between the pro-domain and large subunit (the $TETD^{23}$ site), resulting in the loss of the pro-domain, followed by cleavage at $TEVD^{193}$ and then at $DVVD^{179}$ (Klaiman et al., 2009; X.-J. Wang et al., 2010). This differs from the sequence of cleavage events during C3-mediated activation, which proceeds in the order of cleavage at $DVVD^{179}$, $TETD^{23}$, and $TEVD^{193}$ (Simon et al., 2012; Slee et al., 1999). The autoactivation of C6 is inhibited by phosphorylation at Ser^{257} by the kinase ARK5, which prevents cleavage at the $TEVD^{193}$ site (Cao et al., 2012; Suzuki et al., 2004; Velázquez-Delgado and Hardy, 2012). The cleavage and phosphorylation sites within C6 are illustrated in Figure 1.3.

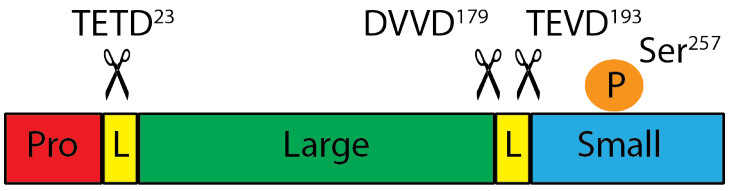

Figure 1.3: Structure, phosphorylation and cleavage sites of caspase-6. The dimeric structure of effector caspase-6 includes a short pro-domain, cleavage sites at the junction between the pro-domain and large subunit ($TETD^{23}$), between the large subunit and inter-subunit linker ($DVVD^{179}$) and between the inter-subunit linker and small subunit ($TEVD^{193}$). The ARK5 phosphorylation site

at Ser^{257} inhibits autoactivation.

C6 possesses several unique features distinct from its effector caspase classmates. It demonstrates more initiator caspase-like substrate specificity (Thornberry et al., 1997) and has a greater basal level of activity in its zymogen form (Fuentes-Prior and Salvesen, 2004). In neurons, C6 is also activated by caspase-1 and -9, as demonstrated by the specific inhibition of these upstream caspases and the subsequent reduction in activity of C6 and prevention of cell death (Akpan et al., 2011; Guo et al., 2006; Kaushal et al., 2015). Recent work has demonstrated cellular stress to human neurons leads to inflammasome activation, followed by C1 and subsequently C6 activation resulting in synchronous neuroinflammation and axonal degeneration (Kaushal et al., 2015).

Notably, given the protective effects of inhibiting C1 in HD mouse models, it is possible that the benefit conferred to these mice is mediated through the downstream inhibition of C6 activity and protection from cell death. C6 expression is also increased by the tumour suppressor protein p53 (MacLachlan and El-Deiry, 2002) through p53 binding in the C6 promoter region (Yang et al., 2008). Interestingly, p53 is upregulated in mHTT-expressing cells and the activation of p53 is associated with a dramatic increase in C6 activity in HD (Ehrnhoefer et al., 2014; MacLachlan and El-Deiry, 2002). Recent work has demonstrated that C6 interacts with the transcription factor Sox11 and that expression of Sox11 attenuates C6 activity and prevents cell death (Waldron-Roby et al., 2015).

C6 is not included in the subset of caspases inhibited by XIAP (Salvesen and Duckett, 2002) but can be non-specifically inhibited by broad-spectrum caspase inhibitors such as carbobenzoxy-valyl-alanyl-aspartyl-[O-methyl]-fluoromethylketone (zVAD-fmk) and baculoviral protein p35 (Garcia-Calvo et al., 1998; Xu et al., 2001). Synthetic C6 inhibitors have been developed that are based on the 4-peptide sequence of its typical substrates (VEID), but these inhibitors often lack specificity and may unintentionally inhibit other caspases (Garcia-Calvo et al., 1998; McStay et al., 2008).

1.3.2 Functions of caspase-6

C6 is broadly expressed in the brain and periphery (Albrecht et al., 2007; Godefroy et al., 2013). As mentioned, it is historically known for its role as an executioner of apoptosis, where it localizes to the nucleus and cleaves C2, C8 and C3 as well as structural proteins resulting in the demise of the nucleus and cell (Cowling and Downward, 2002; Hirata et al., 1998; Orth et al., 1996; Slee et al., 1999; Van de Craen et al., 1999). Importantly, C6 has been demonstrated as a key mediator of several non-apoptotic processes, central among which is its role in facilitating axonal pruning during development (Nikolaev et al., 2009; Park et al., 2010; Schoenmann et al., 2010; Simon et al., 2012). Indeed, constitutive C6 deficient animals are protected against axonal degeneration induced by exposure to myelin *in vitro* and NMDA-induced excitotoxicity (Uribe et al., 2012). C6 is also responsible for regulating B cell activation and differentiation into plasma cells (Watanabe et al., 2008).

Though not traditionally considered an inflammatory caspase, C6 has been recently postulated to play a role in mediating inflammation. In a study conducted by Leblanc and colleagues, the overexpression of C6 in the mouse hippocampus resulted in an increase in astrocytic and microglial activation, canonical signs of inflammation (LeBlanc et al., 2014). In alveolar macrophages, C6-mediated cleavage of an inhibitor of innate immunity IRAK-M was required for the release of TNF-α and subsequent macrophage activation upon pneumonic challenge (Kobayashi et al., 2011). Furthermore, loss of C6 in mice resulted in a blunted inflammatory pain response, while treatment with recombinant C6 elicited TNF-α production and microglia-dependent pain hypersensitivity (Berta et al., 2014).

Several autophagy proteins such as Beclin-1 and p62 are known substrates for C6 (Norman et al., 2010; Wu et al., 2014) and the genetic deletion of C6 in both the YAC128 and BACHD mouse models reduces HTT protein levels, suggesting C6 may also play a role in regulating protein clearance (Gafni et al., 2012; B. K. Y. Wong et al., 2015).

1.3.3 Caspase-6 in other neurodegenerative diseases

In addition to HD, aberrant C6 activity has been implicated in several other neurodegenerative conditions. Significant effort has been dedicated to uncovering the role of C6 in mediating the pathogenesis of Alzheimer's disease (AD), a disease whose mechanisms bear striking resemblance to HD (Ehrnhoefer et al., 2011c; Graham et al., 2011). AD is characterized by progressive cognitive impairment and dementia as well as the hallmark presence of amyloid plaques and neurofibrillary tangles in the hippocampus, entorhinal cortex and amygdala (Duyckaerts et al., 2009).

Familial AD is caused by mutations in genes encoding for the amyloid precursor protein (APP), presenilin 1 (PSEN1) and presenilin 2 (PSEN2) while the apolipoprotein E4 allele is the strongest genetic risk for late-onset sporadic AD (Karch and Goate, 2015). Proteolytic cleavage of the APP protein generates the extracellular amyloid-β (Aβ) peptide, which has a high propensity to aggregate into amyloid plaques seen in AD brains (Bi, 2010). Neurofibrillary tangles consist primarily of hyperphosphorylated tau, a microtubule-associated protein (Bi, 2010).

The notion that amyloid plaques drive AD pathogenesis prevailed for decades. However, the lack of clinical benefit observed following clearance of amyloid plaques in humans pointed to the need for identifying upstream molecular events contributing to the formation of plaques and tangles for the development of therapeutic targets (Holmes et al., 2008). Caspase activation is an early event in AD pathology and contributes to the generation of tangles (de Calignon et al., 2010; Gamblin et al., 2003; Rissman et al., 2004). Active C6 along with C6-cleaved tau have been observed in early- and late-stage familiar and sporadic AD brains (Albrecht et al., 2007; 2009; Guo et al., 2004). Furthermore, increased C6 mRNA has been observed in post-mortem AD brains (Pompl et al., 2003), possibly due to the elevated levels of p53 observed in AD (Kitamura et al., 1997). Increased C6 activation has also been observed in the mouse hippocampus and leads to neurodegeneration and memory impairment (LeBlanc et al., 2014).

Both tau and APP are substrates of C6 (Galvan et al., 2002; H. Zhao et al., 2014; M. Zhao et al., 2003) and prevention of C6-mediated cleavage at the 664 amino acid site within APP confers partial behavioural and neuropathological benefits in an AD mouse model (Galvan et al., 2002). Interestingly, the levels of C6-cleaved tau detected in the CSF of AD patients correlate with disease progression and cognitive scores (Ramcharitar et al., 2013b). The accumulation of aggregates in AD is also facilitated by C6-mediated cleavage of p97, a protein responsible for mediating ubiquitin-proteasome degradation of misfolded proteins (Halawani et al., 2010). These data point to a central role played by C6 in the pathophysiology of AD.

Increased C6 activation has also been observed throughout the normal aging process in both humans and mice, independent of the development of neurodegenerative disease (Albrecht et al., 2007; Graham et al., 2006). Increased C6 activity has also been shown to play a role during stroke and cerebral ischemia (Harrison et al., 2001; Singh et al., 2002). Importantly, modulation of C6 activity protects mice from stroke (Akpan et al., 2011; Shabanzadeh et al., 2015) and treatment of mice with a C9 inhibitor following stroke induction attenuated C6 activation and was protective against neuronal loss (Akpan et al., 2011).

1.4 MODULATION OF CASPASE-6 IN HD

1.4.1 Caspase-6 resistant mutant huntingtin

The identification of caspase cleavage sites within HTT and the toxic repercussions of HTT proteolysis at certain sites led investigators to generate non-cleavable caspase-resistant versions of the mutant protein (Wellington, 2000). This was achieved using site-directed mutagenesis targeting the obligate aspartate residue required by caspases within the substrate recognition site (Thornberry et al., 1997). *In vitro*, mHTT mutated at amino acids sites 513 and 530 (resistant to C3-mediated cleavage) and at the 586 site (resistant to C6-mediated cleavage) demonstrate reduced toxicity to apoptotic stimuli and have a lower propensity to form aggregates (Wellington, 2000).

These findings were then translated *in vivo* when modified YAC128 mice were generated to be resistant to various proteolytic events. Characterization of mice carrying a YAC128 transgene mutated at amino acid sites 513 and 552 and resistant to C3 cleavage revealed no protection from the pathology observed in the parental YAC128 line, suggesting fragments generated by C3-mediated mHTT cleavage are not the primary toxic species driving pathogenesis (Graham et al., 2006). However, mice carrying the mHTT transgene mutated at amino acid 586 and resistant to C6 cleavage are fully protected from behavioural and neuropathological deficits seen in YAC128 mice (Graham et al., 2006; Pouladi et al., 2009). These C6-resistant (C6R) mice do not develop motor function deficits, depressive-like behaviour and also do not exhibit the canonical striatal atrophy or sensitivity to NMDA-induced excitotoxicity observed in YAC128 mice (Graham et al., 2006; Pouladi et al., 2009). This dramatic protection from HD phenotypes was achieved by targeting one proteolytic event and suggests that the 586 fragment itself mediates toxicity, a finding corroborated by the observation that the expression of this particular mHTT fragment is sufficient to cause HD-like phenotypes including progressive motor dysfunction and neuropathology in mice (Tebbenkamp et al., 2011; Waldron-Roby et al., 2012). These data strongly suggest that cleavage at the 586 site of mHTT is a necessary step in the progression of HD pathology in YAC128 mice.

1.4.2 Constitutive genetic loss of caspase-6 and possible compensation mechanisms

Studies investigating the pathogenicity of the 586 fragment highlighted the therapeutic relevance of preventing this proteolytic event, possibly by way of targeting C6 activity. To investigate the impact of modulating C6, a constitutive C6 deficient mouse was generated (*C6*$^{-/-}$). Neuroanatomical and behavioural characterization of these deficient mice revealed an age-dependent increase in striatal and cortical volume, hypoactive behaviour and cognitive learning deficits (Uribe et al., 2012). Furthermore, neurons cultured from *C6*$^{-/-}$ animals are protected from excitotoxicity and myelin-induced neurodegeneration (Uribe et al., 2012), further confirming the indispensable role played by C6 in mediating these

cell processes. Interestingly, a gene dosage effect was observed in heterozygotes where the loss of one *C6* allele still conferred protection against excitotoxic insults (Uribe et al., 2012), suggesting that pharmacological approaches that partially inhibit C6 activity may still provide therapeutic benefit.

The *C6*$^{-/-}$ mouse was subsequently crossed to the BACHD, YAC128 and *Hdh*Q150 mouse models of HD to examine the effects of the constitutive absence of C6 in the context of mHTT. Consistent across all studies was the finding that genetic ablation of C6 did not prevent the generation of the 586 mHTT fragment, which may be due to compensatory cleavage by C8 (Gafni et al., 2012; Landles et al., 2012; B. K. Y. Wong et al., 2015). Interestingly, western blot analysis in striatal lysates of both BACHD;*C6*$^{-/-}$ and YAC128;*C6*$^{-/-}$ mice showed reduced fragment and full-length levels of WT and mHTT (Gafni et al., 2012; B. K. Y. Wong et al., 2015), suggesting that C6 may play a role in modulating protein clearance. BACHD;*C6*$^{-/-}$ mice also displayed reduced aggregate load, delayed body weight gain and modestly improved motor function (Gafni et al., 2012), demonstrating that while the generation of the 586 fragment still occurred in the absence of C6, loss of C6-mediated cleavage at 586 was moderately beneficial.

Similar results were obtained in YAC128;*C6*$^{-/-}$ mice, where levels of the 586 fragment were significantly reduced but not abolished entirely (B. K. Y. Wong et al., 2015). In addition, these mice display delayed body weight gain corresponding with normalized IGF-1 levels, a rescued depressive phenotype, reduced HTT protein levels and a concomitant increase in autophagic activity (B. K. Y. Wong et al., 2015). These results further confirmed the possibility that an alternate protease is capable of cleaving at the 586 site to generate this toxic fragment in the absence of C6. Indeed, *in vitro* studies revealed that C8 and C10 were capable of cleaving at the 586 site, albeit to a lesser extent (B. K. Y. Wong et al., 2015) and indicated that the reduced *in vivo* levels of the 586 fragment may explain the delay in some of the YAC128 phenotypes. As C10 is not present in mice, it is likely the upregulation of C8 in the absence of C6 that is contributing to mHTT proteolysis at 586, particularly in light of the fact that C6 and C8 often

participate in shared cellular pathways (van Raam et al., 2013; B. K. Y. Wong et al., 2015).

The intriguing finding that the depressive phenotype was completely rescued in YAC128;*C6*$^{-/-}$ mice while most other behavioural and neuropathological phenotypes were only partially attenuated points to a distinction between phenotypes governed by C6 activation as opposed to the presence of the 586 fragment. Specifically, in light of the postulated role for C6 in mediating inflammation and cytokine production together with the well-established link between elevated cytokines and depression, the presence or absence of C6 may govern the onset of this affective behaviour through this inflammatory mechanism independent of the presence of the 586 fragment.

In contrast to the first two HD models crossed to *C6*$^{-/-}$ mice, analysis of mHTT fragment patterns in *Hdh*Q150;*C6*$^{-/-}$ mice revealed no reduction in the generation of the 586 fragment and no differences in full length WT or mHTT protein levels (Landles et al., 2012). This opposing finding could be attributed to the differences in mouse models used, as the YAC128 and BACHD are transgenic models containing full-length human mHTT whereas the *Hdh*Q150 is a knock-in mouse containing the polyQ expanded tract within the endogenous mouse *Hdh* gene. Given that the surrounding genomic contexts differ between these models, it is possible that these differences result in distinct mechanisms targeting HTT for clearance pathways.

A caveat with the constitutive deletion of genes is the possibility for developmental reprogramming and compensation, particularly between members of the same genetic family or pathway (Grether, 2005). Compensatory mechanisms have been documented between two members of the *Rb* family of tumour suppressor genes. In the absence of one *Rb* gene, the other is upregulated in an effort to prevent the development of retinoblastoma in mice (Donovan et al., 2006). Compensation has also been observed within the caspase family, specifically between executioner caspases. In the constitutive C3 deficient mouse model, apoptotic stimuli resulted in the compensatory activation

of C6 and C7, resulting in delayed but not full protection against apoptosis (T. S. Zheng et al., 2000). Interestingly, the compensatory activation of alternate executioner caspases in the absence of C3 activity in mice is strain-dependent – loss of C3 on the 129S1/SvImJ genetic background results in perinatal lethality, while *C3*$^{-/-}$ mice on the C57BL/6J genetic background develop normally due to compensatory activation of C7 (Houde et al., 2004). Taken together, these data highlight the need for investigating conditional *C6* deficient models in HD.

1.4.3 Peptide-mediated inhibition of caspase-6

Ideally, modulation of C6 at the post-translational level would be achieved using small molecule inhibitors or peptide-based approaches that specifically perturb a unique enzyme-substrate interaction. Given the overlapping functions of many caspase family members, this has proven particularly difficult to achieve with small molecules (Heise et al., 2012). One strategy to specifically prevent C6-mediated cleavage of mHTT of 586 was employed by Aharony and colleagues, who designed a 24-amino acid peptide based on the HTT sequence surrounding the 586 site of mHTT and fused it to a TAT tag to enable cell permeability (Aharony et al., 2015). *In vitro*, this peptide is protective against mHTT-induced toxicity and prevents the generation of the 586 fragment. Treatment of BACHD mice with this peptide by subcutaneous osmotic pump infusion resulted in reduced body weight gain, improvement in motor and cognitive function as well as the prevention of the depressive phenotype (Aharony et al., 2015), further confirming that inhibiting this specific proteolytic cleavage event is protective in HD.

1.5 THESIS OBJECTIVES

The primary goal of this thesis was to investigate the effects of modulating C6 in the YAC128 mouse and to provide further validation of C6 as a potential drug target. It is clear from the characterization of the C6R mice that preventing C6-mediated cleavage of mHTT could significantly delay or prevent disease progression (Graham et al., 2006). However, we have learned through genetic proof-of-concept studies that the strategy of constitutive deletion of the *C6* gene in several HD mouse models does not prevent cleavage of mHTT at the 586 site (Gafni et al., 2012; Landles et al., 2012; B. K. Y. Wong et al., 2015). This is likely due to compensatory mechanisms at play during development, whereby other caspases and possibly other proteases become responsible for cleaving mHTT at this site. As such, it is imperative to assess the effects of modulating C6 in the adult animal by inducible genetic deletion or small peptide treatment, which are more relevant clinical approaches and bypass the consequences of the absence of C6 during development. Modulation of C6 in the adult mouse is hypothesized to confer benefits and ameliorate the phenotypes observed in YAC128 mice. Furthermore, assessing the impact of C6 modulation on less-well characterized phenotypes such as inflammation could provide insight into the non-apoptotic roles played by C6 in the pathogenesis of HD. The work in this thesis is aimed at further determining the validity of C6 as a therapeutic target through the following specific objectives:

1.5.1 Assess the impact of partial, adult-onset genetic loss of caspase-6 in WT and YAC128 mice

Conditional strategies to delete the C6 gene are required to assess the impact of modulating C6 in the adult animal. This can be achieved using an inducible knockout method, which makes use of the cyclization recombination (Cre)-loxP system and induction of Cre using tamoxifen. Preliminary studies are necessary to optimize the extent of gene deletion using various tamoxifen administration protocols. Following optimization of tamoxifen treatment, characterization of the

effects of *C6* gene deletion in YAC128 mice will be conducted to assess the impact of C6 deficiency on HD phenotypes.

1.5.2 Assess whether peptide-mediated inhibition of caspase-6 activity ameliorates HD phenotypes in YAC128 mice

Alternative methods for modulating C6 are necessary in the development of potential therapeutics. Furthermore, testing existing therapeutics in multiple mouse models of HD is critical for confirming efficacy and validity of therapeutic compounds. To that end, the effects of inhibiting C6-mediated cleavage of mHTT are assessed in YAC128 mice using a peptide previously shown to be therapeutically beneficial in an alternate mouse model of HD.

1.5.3 Investigate the role of caspase-6 in inflammation and its relationship to the inflammatory phenotype in YAC128 mice

If C6 is to be a therapeutic target, ongoing work is required to expand our knowledge of the functions of C6, with an important focus on its less well-understood non-apoptotic roles. There is a need to further investigate the recently proposed roles for C6 in mediating inflammation; particularly as aberrant C6 activity co-exists with enhanced inflammatory phenotypes in many neurodegenerative conditions. The role of C6 in mediating inflammation and its relevance to HD phenotypes will be assessed by comparing the inflammatory responses of WT, constitutive *C6*$^{-/-}$ and YAC128 mice.

2 MATERIALS AND METHODS

2.1 GENERATION OF CASPASE-6 INDUCIBLE DEFICIENT MOUSE

The C6 inducible mouse was engineered by Caliper Life Sciences (now PerkinElmer). LoxP sites, short sequences recognized by the Cre recombinase enzyme, were inserted into the introns flanking exons 2 and 5 of the mouse *C6* gene (~6.5 kb apart) resulting in an expected excision of this region upon expression of Cre (Figure 2.1). This particular region of the gene was chosen due to the presence of the catalytic domain localized to the central region of the protein. The 5' and 3' homology arms and conditional deletion region were amplified by PCR and inserted into the targeting vector at the indicated restriction enzyme sites. The targeting vector carried a loxP-flanked Neomycin (Neo) cassette for positive selection and a diphtheria toxin A (DTA) cassette for selection against random insertion (Figure 2.1).

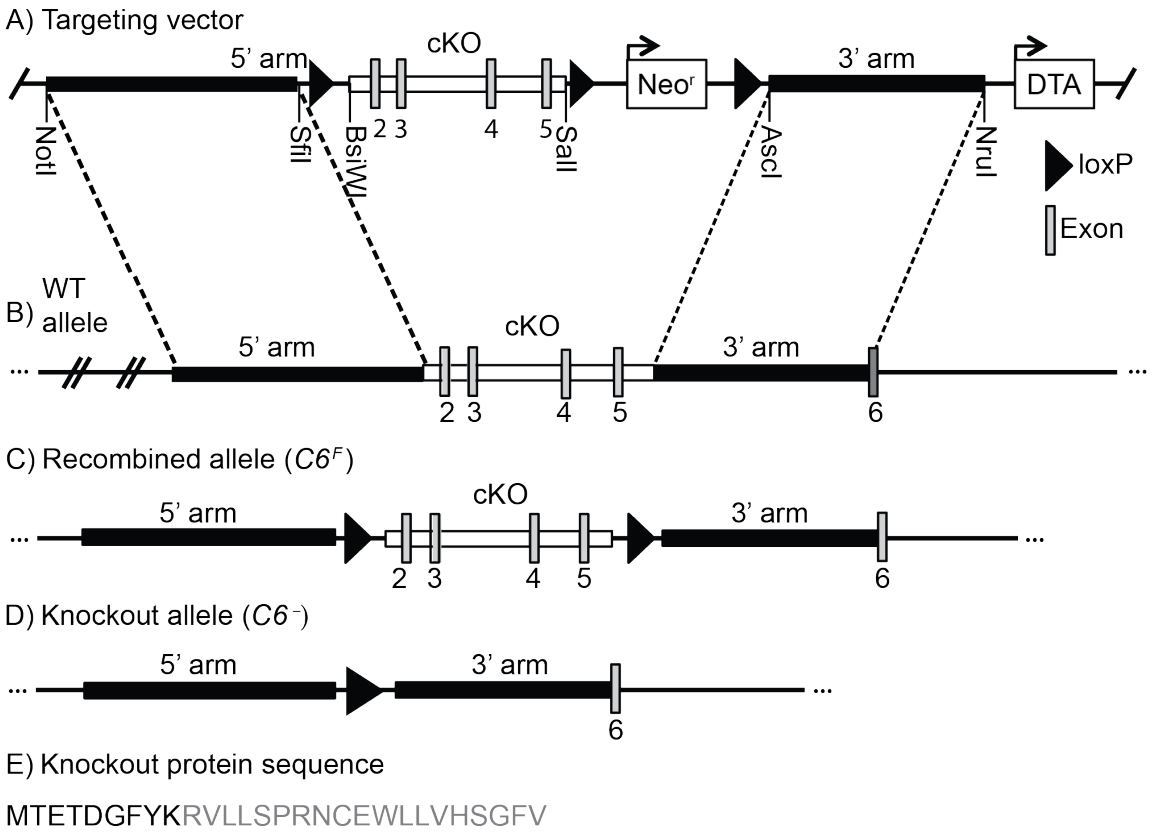

Figure 2.1: Generation of *C6* inducible deficient mice. The targeting vector used (A) was generated through PCR cloning of the 5' and 3' homology arms (4.9 and 5.1 kb, respectively) and the region to be deleted (cKO) with restriction enzyme sites are indicated. The deletion region, in white, includes exons 2-5 as well as upstream and downstream intronic sequence for a total of ~6.5 kb. The WT allele is shown in (B) with the 5' and 3' homology arms and the cKO region indicated. The recombined allele (*C6*^{F}) is shown in (C). The deleted allele resulting from Cre expression is shown in (D) resulting in the frameshifted sequence in grey (E).

C57/BL6 embryonic stem cells were electroporated with the targeting construct DNA and integration was selected for using Geneticin (G418) antibiotic. G418-resistant clones were isolated and Southern blot analysis was carried out to screen for clones that underwent homologous recombination at both arms. The Neo cassette was then removed following electroporation of recombinant ES cells with *Cre* and G418-sensitive clones were isolated. Following confirmation of Neo cassette removal by Southern blot analysis, two clones were microinjected into FVB/NJ blastocysts that were then transferred into pseudo-pregnant females

for the generation of chimeras. Chimeric mice were then bred with C57/BL6 males and resulting black coat progeny indicated germline transmission of the floxed allele ($C6^{F/+}$). Offspring were backcrossed for 10 generations to the FVB/NJ strain. Heterozygote floxed mice were then intercrossed to produce homozygotes ($iC6^{F/F}$). Mice carrying the floxed allele were genotyped using the following primers: 5'-GACTTCCTCATGTGCTACTCTGTCGCA-3' (forward) and 5'- GCAAGCTGCTAACAGCCAACACAAC-3' (reverse).

2.2 MOUSE GENOTYPES AND BREEDING STRATEGY

All experimental mice were maintained on the FVB/NJ strain. The $iC6^{F/F}$ mice were then crossed to a ubiquitously Cre-expressing line (referred to the Cre-ERT2 line (Ruzankina et al., 2007), '$C6^{F/F}$;Cre-ERT2'). Cre expression is driven by the human ubiquitin C (UBC) promoter, and the tamoxifen-inducible feature is conferred by fusion of the *Cre* gene to a mutated version of the entire estrogen receptor (*ERT2)* gene, enabling recognition by tamoxifen and not endogenous estrogen. Mice were then crossed to mice carrying the YAC128 transgene, generating the triple transgenic mouse. Mice carrying the *Cre-ERT2* transgene were genotyped using the following primers against *Cre*: 5'-GCGGTCTGGCAGTAAAAACTATC-3' (forward) and 5'-GTGAAACAGCATTGCTGTCACTT-3' (reverse). Mice carrying the *YAC128* transgene were genotyped using the following two sets of primers against human *HTT*: 5′-CTTGAGATCGGGCGTTCGACTCGC-3′ (primer set 1 forward) and 5′-CCGCACCTGTGGCGCCGGTGATGC-3′ (primer set 1 reverse); 5′-CCTGCTCGCTTCGCTACTTGGAGC-3′ (primer set 2 forward) and 5′-GTCTTGCGCCTTAAACCAACTTGG-3′ (primer set 2 reverse). In order to determine genotypes of triple transgenic mice, DNA extracted from tail lysates were subject to two separate PCR reactions – the first was a multiplex optimized amplify both *Cre* and the floxed *C6* regions, while the second was targeted to amplify the human *HTT* transgene, all of which employed to above-mentioned primers.

The 5 genotypes used in specific objective 1.5.1 (Chapter 3) were obtained from two separate matings. WT mice were obtained by mating two FVB/NJ mice, while the remaining 4 genotypes were obtained by mating *iC6$^{F/F}$;YAC128* females to *iC6$^{F/F}$;Cre*+ males. Mice were born at expected Mendelian ratios. All mice were treated with tamoxifen and the *Cre*+ mice that become *C6* deficient animals following tamoxifen treatment are denoted as *iC6$^{-/-}$* (inducible *C6* deficient mice) while those without *Cre* are denoted as *iC6$^{F/F}$* Controls. A total of 9 experimental cohorts were generated and injected with tamoxifen to induce deletion of *C6*. Eight of these cohorts were behaviour tested at 3, 6, 9 and 12 months, of which 2 were assessed for neuropathological endpoints at 12 months. A separate cohort was kept naïve and harvested for biochemical assessment at 12 months. Separate cohorts were generated to assess the effects of loxP sites on C6 expression. The 5 genotypes are listed in Table 2.1.

Table 2.1: List of genotypes used in the inducible *C6* deficiency study.

Shorthand Name	Genotype	Treatment
WT	*C6$^{+/+}$*	Tamoxifen
iC6$^{F/F}$ Control	*C6$^{F/F}$*	Tamoxifen
iC6$^{-/-}$	*C6$^{-/-}$*;Cre-ERT2	Tamoxifen
iC6$^{F/F}$;YAC128 Control	*C6$^{F/F}$*;YAC128	Tamoxifen
iC6$^{-/-}$;YAC128	*C6$^{-/-}$*;YAC128;Cre-ERT2	Tamoxifen

Mice used in specific objective 1.5.2 (Chapter 4) were obtained by breeding WT FVB/NJ female mice with male YAC128 mice. For all experiments, littermates were used where possible and cohorts consisted equally of both sexes.

Mice used in specific objective 1.5.3 (Chapter 5) were obtained by breeding female and male heterozygous constitutive *C6* deficient mice (*C6$^{+/-}$*). Constitutive *C6$^{-/-}$* mice were genotyped using the following primers: 5'-CCTGTGGGGTCAAAAGACTTTCACAG-3' (forward) and 5'-GCAAGCTGCTAACAGCCAACACAAC-3' (reverse).

All animal experiments were conducted according to protocols approved by the Committee on Animal Care at the University of British Columbia.

2.3 INDUCTION OF *CASPASE-6* DELETION WITH TAMOXIFEN

All tamoxifen treatments were carried out when mice reached 6 weeks of age, at which point mice have reached sexual maturity and the development of the brain is complete (Finlay and Darlington, 1995). The tamoxifen administration regimen was optimized using 3 different administration routes – tamoxifen-embedded food pellets for oral consumption, slow-release dissolvable tamoxifen pellets surgically implanted subcuteanously as well as intraperitoneal (IP) tamoxifen injections. Tamoxifen food pellets were purchased from Harlan Teklad (TD.07694, 250 mg tamoxifen citrate/kg supplemented standard diet Global 2016 pellets) and provided *ad libitum* to mice for 2 or 3 weeks. This formulation provides ~40 mg tamoxifen per kg body weight per day, which corresponds to approximately 1 mg per day under the assumptions that the mouse weights 20-25 g and consumes 3-4 g of food per day. Slow-release tamoxifen pellets for surgical implantation were obtained from Innovative Research of America (E-361, 21-day release) in 50 or 75 mg doses. This delivery method enables a constant, even dose over the release period and results in an estimated blood level of tamoxifen in mice of 5.0 µg/ml and 7.5 µg/ml respectively, according to manufacturers measurements. For IP injections, tamoxifen powder (Sigma, T5648) was dissolved in 98% corn oil with 2% ethanol as previously described (Ruzankina et al., 2007) and administered at 100 or 175 mg/kg for 5-19 consecutive days.

2.4 QUANTITATIVE REAL-TIME PCR

Total RNA was extracted from tissues frozen at -80°C using the RNeasy micro kit (Qiagen, 74004) for striata or mini kit (Qiagen, 74104) for all other tissues. Residual genomic DNA was destroyed using DNAse I (Invitrogen, 18047-019) and cDNA was prepared from 250ng-1µg total RNA using the SuperScript®-III First-Strand Synthesis kit (Life Technologies, 18080-051). Quantitative real-time PCR (qRT-PCR) was performed using the Power SYBR Green PCR master mix

(Applied Biosystems, 4309155) in the ABI 7500 Fast instrument (Applied Biosystems) under default conditions in triplicate. The primers were used are listed in Table 2.2.

Table 2.2: List of primers used in quantitative real-time PCR.

Gene	Forward Primer (5'-3')	Reverse Primer (5'-3')
C6	TTTAACGACCTCAGAGCAGAAG	GGCTCAGGAAGACACAGATG
Htt (mouse)	TGCTACACTGACAGCGAGTCT	ATCCCTTGCGGATCCTATCA
HTT (human)	GAAAGTCAGTCCGGGTAGAAC	CAGATACCCGCTCCATAGCAA
Rpl13a	GGAGGAGAAACGGAAGGAAAAG	CCGTAACCTCAAGATCTGCTTCTT
HPRT	CGTCGTGATTAGCGATGATGA	TCCAAATCCTCGGCATAATGA

2.5 PROTEIN ANALYSIS, WESTERN BLOTTING AND ANTIBODIES

Protein was isolated from tissues by homogenizing in SDP+ buffer (50 mM Tris (pH 8.0), 150 mM NaCl, 1% NP40, 40 mM β-glycerophosphate, 10 mM NaF, 1x Roche complete protease inhibitor, 1 mM sodium orthovanadate and 800 uM PMSF) and incubated on ice for 20 minutes for complete lysis. Cell debris was removed by centrifuging at 15,000x-g at 4°C for 15 minutes and protein was quantified in the supernatant using the DC protein assay (BioRad, 500-0111). Protein was prepared for western blotting by heating at 70°C in 1X LDS sample buffer (Invitrogen, NP0008) with 10 μM DTT, separated by SDS-PAGE and subsequently transferred onto a nitrocellulose membrane. For dot blots, 2 μl of protein sample was directly applied on to the membrane and allowed to dry. Membranes were blocked in a 5% milk-PBS solution for 1 hour at room temperature and then incubated with primary antibody overnight at 4°C.

Fluorescently conjugated secondary antibodies Alexa Fluor 680 (Molecular Probes, A21076, 1:10000) and/or IRDye 800CW (Rockland, 610-131-121, 1:10000) were applied the following day in Odyssey Blocking Buffer (Li-COR, 927-40000) for one hour and blots scanned and quantified using the Odyssey Infrared Imaging system (Li-COR). Primary antibodies used were C6 (in-house, 1:500), β-actin (Millipore, MAB1501R, 1:10000), huntingtin (BKP1, in-house 1:400 and Millipore, MAB2166, 1:1000), calnexin (Sigma, C4731, 1:5000), TAT

(Abcam, 63957,1:500) and diluted in 5% BSA-PBS-T (bovine serum albumin in phosphate buffered saline with 0.05% Tween-20).

2.6 SURGICAL PUMP AND PELLET IMPLANTATION

The 24-amino acid ED11 peptide (sequence GRKKRRQRRRPPQSSEIVLDGTDN) was synthesized, purified to >95% and analyzed using high performance liquid chromatography (HPLC) and mass spectrometry by Applied Biological Materials Inc. (ABM). Alzet osmotic pumps (DURECT, 1004) containing ED11 initially dissolved in water and further diluted in sterile 0.9% saline were prepared by as previously described (Aharony et al., 2015). Mice were anesthetized with isofluorane and a 5x5 cm region below the scapulae was shaved and disinfected with 70% ethanol and betadine. A 3-4 mm lateral incision was made and the pump or pellet was inserted subcutaneously approximately 3 mm caudally from the incision. The incision was closed with sutures and mice were allowed to recover on a heating pad until awoken from anesthetic. Mice were monitored for 3 days following surgery and any remaining sutures were removed after 7 days. Pumps released ED11 compound at a concentration of 8 mg/kg/day for 28 days and were replaced every 28 days until the mice were sacrificed at 6 months of age. Tamoxifen pellets were implanted the same way as ED11 osmotic pumps and released compound for 21 days and mice were sacrificed one month after the last day of release.

2.7 BEHAVIOUR ANALYSES

All behaviour-tested mice were housed on a 12-hour light/dark cycle and the experimenter was blind to all genotypes. All behaviour analyses were conducted during the dark phase of the cycle. Behaviour testing for *iC6* mice (Chapter 4) was conducted at 3, 6, 9 and 12 months of age and at monthly intervals for ED11-treated mice starting at 2 months of age. Behaviour testing on ED11-treated mice was staggered with monthly pump implant surgeries in order to ensure the mice were fully recovered prior to behavioural assessment.

2.7.1 Motor tests

Motor learning and function was assessed using the rotarod apparatus (UGO Basile, Comerio, Italy) as previously described (Slow et al., 2003). Briefly, naïve mice were trained for three consecutive days at a fixed speed setting of 18 rpm for 120 seconds three times a day for a total of 9 trials over three days. Trials on any given day were separated by 2 hours and the latency to the first fall as well as the number of falls was recorded for each trial. The average of the three trials is reported as a measure for motor learning. On the fourth day and subsequently at 2-3 month intervals, mice were tested on a rotarod that accelerated from 5 to 40 rpm over 300 seconds and the latency to fall was recorded. For this assessment of motor function, an average of three trials per day is reported.

Motor function is also assessed using a climbing apparatus as previously described (Southwell et al., 2009). Two- to three-month old mice were placed in a 10x15 cm enclosed wire mesh cylinder and videotaped for 300 seconds as they freely explored the apparatus. A climbing event was noted when all four paws were lifted from the surface and the time spent climbing was recorded from when all four paws were lifted to when the first paw touched back down. Rearing events were also recorded when the two front paws were lifted as an indication of active behaviour and exploratory ability.

2.7.2 Cognitive tests

Spatial and novel object learning was determined using the novel object location and novel object preference tests as previously described (Southwell et al., 2009). Briefly, on the first day, 5 minutes following the open field test (refer to section 2.6.3) mice were placed back in the lower left corner of the 50x50cm black Plexiglas box with 16 cm high edges in a brightly lit room, now containing two different novel objects in the two upper corners of the box. The number of investigations of each object was recorded using EthoVision® XT 7 tracking software (Noldus) using a video camera mounted on the ceiling above over a period of 5 minutes. Mice were then removed from the box and re-introduced after 5 minutes, by which point the object in the top right corner had been moved

to the bottom right corner. Mice were tracked for 5 minutes and the percentage of investigations to the newly located object out of the total number of investigations was calculated to determine novel object location learning. To assess novel object preference, the procedure was repeated on day 2 but rather than move the object in the top right corner, it was replaced entirely with a novel object. Again, the percentage of investigations to the novel object out of the total number of investigations was calculated.

2.7.3 Psychiatric tests

Anxiety was assessed using the open field and elevated plus maze tests. The open field is previously described (Southwell et al., 2009) and consists of placing the mice in an empty 50x50cm black Plexiglas box with 16 cm high edges in a brightly lit room. Mice were allowed to explore the box and were tracked using EthoVision® XT 7 tracking software (Noldus). The total distance travelled, average velocity, time spent in the center and total entries in to the center were recorded.

The elevated plus maze test was conducted as previously described (Southwell et al., 2013). The apparatus consists of two open arms and two closed arms with 20 cm walls 50 cm above the ground, with arm lengths of 30x10 cm. Mice were placed in the center of the maze and allowed to freely explore for 5 minutes while being tracked using EthoVision® XT 7 tracking software (Noldus). The distance travelled and time spent in the open arms were recorded.

Depressive-like behaviour was measured using the Porsolt forced swim test as previously described (Porsolt et al., 1977),(Pouladi et al., 2009). Mice were placed in transparent cylinders 25 cm tall x 19 cm wide filled with room temperature water to a depth of 15 cm. Mice were recorded for 6 minutes using a camera located above the cylinders, with the last 5 minutes scored for time spent immobile as a readout for depressive-like behaviour.

Anhedonia, the loss of pleasure-seeking behaviour, was assessed using the sucrose preference test as previously described (Pouladi et al., 2009). Mice were individually housed and two bottles containing water were placed in their cages

for a one-week acclimatization period. On the seventh day, the right side water bottle was replaced with a bottle containing 2% sucrose solution and both bottles were weighed. After 24 hours, the amount of water and sucrose consumed was measured by weighing both bottles. Sucrose preference was computed by first normalizing sucrose intake to body weight and calculating the normalized sucrose intake as a percentage of total fluid intake.

2.8 NEUROPATHOLOGY

Neuropathological assessments were conducted as previously described (Southwell et al., 2013). Mice were terminally anesthetized with a single 2.5% avertin IP injection and intracardially perfused with cold 4% paraformaldehyde. Brains were extracted and submerged in 4% paraformaldehyde for 24 hours at 4°C for post-fixation. After 24 hours, brains were transferred to a 30% sucrose solution in PBS for cryopreservation. Prior to sectioning, olfactory bulbs and brain stem were removed and discarded. The remaining brain was weighed and the cerebellum was subsequently removed and weighed separately. Forebrain weight was calculated by subtracting cerebellum weight from whole brain weight. Following weight measurements, forebrains were flash frozen on dry ice. Brains were sectioned coronally on a cryostat (Microm HM 500 M) at 25 µm thickness spaced 200 µm apart. A series of sections spanning the striatum was stained with a NeuN antibody at room temperature overnight revealing all neurons. The 586 fragment staining on sections spanning the striatum was conducted using an anti-IVLD antibody (in-house, 1:500). Volumetric measurements of the striatum, cortex and corpus callosum were determined using Stereoinvestigator software (Microbrightfield) and the experimenter was blind to all genotypes.

2.9 NEURONAL CULTURE AND TREATMENT

Embryonic day 15.5-17.5 cortical neurons were cultured as previously described (Metzler et al., 2010) from timed-pregnant FVB and *C6*$^{-/-}$ females each from homozygous breedings. Cultures were incubated at 37°C and 5% CO_2 and half the media was changed every 4-5 days. On the tenth day *in vitro*, cells were treated with 500 µM NMDA for 10 minutes and 48 hours later, the media was

removed and subject to an adenosine triphosphate (ATP) assay (Promega) and carried out according to manufacturer's instructions.

2.10 MICROGLIAL CULTURE AND TREATMENT

Microglia were isolated from individual hemispheres of 0- to 2-day old post-natal mice. Hemispheres were minced, triturated, centrifuged and plated in DMEM media (Invitrogen). Ten to 14 days later, the mixed cultures were gently shaken for 4 hours and floating cells (microglia) were collected and plated separately in DMEM. Cells were seeded into a 96-well plate and the following day switched to media containing 1% FBS. The next day, microglia were treated with varying concentrations of control standard endotoxin (CSE, Associates of Cape Cod) combined with 2.5 ng/µl interferon-gamma (IFN-γ) for 24 hours. Following treatment, the media was harvested for the quantification of cytokines. For treatment with conditioned neuronal media, microglia were incubated for 1 day in 1% FBS-containing media (100 µl/well) before 50 µl/well neuronal media was added. Media was harvested 24 hours after treatment for the quantification of cytokines.

2.11 MACROPHAGE CULTURE AND TREATMENT

Alveolar macrophages were isolated using the brochoalveolar lavage method previously described (Everett et al., 1996). Mice were terminally anesthetized with a single 2.5% avertin IP injection and the intact lungs and trachea removed. Approximately 300 µl of ice-cold PBS was slowly injected into the cannulated lung and the lavage retrieved while gently massaging tissue to disperse liquid. This was repeated 4 additional times and the extracted fluid was centrifuged at 1200 rpm and 4°C for 10 minutes. The cell pellet was re-suspended in warm RPMI 1640 media (Invitrogen) containing 5% FBS, 1% penicillin/streptomycin and plated at a density of $1x10^5$ cells/well in a 96-well plate. Cells were incubated at 37°C, 5% CO_2 and media replaced 2-3 hours later. After 24 hours, media was changed to 1% FBS RPMI and following an additional 24 hours, cells were treated with 10 µg/L IFN-γ with or without 100 µg/L CSE (Associates of Cape

Cod) in fresh media. Supernatants were collected 24 hours after treatment initiation.

2.12 LPS INJECTIONS

Lipopolysaccharide (LPS) derived from *Escherichia coli* (Sigma L2630 serotype O111:B4) was dissolved in 0.9% sterile saline. WT and *C6*$^{-/-}$ mice were IP injected with LPS at ranging doses of 0.5 mg/kg to 5 mg/kg and plasma collected 4-48 hours post-injection. Behaviour testing on LPS-injected animals was conducted 24 hours post-injection.

2.13 PLASMA AND SERUM COLLECTION

Blood was collected either by cardiac puncture following terminal anesthetization with a single 2.5% avertin IP injection or saphenous vein survival bleeding. Plasma was isolated by collecting blood in EDTA-coated tubes (Sarstedt, Numbrecht), kept on ice and centrifuged at 6,000 rpm and 4°C for 10 minutes. For serum collection, blood was allowed to coagulate at room temperature for 30 minutes and then centrifuged at 15,000 g for 10 minutes. Clear supernatant was then removed for analysis.

2.14 ENZYME-LINKED IMMUNOSORBENT ASSAYS (ELISA)

Cytokine ELISAs were conducted according to manufacturer's instructions for IL-6, TNF-α, IL-1β (eBioSciences) and for CXCL1/KC (R&D Systems).

The ED11 was adapted from Ehrnhoefer et al., (Ehrnhoefer et al., 2011a) and conducted using the Mesoscale Discovery platform (Meso Scale Diagnostics, Maryland, USA). The protocol followed was identical with the exception of the primary antibody being anti-TAT (Abcam, 63957,1:500).

2.15 FLUORESCENCE RESONANCE ENERGY TRANSFER (FRET)

A FRET assay for assessing the inhibitory capacity of ED11 on caspase-6 activity was conducted as previously described (Aharony et al., 2015). Briefly, COS-7 cells were transfected with an N-terminal construct of HTT containing 1212 amino acids and 15Q, lysed in SDP buffer (50 mM Tris (pH 8.0), 150 mM NaCl, 1% NP40, 40 mM β-glycerophosphate, 10 mM NaF, 1x Roche complete

protease inhibitor) and used as a substrate. Recombinant caspase-6 (Enzo Life Sciences, BML-SE170-5000) was diluted in FRET buffer (10 mM HEPES pH 7.4, 100 mM NaCl, 0.05% gelatin, 0.1% CHAPS and 2 mM DTT) to a concentration of 0.125 units/ul, mixed with various batches and concentrations of ED11 for a final volume of 22ul and incubated at room temperature for 30 minutes in a white 384-well plate. Subsequently the HTT-expressing COS lysate was diluted in FRET buffer containing terbium-labeled BKP1 antibody (36 ng/ml, FRET donor) after which a D2-labeled monoclonal 586 neo-epitope antibody (360 ng/ml, FRET acceptor) was added. The plate was incubated at 37°C for 4 hours and then at 4°C overnight. The following day, the plates were read using a Xenon lamp Victor Plate Reader (Perkin Elmer) at an excitation wavelength of 340 nm, after which the FRET signal was computed as the ratio of D2 (655 nm) to terbium (615 nm) emission. Data represents an average of triplicate.

2.16 STATISTICAL ANALYSIS

Data were analyzed using Prism 5 statistical software and error bars represent standard error of the mean. For data with one independent variable, an unpaired t-test or one-way ANOVA was conducted as appropriate. For two independent variables, a two-way ANOVA was used. In cases where repeated measurements on the same subject were carried out with no missing values (e.g. longitudinal body weight measurements or rotarod training assessment), a two-way repeated-measures (RM) ANOVA was used. Tukey's post-hoc tests were conducted following 1- or 2-way ANOVA analyses. Asterisks refer to significant differences by t-test or by post-hoc following an ANOVA (as appropriate) unless otherwise indicated.

3 CHARACTERIZATION OF INDUCIBLE CASPASE-6 DEFICIENT MICE

Conditional gene targeting strategies have become a powerful tool for interrogating the effects of spatially and/or temporally controlled gene expression. The most common strategy utilizes the naturally occurring Cre-loxP system derived from bacteriophage, whereby the Cre recombinase enzyme recognizes target 34-base pair loxP sequences and excises the intervening DNA (A. J. Smith et al., 1995); (Schmidt-Supprian and Rajewsky, 2007). Cre recombinase driven by tissue- or cell-specific promoters allow for spatial control while temporal control can be achieved using developmentally regulated promoters or tamoxifen-inducible Cre transgenes (Feil et al., 2009). The latter, used here, involves the fusion of the Cre transgene to a mutated form of the ligand-binding domain of the estrogen receptor rendering it recognizable only to 4-hydroxytamoxifen (4-OHT, active metabolite of tamoxifen) and not to its natural ligand 17β-estradiol (Hayashi and McMahon, 2002). Under basal conditions, the Cre-ERT2 complex is bound to Hsp90 and sequestered in the cytosol. Upon tamoxifen administration, 4-OHT binds to Cre-ERT2, the complex dissociates from Hsp90 and translocates to the nucleus where Cre recombinase excises at the loxP sites resulting in the removal of the intervening sequence (Feil et al., 2009) (Figure 3.1).

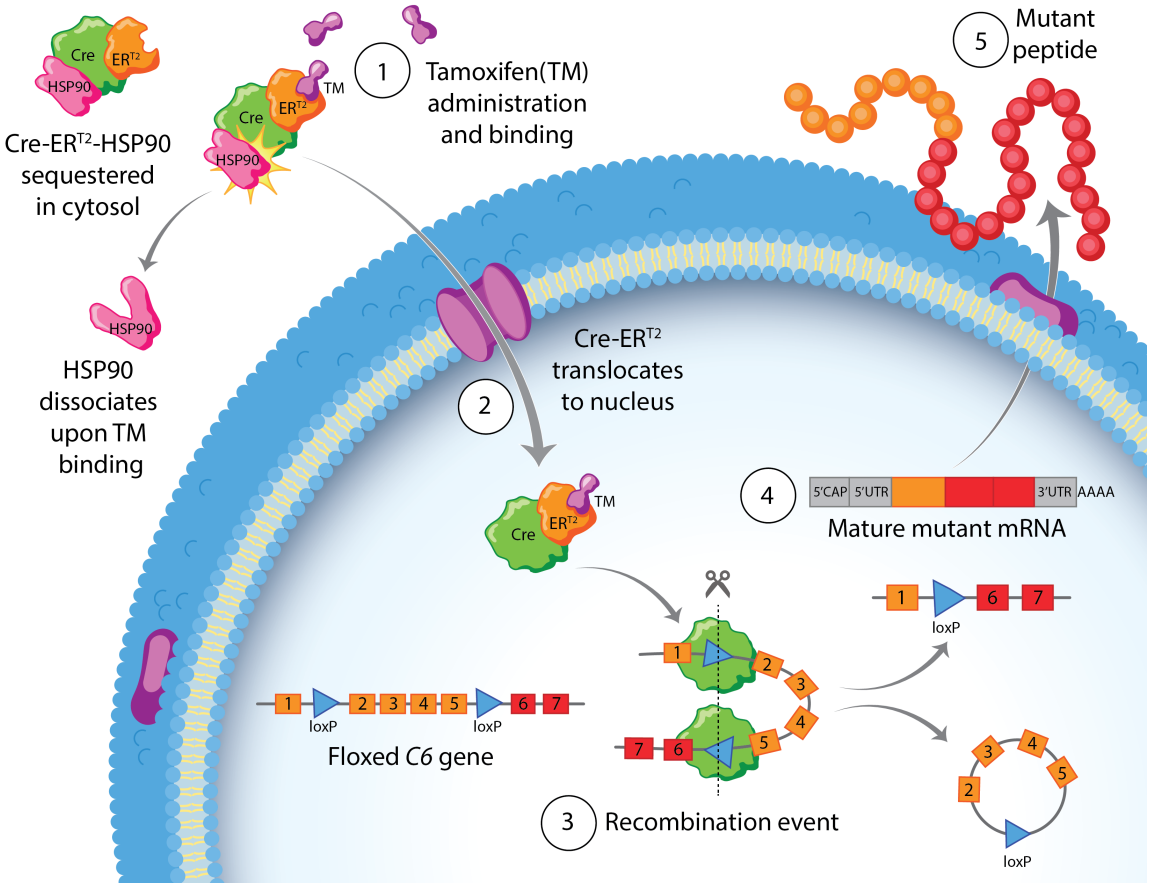

Figure 3.1: Tamoxifen-inducible deletion strategy using Cre-loxP system. Figure by Erin Kenzie, reprinted with permission. Under basal conditions in the absence of tamoxifen, Hsp90 is bound to Cre-ERT2 and kept inactive in the cytosol. Upon exposure to 4-OHT, the active metabolite of tamoxifen, Hsp90 dissociates from the complex (1), which allows Cre-ERT2 to translocate to the nucleus (2) where it excises DNA flanked by loxP sites of the *C6* gene (3), resulting in the production of mutant mRNA (4) and a mutant peptide (5).

3.1 OPTIMIZATION OF TAMOXIFEN TREATMENT

Various doses and routes of administration have been reported to achieve recombination, however efficiency of recombination can vary widely depending on the mouse strain used, genetic background, age and design of targeting vector, among other factors (Feil et al., 2009; Hébert and McConnell, 2000; L. Smith, 2011; S.-Z. Wang et al., 2009). Thus, thorough testing is required to achieve the optimal dose and route of administration in order to maximize recombination efficiency while minimizing potential tamoxifen-induced toxic side effects. To that end, recombination efficiency was tested by treating *iC6*$^{F/F}$ mice

with varying doses of tamoxifen administered orally through food pellets, subcutaneously using surgically-implanted slow-release pellets and intraperitoneally through daily injections.

3.1.1 Tamoxifen-embedded food pellets

While tamoxifen is most commonly administered by IP injection (Kiermayer et al., 2007); (Andersson et al., 2010); (Feil et al., 2009), it is a labour-intensive approach and poses considerable stress to the animals. Incorporating tamoxifen into the food represents a less stressful treatment approach. To that end, tamoxifen-embedded food pellets were provided *ad libitum* to *iC6*$^{F/F}$ mice. Three different protocols were tested for recombination efficiency as follows: (1) two-week tamoxifen food pellet exposure with 1 week post-administration analysis; (2) three-week tamoxifen food pellet exposure with 1 week post-administration analysis; and (3) three-week tamoxifen food pellet exposure with 6 weeks post-administration analysis. Protocols 1 and 2 were conducted simultaneously and collection of tissues was carried out one week following the last day of exposure to tamoxifen feed.

Western blot assessment of full length C6 protein in cortical and spleen tissues, representative of the central nervous system (CNS) and periphery, respectively, was used as a primary readout for recombination efficiency. Protein quantification reveals no change in C6 protein in the cortex but a mild reduction in the spleen (~20%) after two weeks of tamoxifen food (Figure 3.2A), which becomes significant (~40%) in spleen samples exposed to tamoxifen food for three weeks (Figure 3.2B). As a greater extent of excision was desired for the brain, protocol 2 was repeated but modified to extend the post-exposure interval before collecting tissues, as it has been reported that a longer post-tamoxifen interval can result in greater extents of deletion (Andersson et al., 2010; Reinert et al., 2012). With this paradigm, we did not find any further decrease in C6 protein levels compared to protocol 2 with again no changes in C6 protein in the brain and again only moderately (~40%) reduced in the spleen. In this cohort, the

levels of C6 were also assessed in the liver and were significantly reduced by 95% (Figure 3.2C).

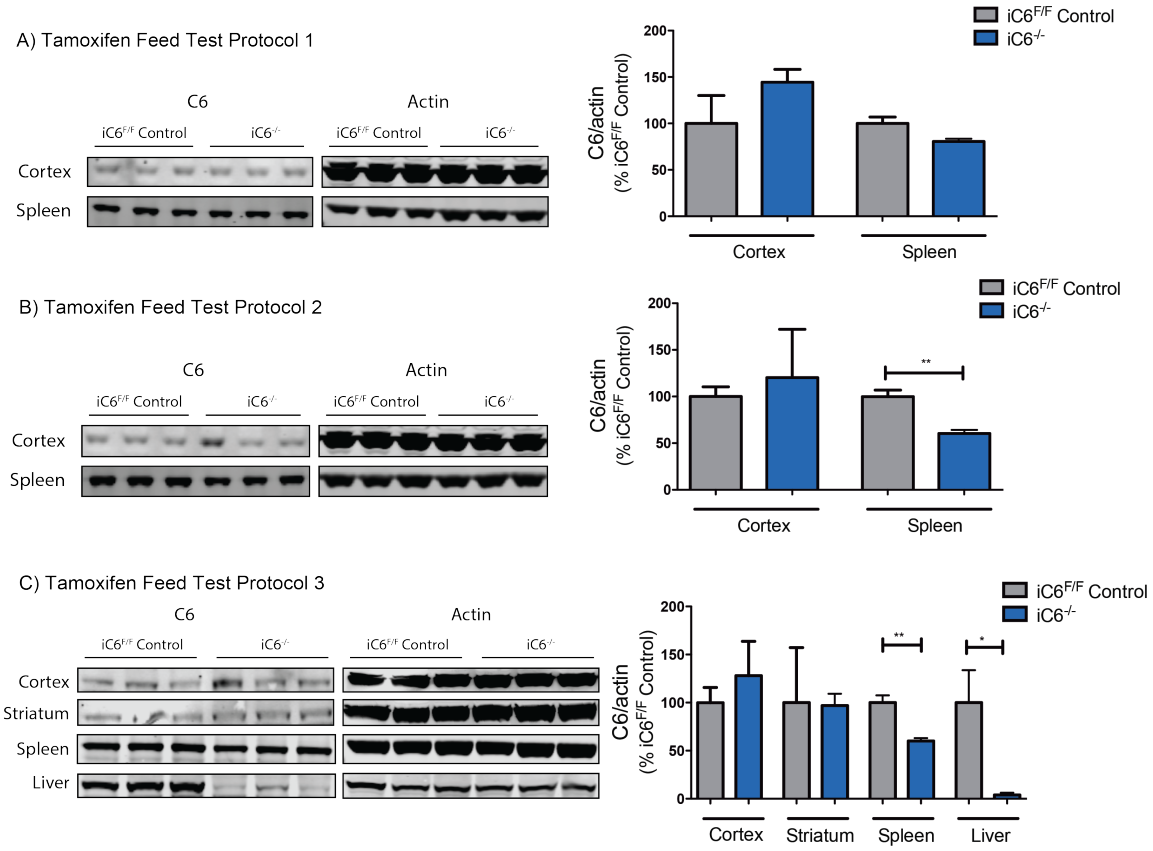

Figure 3.2: Extent of *C6* deletion obtained following oral administration of tamoxifen by food pellets. Western blot analysis of C6 protein levels and corresponding quantification 1 week post-tamoxifen administration for cortex and spleen tissue of animals exposed to tamoxifen feed for 1 week (A) or 2 weeks (B). Western blot analysis on cortex, striatum, spleen and liver of a third cohort of animals tested using protocol 3, which differed from protocol 2 only in that analysis of C6 levels was conducted 6 weeks post-administration instead of 1 week (C). C6 protein expression was quantified relative to actin expression and graphed as a percent of *iC6$^{F/F}$* control (N=2-3, unpaired two-tailed t-test; * p<0.05, ** p<0.01, *** p<0.001).

While this strategy for tamoxifen administration is less stressful for the animals and more cost-efficient, the lack of excision in the brain and high degree of variability in excision between animals is not ideal and could be in part due to differential amounts of food intake. These observations highlighted the need for testing alternative routes of tamoxifen administration.

3.1.2 Implanted subcutaneous tamoxifen pellets

In order to standardize the exact dose of tamoxifen for each animal whilst minimizing distress to the animals, we tested surgically implantable subcutaneous pellets that are dissolvable and slowly release a steady amount of tamoxifen every day for 21 days. Two dosing protocols of 50 mg and 75 mg were tested, which correspond to a daily administration of 2.38 mg and 3.33 mg of tamoxifen, respectively. This strategy limits the handling of the mouse to one surgery during which they are anaesthetized and monitored for 3 days during recovery. Mice were sacrificed 4 weeks following the last day of release and C6 protein levels were assessed in brain and peripheral tissues.

Western blot analysis of the cortex, striatum and spleen tissues of mice implanted with a 50 mg tamoxifen pellet reveal no differences in C6 protein expression between *iC6*$^{-/-}$ and *iC6*$^{F/F}$ brain tissues but a trend toward reduction in the liver of *iC6*$^{-/-}$ mice (Figure 3.3A). Treatment with the higher dose pellet, 75 mg, did not yield any additional reduction in C6 protein except for in the liver where C6 is significantly reduced by ~80% (Figure 3.3B).

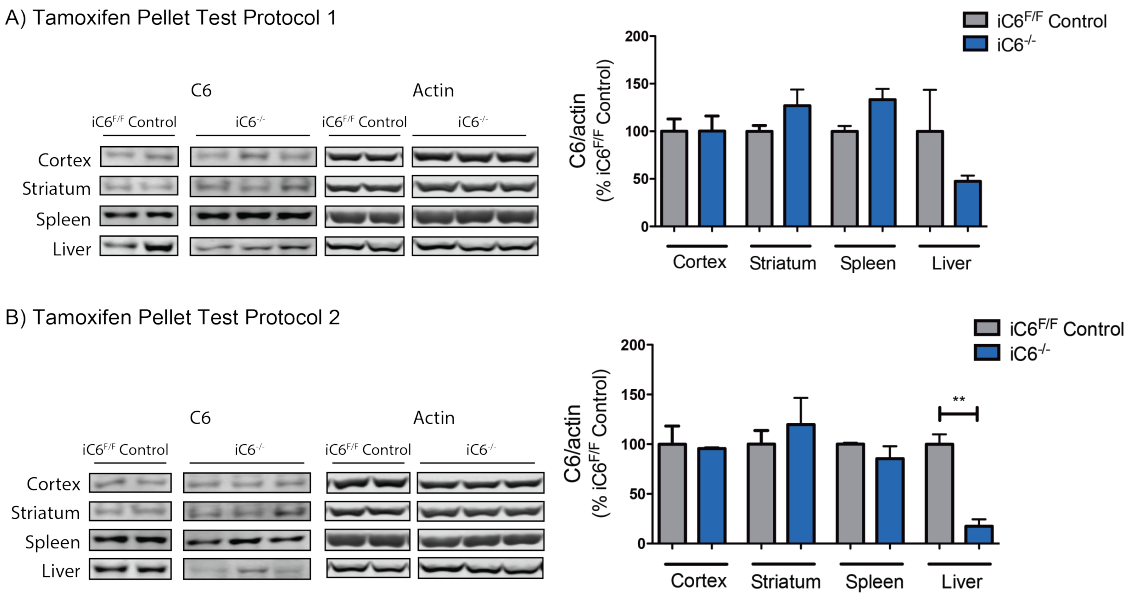

Figure 3.3: Extent of *C6* deletion obtained following subcutaneous administration of tamoxifen by surgically implanted dissolvable pellets. Western blot analysis of C6 protein levels and corresponding quantification of cortex, striatum, spleen and liver tissues assessed 4 weeks following treatment of 50 mg subcutaneous slow-release tamoxifen pellets (A) or 75 mg subcutaneous slow-release tamoxifen pellets (B). C6 protein expression was quantified relative to actin expression and graphed as a percent of iC6F/F control (N=2-3, unpaired two-tailed t-test; * $p<0.05$, ** $p<0.01$, *** $p<0.001$).

It is worth nothing that upon sacrificing the animals, several mice still had a residual portion of the pellet that was undissolved in the subcutaneous space, indicating that they had not received the full dose and perhaps not a consistent dose over time. Additionally, the pellets were quite large in size (approximately 1-1.5 cm in diameter) relative to the animal and although they were implanted dorsally below the scapulae, the pellets moved over time and were often localized to the sides of the animal soon after surgery. This prompted scratching, resulting in irritation and inflammation around the pellet. In light of these observations and the lack of excision in the CNS, we proceeded to test the efficacy of IP injections of tamoxifen.

3.1.3 Intraperitoneal injection of tamoxifen

In optimizing the tamoxifen administration with IP injections, 3 different regimens were tested: (1) injection of 200 mg/kg/day for 5 consecutive days; (2) injection of 200 mg/kg for 21 days; and (3) injection of 100 mg/kg for 19 days. Protein analysis was conducted 4 weeks following the last injection in all paradigms.

We began testing recombination efficiency by tamoxifen injections with a previously published regimen of 200 mg/kg tamoxifen per day for 5 consecutive days, which was shown to result in near-complete recombination in the brain and peripheral tissues with the Cre-ERT2 transgene (Ruzankina et al., 2007). Treatment of *iC6* mice with this regimen and analysis of C6 protein levels 4 weeks post-injection revealed recombination was limited to the periphery and did not occur in the CNS. No significant reduction in C6 protein expression was observed in cortical or striatal tissues, while C6 levels were reduced by approximately 75% in the spleen and by 95% in the liver (Figure 3.4).

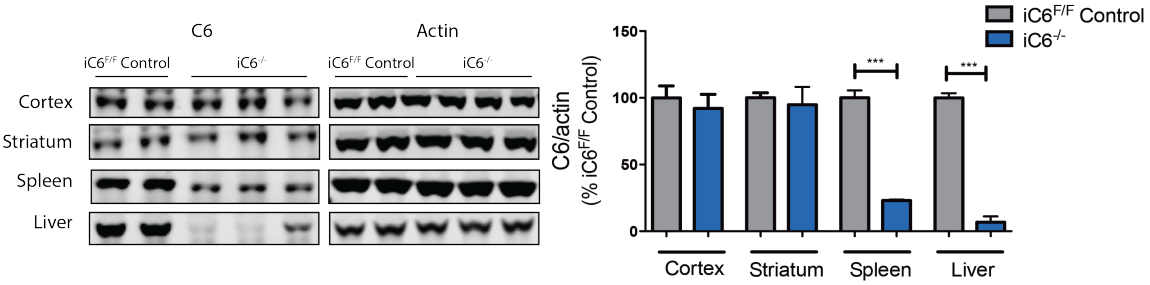

Figure 3.4: Extent of *C6* deletion obtained following intraperitoneal injection of tamoxifen at 200 mg/kg for 5 days. Western blot analysis of C6 protein levels and corresponding quantification of cortex, striatum, spleen and liver tissues assessed 4 weeks following intraperitoneal injection of 200 mg/kg/day tamoxifen for 5 consecutive days. C6 protein expression was quantified relative to actin expression and graphed as a percent of *iC6$^{F/F}$* control (N=2-3, unpaired two-tailed t-test; * p<0.05, ** p<0.01, *** p<0.001).

While this was the greatest extent of deletion observed thus far in peripheral tissues, recombination was still not observed in brain tissues. Further evidence that this particular protocol does in fact result in excision in the CNS came from another member of our lab who was also working with an inducible floxed mouse model, the *huntingtin-interacting protein 14* inducible mouse (*Hip14$^{F/F}$*) on the

same FVB/NJ genetic background and using the same Cre-ERT2 transgene. This identical protocol in the *Hip14*$^{F/F}$ mouse resulted in 90-95% deletion in all brain and peripheral tissues without overt toxicity (Shaun Sanders, unpublished data). With all other experimental conditions seemingly identical, we suspected that the lack of excision observed in the iC6 model was due to the original vector design.

It has been reported that the recombination efficiency of Cre decreases with increasing genetic distance between loxP sites (Coppoolse et al., 2005; S.-Z. Wang et al., 2009; B. Zheng et al., 2000). The loxP sites are ~6.5 kb apart in the *iC6* mouse, while distances of 1-3 kb are most commonly used (Coppoolse et al., 2005; B. Zheng et al., 2000). This suspicion is corroborated by the fact that the loxP sites in the *Hip14* mouse model are located ~1.1 kb apart. Thus, in order to increase recombination in the existing *iC6* model, it was decided to continue this treatment paradigm at the same dose but for an extended period of time for up to 28 days, a previously published strategy (Turlo et al., 2010). However, following the seventh consecutive day of injections, the mice exhibited severe signs of toxicity and sickness and several animals had to be euthanized as they had reached humane endpoints. We halted tamoxifen injections following day 7 to allow the mice to recover and subcutaneous fluids of 0.9% saline were administered to assist in recovery. Following two days of recovery and fluids, most of the animals had not improved and their health conditions were deteriorating; thus, I decided to cease testing of this protocol.

I next settled on a dosing protocol of 100 mg/kg/day for 19 days, which has been optimized in a similar setting for achieving global deletion particularly in the brain (Huda Zoghbi, personal communication). This third protocol showed minimal toxicity and C6 protein analysis of these mice revealed approximately 40-60% deletion in the cortical, striatal, hippocampal and cerebellar tissues and 80-95% deletion in the spleen, liver and muscle tissues (Figure 3.5A). RT-qPCR analysis for C6 mRNA expression was also conducted on brain tissues and revealed a 40-60% reduction in mRNA expression corresponding well to the protein data (Figure 3.5B).

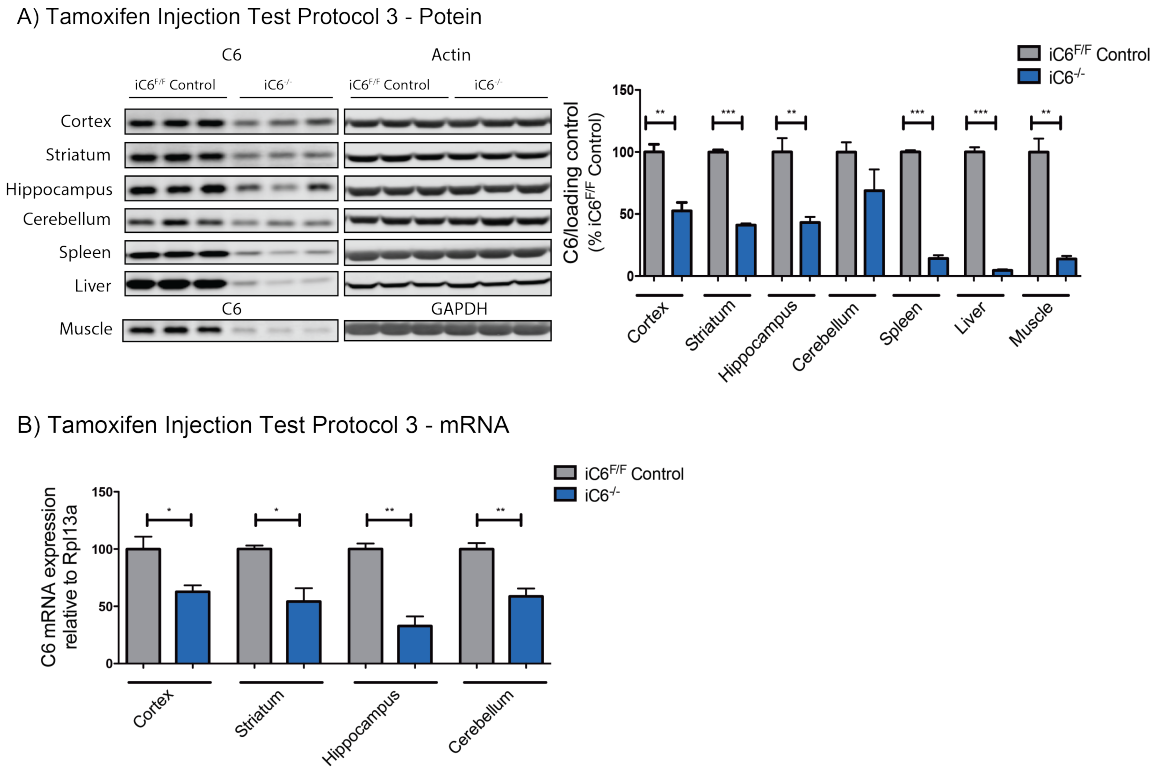

Figure 3.5: Extent of *C6* deletion obtained following intraperitoneal injection of tamoxifen at 100 mg/kg for 19 days. A) Western blot analysis of C6 protein levels and corresponding quantification of cortex, striatum, hippocampus, cerebellum, spleen, liver and muscle tissues assessed 4 weeks following intraperitoneal injection of 100 mg/kg/day tamoxifen for 19 consecutive days. B) C6 transcript levels in brain tissues as assessed by RT-qPCR reveal corresponding reductions in mRNA. C6 protein expression was quantified relative to actin or GAPDH expression, while C6 transcript levels were quantified relative to Rpl13a and graphed as a percent of *iC6$^{F/F}$* control (N=2-3, unpaired two-tailed t-test; * p<0.05, ** p<0.01, *** p<0.001).

An additional test cohort was repeated with the same tamoxifen administration protocol to confirm results (data not shown) and consistent levels of deletion were observed. With levels of deletion hovering at 50% in the brain and 90% in the periphery, this dosing regimen was superior to all other protocols tested. Additionally, the therapeutic modulation of C6 activity in a human clinical context, a situation I was attempting to mimic, would likely not be complete. I thus proceeded with the characterization of the effects of partial C6 deletion on HD phenotypes in the YAC128 mouse.

3.2 INFLUENCE OF LOXP SITES ON CASPASE-6 EXPRESSION

WT (+/+), heterozygous (+/F) and homozygous floxed (F/F) littermates were collected and tissues analyzed for C6 expression. Western blot analysis revealed no changes in C6 protein expression in cortex, liver and muscle of heterozygous or homozygous samples compared to WT (Figure 3.6A, E, and G respectively). Interestingly, we found an increase in C6 protein expression in the striatum of homozygous floxed mice (Figure 3.6B) and a decrease in protein expression in hippocampus, cerebellum and spleen (Figure 3.6C, D and F, respectively) suggesting that the insertion of loxP sequences resulted in certain region-specific changes in C6 protein expression, a caveat that should be kept in mind in the interpretation of experimental results.

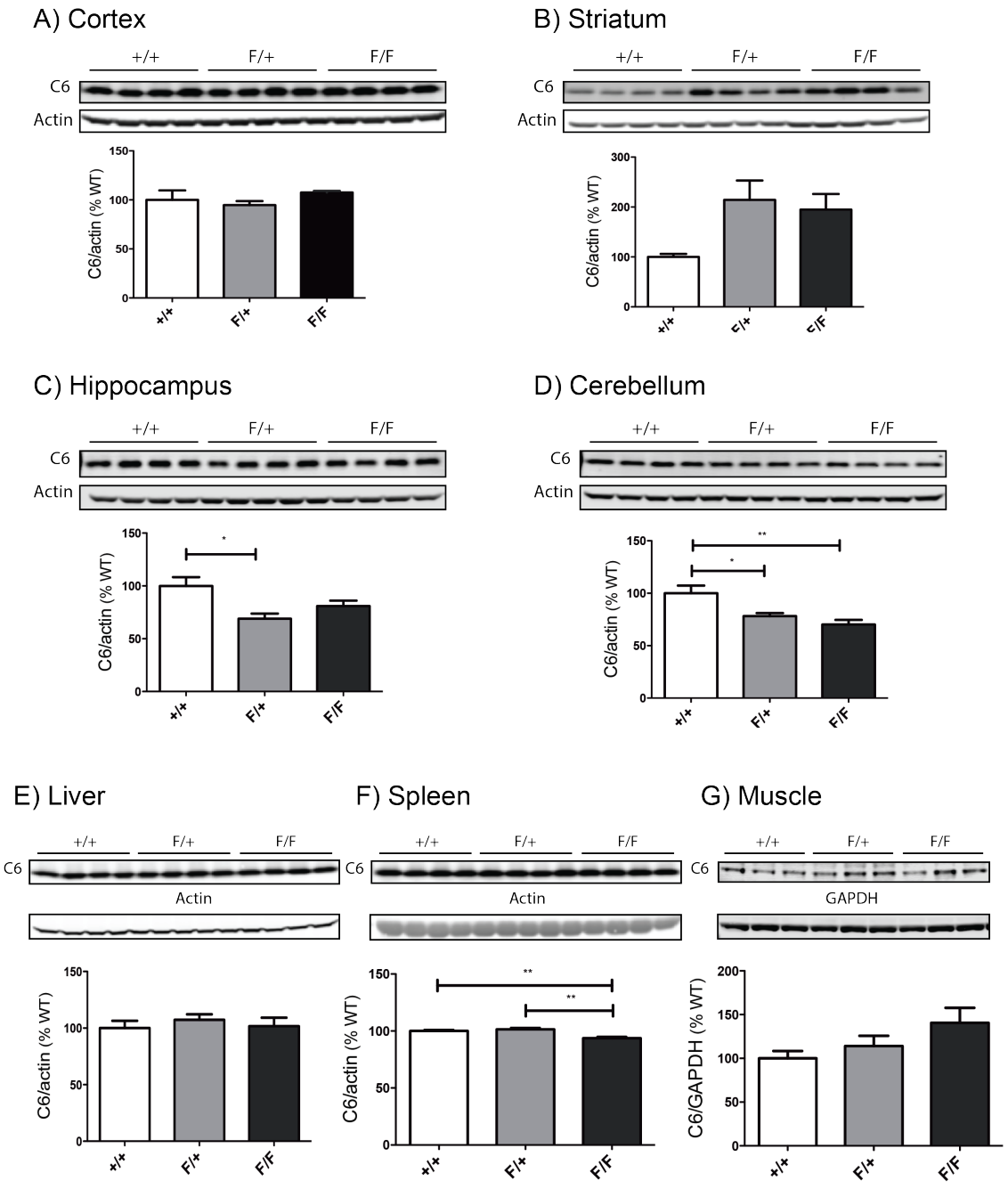

Figure 3.6: Region-specific changes in C6 protein expression as a result of the insertion of loxP sequences. Brains were microdissected and peripheral tissues harvested from WT, heterozygous and homozygous floxed mice and samples were subject to western blot analysis. Quantification of C6 protein revealed no change in protein expression in cortex (A: 1-way ANOVA: $F(2,9)=1.09$, $p=0.3752$; N=4), an increase in the striatum(B: 1-way ANOVA: $F(2,9)=4.43$, $p=0.0457$; N=4), a decrease in the hippocampus (C: 1-way ANOVA: $F(2,9)=6.08$, $p=0.0213$; N=4) and cerebellum (D: 1-way ANOVA: $F(2,9)=8.79$, $p=0.0077$; N=4), no change in the liver (E: 1-way ANOVA: $F(2,9)=0.365$,

p=0.7039; N=4), a decrease in the spleen (F: 1-way ANOVA: $F(2,9)=13.32$, *p*=0.0020; N=4) and no change in the muscle (G: 1-way ANOVA: $F(2,9)=2.56$, *p*=0.1317; N=4). All data was normalized to the average of WT (+/+) samples. * $p<0.05$, ** $p<0.01$. *** $p<0.0001$. Asterisks refer to significant differences following post-hoc analysis.

3.3 EXTENT OF *CASPASE-6* DELETION OBTAINED POST-TAMOXIFEN TREATMENT

Western blot analysis was conducted in the naïve cohort at 12 months to assess C6 protein expression. In the hippocampus, lung and spleen C6 protein levels were reduced by 50-60% and by 95% in the liver compared to $iC6^{F/F}$ controls. However, the reduction in C6 observed in the cortex, striatum and muscle tissues was less than that observed in the initial trial cohorts tested with the same protocol during the optimization of tamoxifen treatment. Protein expression in the $iC6^{-/-}$ cortex was not significantly different from $iC6^{F/F}$ controls and was reduced by 25% in the striatum and 60% in the muscle (Figure 3.7).

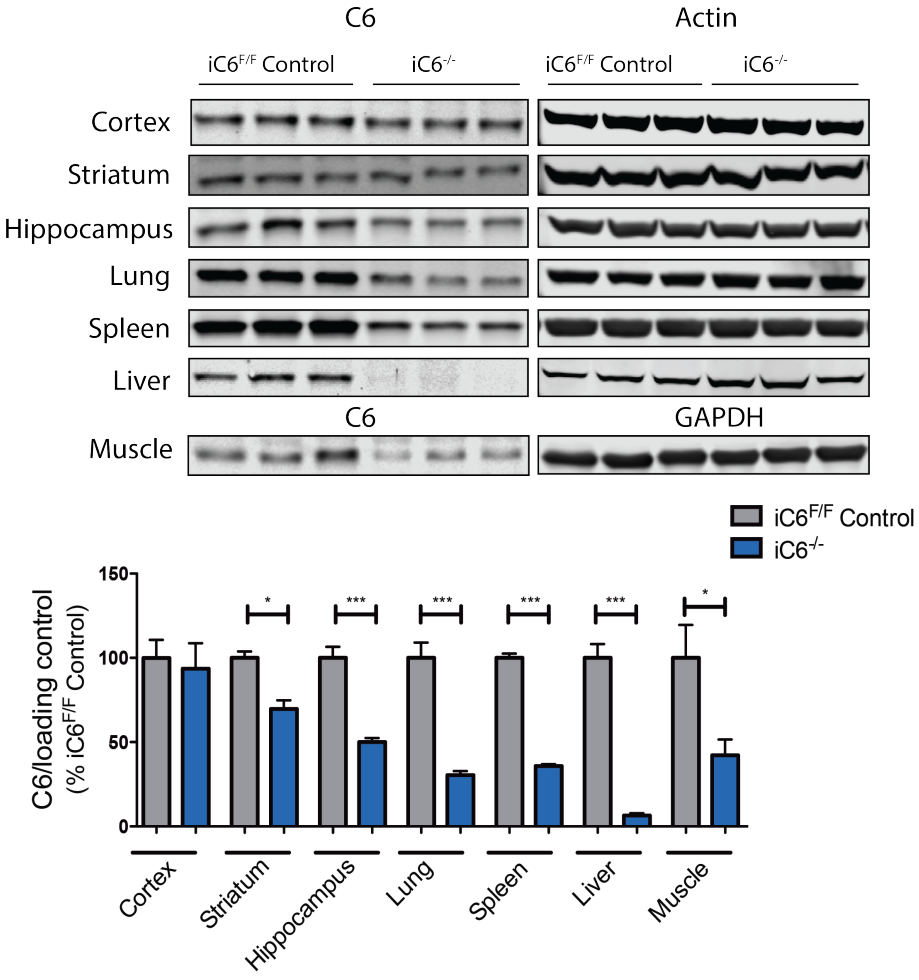

Figure 3.7: Extent of *C6* deletion in 12-month brain and peripheral tissues. Western blot analysis of C6 protein levels and corresponding quantification of cortex, striatum, hippocampus, cerebellum, spleen, liver and muscle tissues assessed at 12 months (~10 months following tamoxifen injection). C6 protein expression was quantified relative to actin or GAPDH expression and graphed as a percent of $iC6^{F/F}$ control (N=6-10, unpaired two-tailed t-test; * $p<0.05$, ** $p<0.01$, *** $p<0.001$).

3.4 NEUROPATHOLOGICAL PHENOTYPES

3.4.1 Brain weights

Assessment of neuropathology was conducted at 12 months and whole brain, forebrain and cerebellar weights were determined. Interestingly, partial loss of *C6* resulted in decreased whole brain, forebrain weight and unchanged cerebellar

weight, compared to WT controls (Figure 3.8A-C, respectively). The reduction in whole brain and forebrain weights was also observed in *iC6*$^{F/F}$;YAC128 control mice, consistent with previous findings (Slow et al., 2003; Van Raamsdonk et al., 2005a).

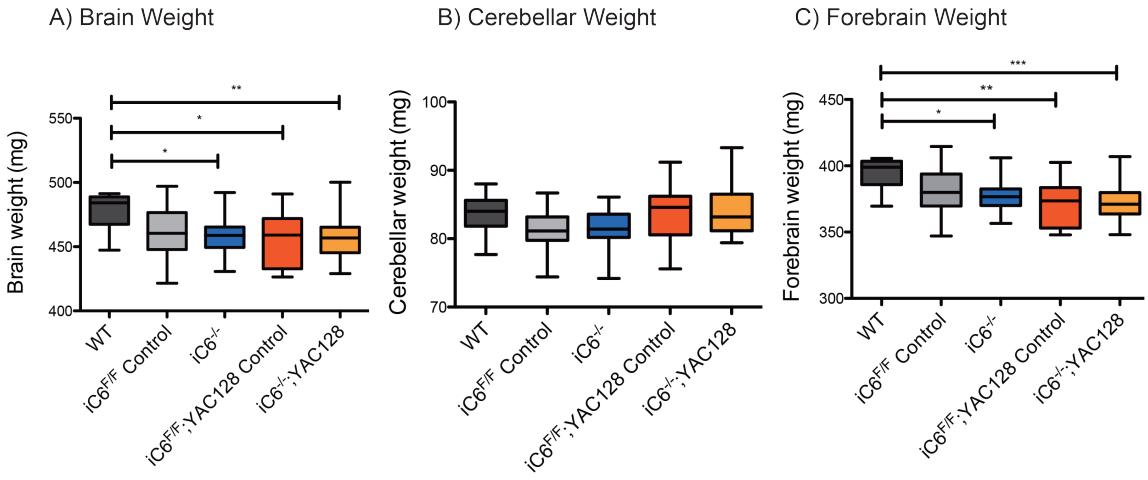

Figure 3.8: Partial loss of *C6* results in reduced whole brain and forebrain weight. Mice were perfused after which brains were removed and weighed. *iC6*$^{-/-}$ mice have decreased brain weight compared to control mice (A; 1-way ANOVA: $F(4,85)=4.09$, $p=0.0044$; N=15-22), unchanged cerebellum weight (B; 1-way ANOVA: $F(4,87)=4.16$, $p=0.0039$; N=15-22), and reduced forebrain weight (C; 1-way ANOVA: $F(4,87)=5.78$, $p=0.0004$; N=15-22). * p<0.05, ** p<0.01, *** p<0.001. Asterisks refer to significant differences following post-hoc analysis.

3.4.2 Volumetric measurements

Perfused brains were then sectioned and stained with a neuronal marker and structural volumes were determined by stereology. YAC128 mice have reduced striatal volume compared to WT controls, reflecting a loss of MSNs (Slow et al., 2003; Van Raamsdonk et al., 2005a; 2007c). This finding is reproduced here in *iC6*$^{F/F}$;YAC128 controls and partial loss of C6 does not prevent this striatal volume loss (Figure 3.9A). There were no genotypic differences observed for cortical volume (Figure 3.9B) and interestingly, partial loss of C6 resulted in reduced corpus callosum volume (Figure 3.9C).

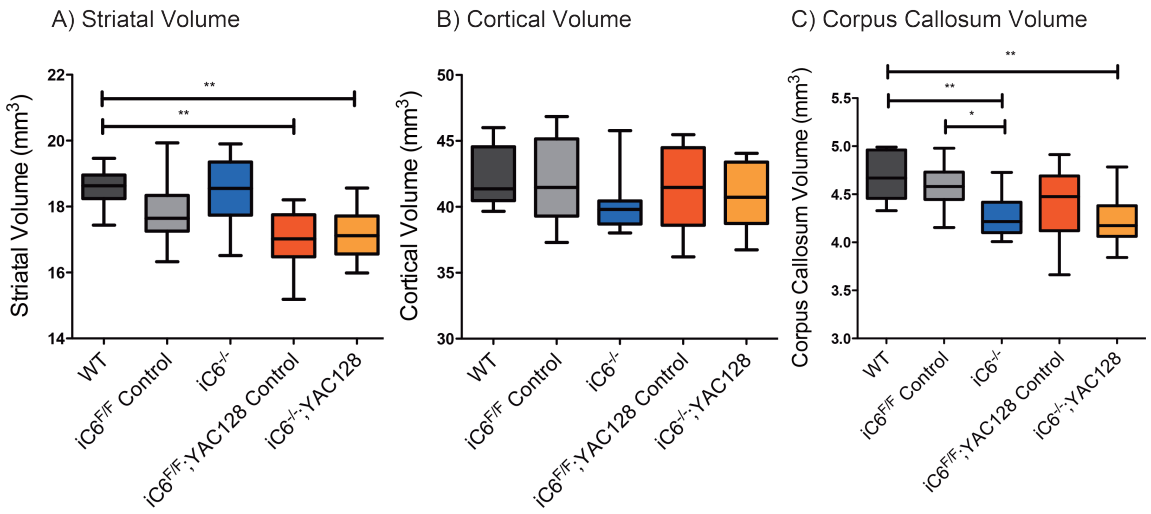

Figure 3.9: Partial loss of C6 does not prevent striatal volume loss and results in reduced corpus callosum volume. Perfused brains were sectioned, stained with NeuN and volumes assessed by stereology. Partial loss of C6 does not prevent striatal volume loss in YAC128 mice (A; 1-way ANOVA: $F(4,54)=7.62$, $p<0.0001$; N=8-13), and has no effect on cortical volume (B; 1-way ANOVA: $F(4,54)=1.09$, $p=0.3694$; N=8-13). Partial loss of C6 results in reduced corpus callosum volume (C; 1-way ANOVA: $F(4,54)=6.12$, $p=0.0004$; N=8-13). * p<0.05, ** p<0.01, *** p<0.001. Asterisks refer to significant differences following post-hoc analysis.

3.5 BEHAVIOURAL ASSESSMENT

Extensive characterization of YAC128 mice has revealed that these mice exhibit a number of behavioural abnormalities (Graham et al., 2006; Slow et al., 2003; Southwell et al., 2009; Van Raamsdonk et al., 2007a; 2005c). Inducible *C6* deficient mice were tested for motor, cognitive and psychiatric function to determine if partial loss of C6 alters these behavioural phenotypes.

3.5.1 Motor function assessment

It has long been noted that YAC128 mice have progressive motor dysfunction, as demonstrated by a decrease in the latency to fall from an accelerating rotarod (Graham et al., 2006; Slow et al., 2003; Southwell et al., 2009; Van Raamsdonk et al., 2007a; 2005c). This accelerating rotarod task is often used as a primary readout for motor function but also involves cognitive capacity to adapt to the increasing speed of the rotarod. Inducible *C6* deficient mice were trained on the fixed-speed rotarod at 3 months of age and longitudinally tested on the

accelerating rotarod every 3 months. The characteristic and progressive rotarod deficit is observed in *iC6*$^{F/F}$;YAC128 control mice and the latency to fall from the accelerating rotarod is not improved in YAC128 mice with partial loss of C6 compared to WT controls (Figure 3.10).

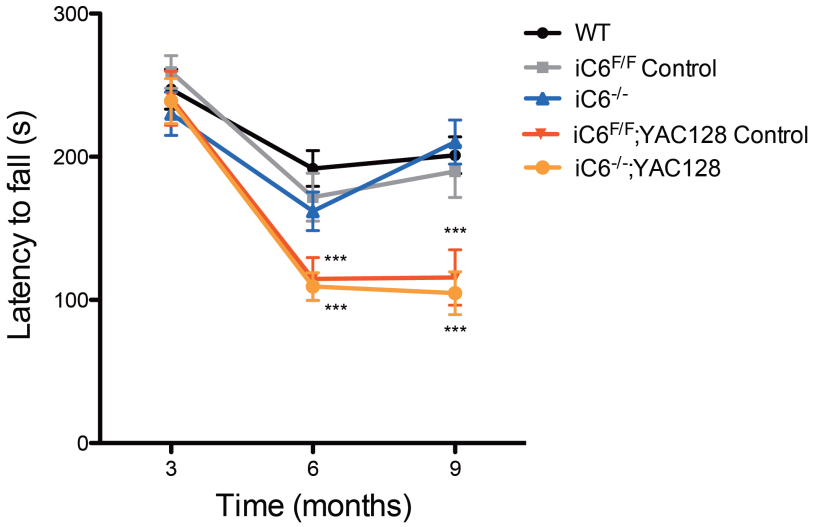

Figure 3.10: Partial loss of C6 does not improve motor dysfunction on the accelerating rotarod. Inducible C6 deficient mice were tested longitudinally on the accelerating rotarod at 3-month intervals to assess motor function. Partial loss of C6 does not improve rotarod performance in YAC128 mice compared to WT (A; 2-way ANOVA: genotype $F(4)=10.37$, $p<0.0001$; time $F(2)=25.09$, $p<0.0001$; interaction $F(8)=5.42$, $p=0.0024$; N=18-20). * p<0.05, ** p<0.01, *** p<0.001. Asterisks refer to significant differences compared to WT following post-hoc analysis.

As the rotarod test is a trained, forced assessment of motor function, it is considered less sensitive to basal ganglia dysfunction than a spontaneous, voluntary test for motor ability such as climbing behaviour (Hickey et al., 2008; Southwell et al., 2009). Previous studies have shown that YAC128 mice display a climbing deficit (Southwell et al., 2009) and this climbing test was conducted on inducible *C6* deficient mice. No improvement in climbing behaviour was observed with partial loss of C6 in YAC128 mice (Appendix Figure S1).

3.5.2 Cognitive function by fixed speed rotarod training

Cognitive dysfunction is a feature observed both in HD patients (Duff et al., 2007; Paulsen, 2011; Paulsen et al., 2001) as well as in mouse models of HD

(Menalled et al., 2009; Southwell et al., 2009; Van Raamsdonk et al., 2005c). Cognitive function can be assessed with several behavioural tests, including the fixed-speed training phase of the rotarod test (Pouladi et al., 2012; Shiotsuki et al., 2010; Van Raamsdonk et al., 2005c). Mice are placed on the rotarod for 120 seconds at a constant speed for three consecutive days and the latency to fall as well as the number of falls are recorded as measures of motor learning. YAC128 mice have been shown to have a reduced latency to fall and a greater number of falls compared to WT, indicating a deficit in motor learning (Pouladi et al., 2012; Van Raamsdonk et al., 2005c). This impairment is more pronounced on the first day of training, and previous studies have shown that when WT and YAC128 mice are trained at 2 months of age, their ability to stay on the rotarod during the training phase improves to WT levels by day 3, suggesting they are capable of learning this motor task eventually but at a slower rate than their WT counterparts (Van Raamsdonk et al., 2005c).

Rotarod training on inducible C6 deficient mice reveals that YAC128 mice with partial loss of C6 fall just as quickly (Figure 3.11A) and as many times (Figure 3.11B) as their YAC128 counterparts, suggesting that partial loss of C6 does not ameliorate the motor learning deficit at 3 months.

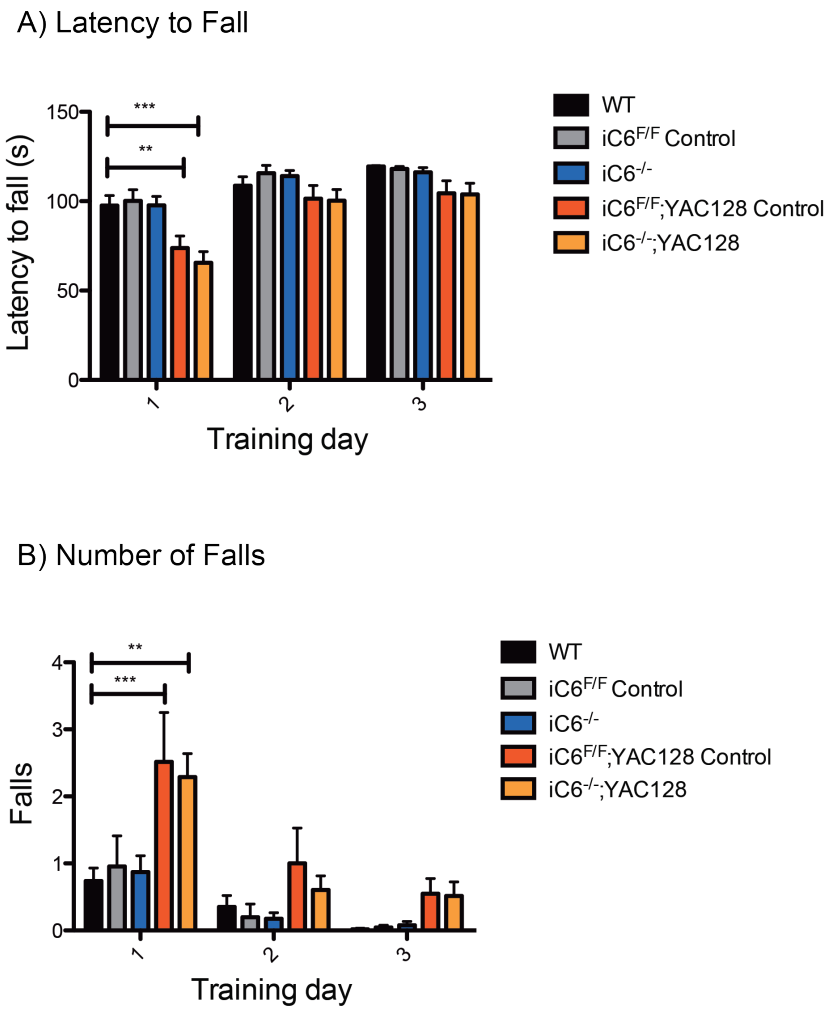

Figure 3.11: Partial loss of C6 does not improve motor learning on the fixed speed rotarod. Inducible *C6* deficient mice were trained on a non-accelerating rotarod for 3 consecutive days at 3 months of age to assess their ability to learn a motor task. Partial loss of C6 results in similar latencies to fall (A; 2-way ANOVA: training day $F(2)=15.75$, $p<0.0001$; genotype $F(4)=10.58$, $p=0.0003$; interaction $F(8)=2.15$, $p=0.0527$; N=19-22) and numbers of falls (B; 2-way ANOVA: training day $F(2)=11.70$, $p<0.0001$; genotype $F(4)=7.46$, $p=0.0064$; interaction $F(8)=2.47$, $p=0.0414$; N=19-22), demonstrating a motor learning deficit not different from YAC128 controls. * p<0.05, ** p<0.01, *** p<0.001. Asterisks refer to significant differences following post-hoc analysis.

Assessment of cognitive function was complemented with the novel object location and novel object preference tests to assess spatial learning and novel object learning, respectively. YAC128 mice demonstrate deficits in both of these tasks beginning at 7 months of age (Southwell et al., 2009). Inducible *C6*

deficient mice were tested for these phenotypes at 9 months of age, however the deficits in YAC128 mice could not be reproduced and thus the effect of partial loss of C6 could not be assessed in this paradigm (Appendix Figure S2).

3.5.3 Psychiatric assessment

Psychiatric disturbances such as anxiety, depression and apathy have been observed in HD patients (Dale and van Duijn, 2015; Duff et al., 2007; Paulsen et al., 2001) as well as HD mouse models (Menalled et al., 2009; Southwell et al., 2009). Several studies have shown that YAC128 mice display psychiatric deficits such as increased anxiety-like behaviour (Menalled et al., 2009; Southwell et al., 2009) as well as anhedonia and depressive behaviour (Pouladi et al., 2009). Modulation of C6 by constitutive genetic deletion in YAC128 mice and peptide-mediated inhibition in BACHD mice has shown to improve these phenotypes (Aharony et al., 2015; B. K. Y. Wong et al., 2015).

Thus, inducible *C6* deficient mice were tested for anxiety-like behaviour using the open field test at 3 months and the elevated plus maze test at 9 months of age. In the open field test, mice are placed in a large, brightly-lit box and anxious mice including YAC128 mice will spend less time in the center and cross the center space less frequently than WT mice (Southwell et al., 2009). To ensure all mice are equally active and exploring the apparatus, the total distance travelled was computed and no genotypic differences were seen (Figure 3.12A). *iC6*$^{F/F}$;YAC128 control mice enter the center less frequently than WT and YAC128 mice partially lacking C6 show a trend toward entering the center of the field more often, though this is not statistically significant (Figure 3.12B).

In parallel, mice can be tested for anxiety-like behaviour using the elevated plus maze. This test involves placing the mouse in the center of a plus maze located above the ground with two open arms and two closed arms. Anxious mice will spend less time exploring the open arms (Southwell et al., 2013). No genotypic differences in distance travelled were observed (Figure 3.12C) and while *iC6*$^{F/F}$;YAC128 expectedly spent significantly less time in the open arms, YAC128 mice partially lacking C6 spent a greater proportion of their time in the open arms

and were not statistically different from WT by post-hoc analysis (Figure 3.12D), suggesting a trend toward improvement in anxiety-like behaviour.

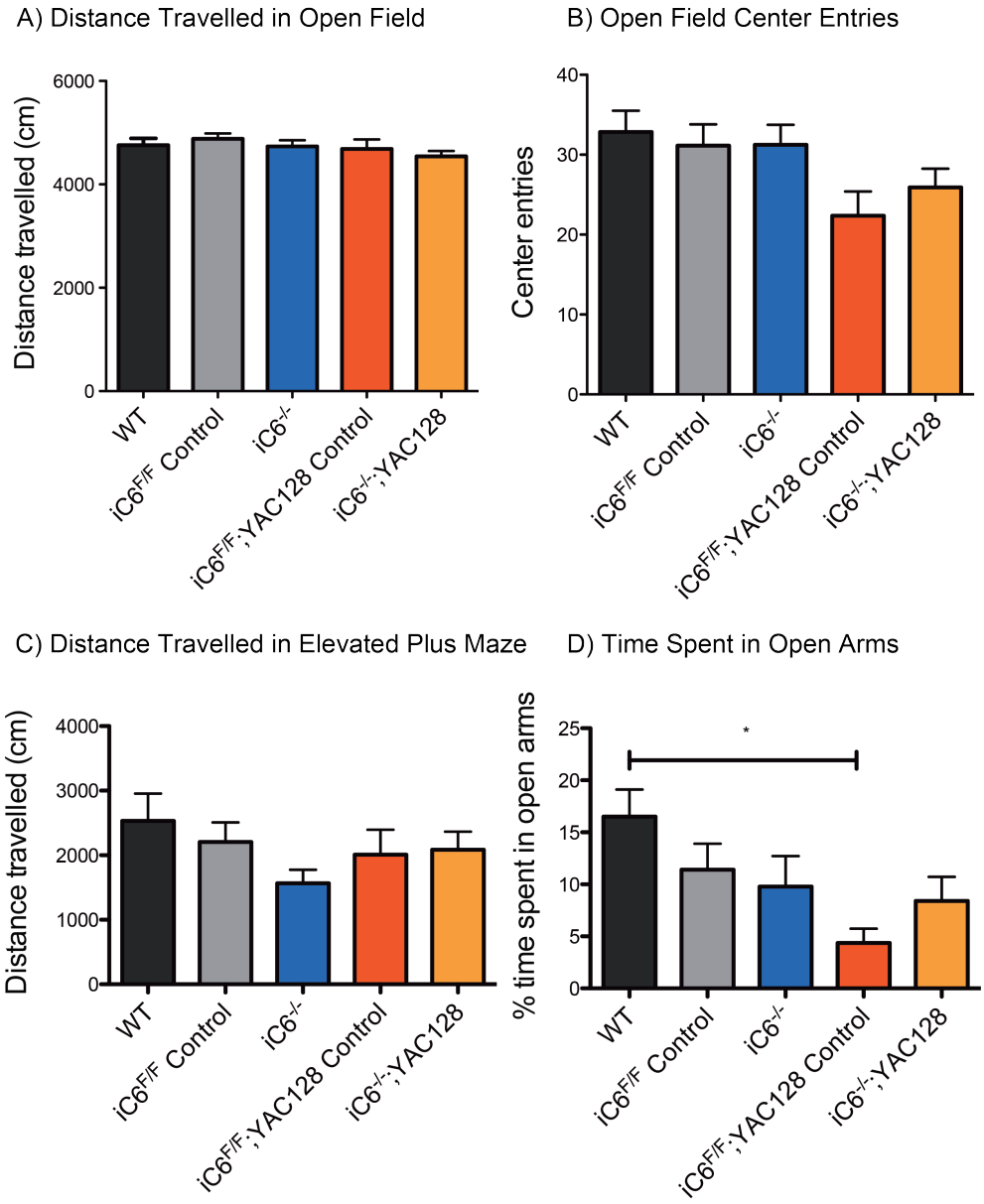

Figure 3.12: Partial loss of C6 results in mild improvement of anxiety phenotypes in YAC128 mice. Inducible *C6* deficient mice were tested for anxious behaviour in the open field and elevated plus maze. While all mice travelled similar distances (A, 1-way ANOVA: $F(4,99)=0.948$, $p=0.4395$; N=19-22), YAC128 mice partially lacking C6 show a trend toward increased center entries (B; 1-way ANOVA: $F(4,99)=2.69$, p=0.0357; N=19-22). In the elevated plus maze, no differences were observed in distance travelled (C; 1-way ANOVA: $F(4,93)=1.35$, p=0.2577; N=19-22), while *iC6$^{-/-}$;*YAC128 mice spent more time in the open arms compared to YAC128 controls (D; 1-way ANOVA: $F(4,99)=2.92$,

p=0.0255; N=19-22). * p<0.05, ** p<0.01, *** p<0.001. Asterisks refer to significant differences following post-hoc analysis.

Affective behaviours such as anhedonia and depression can also be modeled in rodents. The sucrose preference test is an assessment of anhedonia, or lack of pleasure-seeking behaviour. In this test, mice are given access to two bottles, one of which contains water and the other contains a 2% sucrose solution. WT mice will prefer to drink the sweet sucrose solution over the water, but this is not the case in YAC128 mice, who show a reduced preference for sucrose (Pouladi et al., 2009). Inducible *C6* deficient mice were exposed to both bottles for a 24-hour period and while *iC6*$^{F/F}$;YAC128 consumed less sucrose than WT mice, *iC6*$^{-/-}$;YAC128 mice consumed more sucrose than YAC128 control mice (Figure 3.13A). In order to ensure the reduced sucrose intake is not a reflection of reduced overall fluid intake, total fluid consumed was measured and no statistical differences were observed between groups despite trends toward reduced total fluid intake in YAC128 animals (Figure 3.14B). However, when sucrose intake is normalized to total fluid intake to determine sucrose preference, the genotypic difference between WT and *iC6*$^{F/F}$;YAC128 mice is lost but the trends remain (Figure 3.13C).

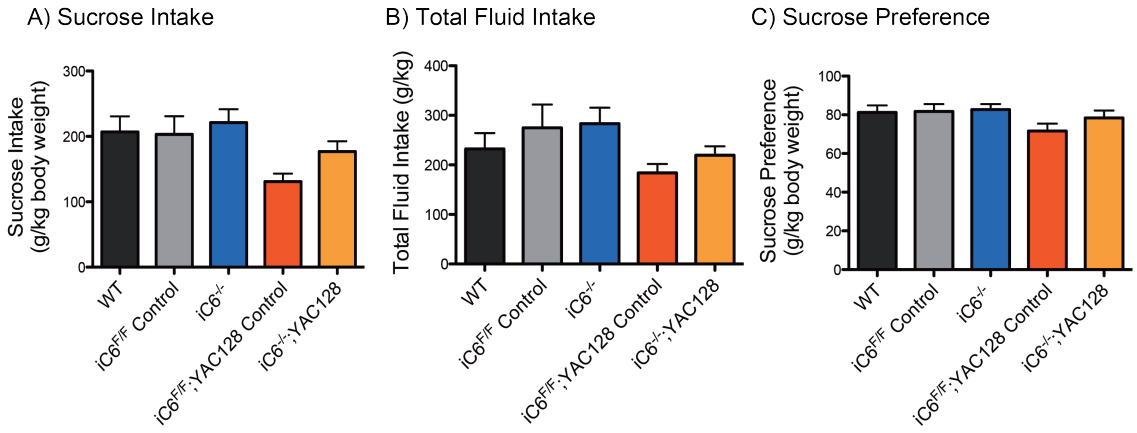

Figure 3.13: *iC6*$^{-/-}$;YAC128 mice consume more sucrose than *iC6*$^{F/F}$;YAC128 mice. Inducible *C6* deficient mice were tested for anhedonic behaviour using the sucrose preference test. YAC128 mice partially lacking C6 display increased sucrose consumption (A, 1-way ANOVA: $F(4,83)=3.04$, $p=0.0218$; N=17-19). No significant differences were observed in total fluid intake (B; 1-way ANOVA: $F(4,41)=1.65$, $p=0.1797$; N=17-19). When intake is normalized to total fluid

intake, genotypic differences in sucrose preference are lost (C; 1-way ANOVA: $F(4,84)=1.52$, $p=0.2034$; N=17-19). * p<0.05, ** p<0.01, *** p<0.001.

Mice were also tested for depressive-like behaviour using the Porsolt forced swim test. Mice are placed in a cylinder containing water and the time they spend not swimming, or immobile, is measured. YAC128 mice spend significantly more time immobile than WT mice beginning at 3 months of age, suggesting depressive-like behaviour (Pouladi et al., 2009). Inducible *C6* deficient mice were tested for this phenotype at 9 months of age and the WT/YAC128 difference could not be reproduced; however, there was a significant increase in immobility time in *iC6*$^{-/-}$;YAC128 mice, suggesting these mice are not be protected from the depression phenotype (Appendix Figure S3).

Another assessment of affective behaviour is the splash test, which measures the motivation to groom. A viscous sucrose solution is sprayed on the fur coat of the mouse and the amount of time spent grooming is recorded. HD knock-in mice have been shown to spend less time grooming compared to their WT counterparts at 14 weeks of age (Orvoen et al., 2012; Pla et al., 2014). Inducible *C6* deficient mice were tested for grooming behaviour at 12 months of age and these findings could not be reproduced in our YAC128 cohort and therefore the effects of partial loss of C6 on this phenotype could not be assessed (Appendix Figure S4).

3.6 PERIPHERAL PHENOTYPES

Peripheral phenotypes have been well documented in HD patients (Ribchester et al., 2004; Sassone et al., 2009; van der Burg et al., 2009; Zielonka et al., 2014) and several signs of peripheral pathology has been observed in mouse models of HD (Björkqvist et al., 2008; Carroll et al., 2015; Ehrnhoefer et al., 2014; Magnusson-Lind et al., 2014; Pouladi et al., 2010; Träger et al., 2014a). Given that the extent of deletion is greatest in peripheral tissues, we aimed to characterize the impact of loss of *C6* on peripheral phenotypes.

3.6.1 Body weight changes

YAC128 mice, along with several full-length transgenic mouse models of HD, gain a significant amount of body weight compared to WT mice (Gray et al., 2008; Pouladi et al., 2010; Southwell et al., 2013; Van Raamsdonk et al., 2006a). It has been demonstrated that the presence of HTT influences body weight by modulating the insulin-like growth factor 1 (IGF-1) pathway (Pouladi et al., 2010; Van Raamsdonk et al., 2006a). Interestingly, this body weight gain in YAC128 mice is delayed and IGF-1 levels are normalized with the constitutive absence of C6 (B. K. Y. Wong et al., 2015).

Thus, we sought to determine whether body weight was altered in inducible *C6* deficient mice. Mice were weighed daily throughout the tamoxifen injection period and subsequently at 3-month intervals. At 13 weeks of age (~3 months), *iC6*$^{F/F}$;YAC128 female and male mice are expectedly significantly heavier than their WT counterparts, while *iC6*$^{-/-}$;YAC128 females and males are not significantly heavier than control animals (Figure 3.14A-B). However, when body weight is visualized over time including during the tamoxifen injection period, it is apparent that both *iC6*$^{-/-}$ and *iC6*$^{-/-}$;YAC128 mice experience a sharp decline in body weight compared to controls during the injection period, suggesting that this body weight loss occurs as a result of tamoxifen toxicity. However, over time, both male and female mice recover and gain significant body weight comparable to *iC6*$^{F/F}$;YAC128 control mice (Figure 3.14C-D). Thus, this attenuation of body weight gain is only transient and not sustained over time, and is unlikely to be a result of partial loss of C6.

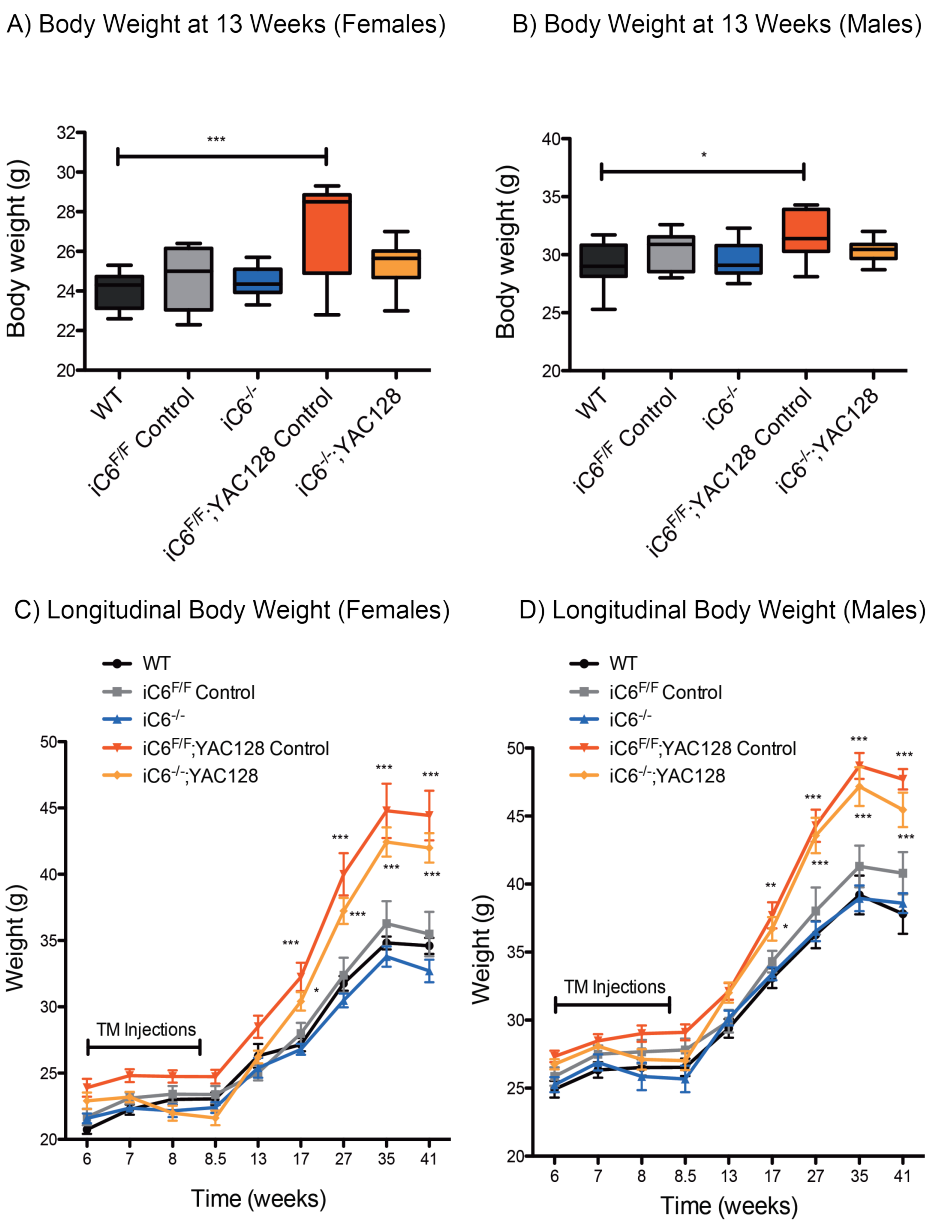

Figure 3.14: *iC6*$^{-/-}$*;*YAC128 mice have transiently reduced body weight not sustained over time. Inducible *C6* deficient mice were weighed throughout the injection period and subsequently at 3-month intervals. YAC128 female and male mice partially lacking C6 do not weigh as much as their YAC128 littermates (A, 1-way ANOVA: $F(4,43)=6.98$, $p=0.0002$; N=9-10) and (B, 1-way ANOVA: $F(4,43)=3.40$, $p=0.0167$; N=9-10), respectively. This effect is transient and longitudinal body weight measurements reveal that *iC6*$^{-/-}$*;*YAC128 female and male mice do eventually gain significant body weight comparable to YAC128 mice (C, 2-way ANOVA: time $F(8)=75.37$, $p<0.0001$; genotype $F(4)=7.95$, $p<0.0001$; interaction $F(32)=5.33$, $p<0.0001$; N=9-10) and (D, 2-way ANOVA: time $F(8)=75.35$, $p<0.0001$; genotype $F(4)=7.22$, $p<0.0001$; interaction $F(32)=3.60$, $p<0.0001$; N=9-10), respectively. * p<0.05, ** p<0.01, *** p<0.001,

Asterisks refer to significant differences compared to WT following post-hoc analysis.

3.6.2 Inflammatory responses

Alterations in inflammation as demonstrated by increased circulating cytokines and hyperactive responses to inflammatory stimuli have been documented in HD patients (Björkqvist et al., 2008; Politis et al., 2015; Wild et al., 2011) and in HD mouse models (Björkqvist et al., 2008; Franciosi et al., 2012; Kwan et al., 2012b; Träger et al., 2014b). Additionally, C6 has been postulated to play a role in mediating the inflammatory response in mice (Baburamani et al., 2015; Berta et al., 2014; Kaushal et al., 2015; Kobayashi et al., 2011; Ye et al., 2013). Therefore we wondered whether the partial deletion of *C6* influenced the hyperactive inflammatory response in YAC128 mice. To that end, alveolar macrophages were isolated and cultured from C6 floxed mice and subjected to stimulation by treatment with control standard endotoxin (CSE), after which the levels of secreted cytokine interleukin-6 (IL-6) were measured. Partial loss of C6 resulted in significantly reduced secretion of IL-6 by macrophages (Figure 3.15A). Basal circulating levels of cytokines IL-6, tumor necrosis factor-alpha (TNF-α) and KC (mouse equivalent of IL-8) were also measured in the serum of 9-month old inducible C6 deficient mice and no differences were found (Figure 3.15B-D), suggesting that C6 may play a more significant role in mediating the inflammatory response to an inflammatory challenge as opposed to under basal conditions.

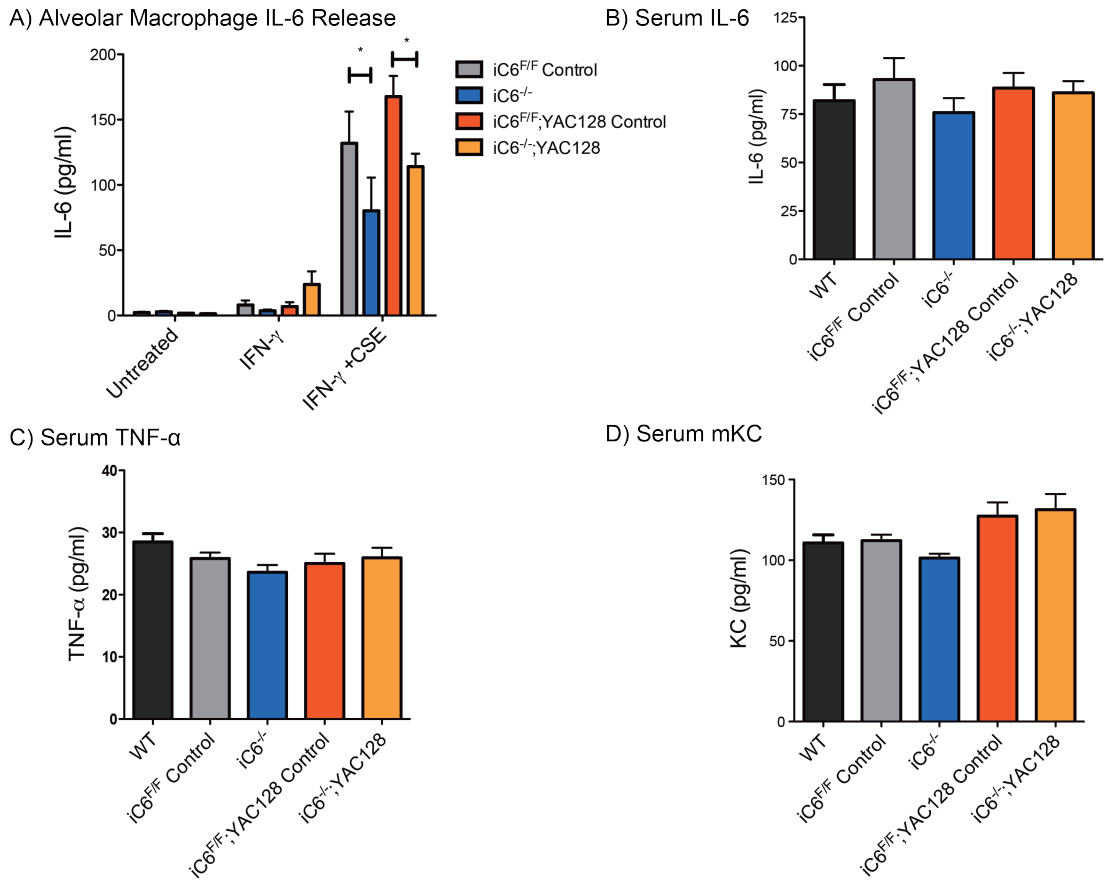

Figure 3.15: Mice partially lacking C6 have reduced responses to inflammatory stimuli but no differences in basal circulating cytokine levels. Alveolar macrophages cultured from inducible *C6* deficient mice show reduced IL-6 release following CSE stimulation (A, 2-way ANOVA: genotype $F(3)=3.29$, $p=0.0453$; treatment $F(2)=70.30$, $p<0.0001$; interaction $F(6)=6.14$, $p=0.0238$; N=5-9). No genotypic differences were observed in serum of 9-month old mice for circulating IL-6 (B, 1-way ANOVA: $F(4,87)=0.618$, $p=0.6505$; N=17-19), TNF-α (C, 1-way ANOVA: $F(4,70)=1.68$, $p=0.1646$; N=15-17) or KC (D, 1-way ANOVA: $F(4,74)=3.18$, $p=0.0181$; N=14-18). * p<0.05, ** p<0.01, *** p<0.001. Asterisks refer to significant differences following post-hoc analysis.

3.6.3 Liver huntingtin protein levels

Hepatic phenotypes have been observed in HD mouse models (Carroll et al., 2015; Chiang et al., 2011) and C6 is highly expressed in human liver (Godefroy et al., 2013). Additionally, C6 has been implicated in mediating the apoptotic response in liver tissue (Rust et al., 2009), and constitutive genetic ablation of C6 results in reduced striatal HTT levels (B. K. Y. Wong et al., 2015). WT and mHTT protein levels were measured in the livers of 12-month old inducible *C6* deficient

mice and the full-length levels of both WT and mHTT were significantly increased in *iC6*$^{-/-}$;YAC128 mice compared to all other genotypes tested (Figure 3.16), suggesting that the absence of C6 influences huntingtin levels in the liver.

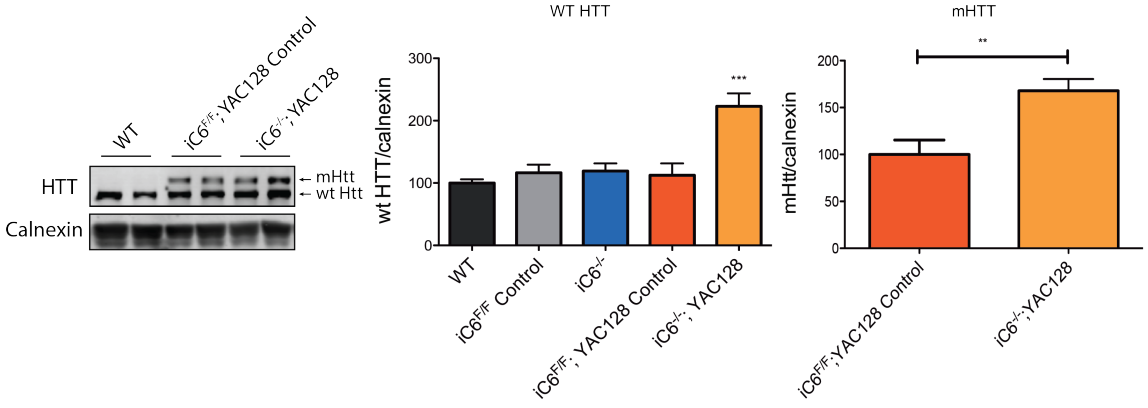

Figure 3.16: *iC6*$^{-/-}$;YAC128 mice have significantly elevated levels of WT and mHTT. Western blot analysis of liver HTT levels show a significant increase in WT compared to all other genotypes (1-way ANOVA: $F(4,37)=12.82$, $p<0.0001$; N=5-10) and mHTT (unpaired two-tailed t-test: $p=0.0021$; N=5-10) in the livers of *iC6*$^{-/-}$;YAC128 mice at 12 months of age. * p<0.05, ** p<0.01, *** p<0.001. Asterisks refer to significant differences following post-hoc analysis.

3.7 SUMMARY OF FINDINGS

Following the optimization of a tamoxifen treatment protocol, 19 consecutive daily IP injections of 100 mg/kg resulted in a partial loss of C6 in the brain ranging between 50-10% loss. In peripheral tissues of experimental animals, C6 levels were reduced by 60-95%. Inducible *C6* deficient mice were assessed for changes in brain structures, behavioural and peripheral phenotypes. Partial loss of C6 resulted in reduced whole brain weight, forebrain weight and corpus callosum volume irrespective of the presence of the YAC128 transgene. In YAC128 mice specifically, partial loss of C6 did not protect against striatal volume loss, motor or cognitive dysfunction. Psychiatrically, a modest improvement in anxiety and anhedonia were observed. This lack of amelioration in HD phenotypes is likely due to incomplete *C6* gene deletion and the observation that C6 levels in brain tissues were only moderately reduced. Characterization of peripheral phenotypes, where the extent of gene deletion is greater, revealed a transient delay in body weight gain in *iC6*$^{-/-}$;YAC128 mice due

to tamoxifen-induced weight loss, an attenuation of IL-6 release from *iC6*$^{-/-}$ and in *iC6*$^{-/-}$;YAC128 macrophages as well as an accumulation of full-length WT and mHTT levels in the liver.

4 EFFECTS OF PEPTIDE-MEDIATED INHIBITION OF CASPASE-6 IN YAC128 MICE

Given the numerous studies highlighting the important pathogenic role of the 586 fragment, significant efforts have been dedicated to investigating ways of preventing its generation. In a study conducted by Aharony and colleagues, a peptide-based approach was devised for inhibiting HTT cleavage at this amino acid site (Aharony et al., 2015). The investigators designed a 24-amino acid peptide, named ED11 – the C-terminal of which mimics the C6 cleavage site in exon 13 of HTT at amino acid 586 and thus acts as a competitive inhibitor for cleavage at that site. The sequence surrounding the IVLD cleavage site was fused to an N-terminal TAT tag to enable cell permeability (Figure 4.1).

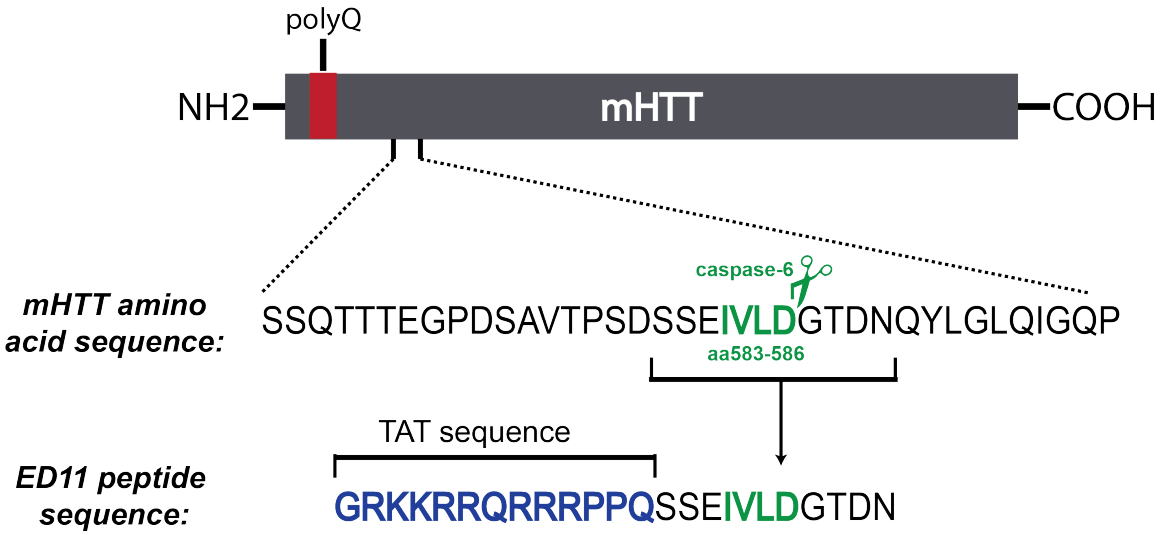

Figure 4.1: ED11 peptide structure. The ED11 24-amino acid peptide was designed to mimic the region surrounding the C6 cleavage site at amino acid 586 of the mHTT protein and fused to a TAT tag to enable cell permeability.

In the study conducted by Aharony and colleagues, the ED11 peptide was administered to pre-symptomatic BACHD mice beginning at 5 weeks of age as well as to post-symptomatic BACHD mice aged to 35 weeks by chronic infusion of 4 mg/kg/day of ED11 using a subcutaneously implanted osmotic pump (Aharony et al., 2015). Treatment of presymptomatic BACHD mice with ED11 resulted in improved motor learning and rotarod performance, partially attenuated

body weight gain, prevention of depressive-like behaviour and an improvement in the anxiety phenotype (Aharony et al., 2015). In the post-symptomatic group, ED11 treatment partially improved rotarod performance, rescued depressive-like behaviour and restored cognitive function in the reversal phase of the swimming T-maze test (Aharony et al., 2015).

In light of the significant attenuation of phenotypes conferred by this peptide in BACHD mice, we sought to assess the impact of ED11 treatment on HD phenotypes in an alternate mouse model of HD, the YAC128 mouse. To that end, WT and YAC128 mice were treated at 6 weeks of age with either saline or 8 mg/kg/day of ED11 using a surgically implanted 28-day release osmotic pump. ED11 treatment continued by pump replacement until 6 months of age and behaviour testing was conducted on a monthly basis starting at 2 months of age until mice were sacrificed at 6 months of age. An additional cohort of mice was collected at 6 months for biochemical assessment. The higher dose of 8 mg/kg/day was used in order to maximize therapeutic efficacy and all other methodological procedures remained the consistent between both studies.

4.1 MOTOR, COGNITIVE AND PSYCHIATRIC ASSESSMENT

Performance on the rotarod test was used as a primary readout for motor function and male BACHD mice treated with 4 mg/kg ED11 per day showed dramatic improvement in rotarod performance compared to controls (Aharony et al., 2015). Longitudinal rotarod testing in YAC128 mice treated with ED11 reveals no improvement in rotarod performance compared to saline-treated YAC128 controls (Figure 4.2).

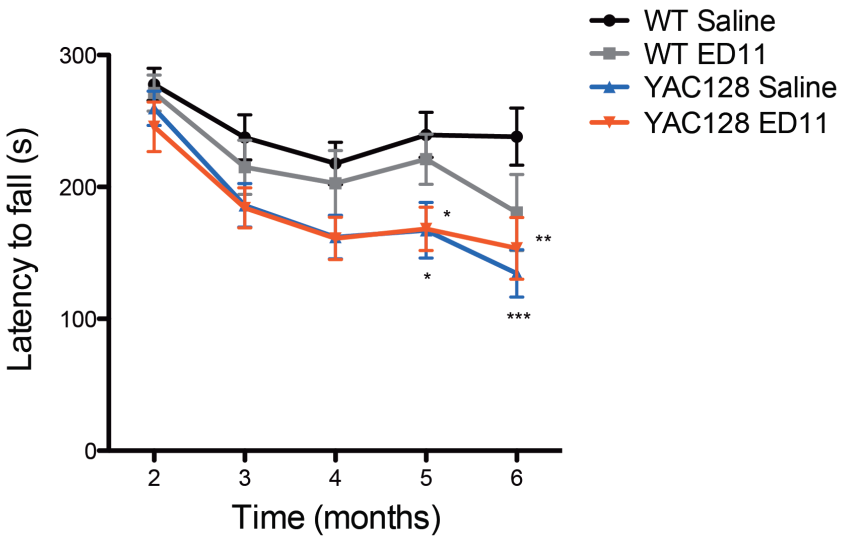

Figure 4.2: ED11-treated YAC128 mice are not protected from rotarod deficits. WT and YAC128 mice were treated with saline or 8 mg/kg/day beginning at 6 weeks of age until 6 months of age, during which they were tested on the rotarod each month. YAC128 mice treated with ED11 are not protected from the rotarod deficit (2-way RM ANOVA: time $F(4)=14.10$, $p<0.0001$; treatment group $F(3)=10.20$, $p=0.0130$; subjects (matching) $F(56)=48.48$, $p<0.0001$; interaction $F(12)=1.77$, $p=0.2287$; N=14-16). * p<0.05, ** p<0.01, *** p<0.001. Asterisks refer to significant differences compared to WT following post-hoc analysis.

As sex-specific differences were observed in the rotarod performance of BACHD mice, longitudinal rotarod data for YAC128 mice was separated by sex and no improvements in performance were observed in either sex (data not shown). Mice were also tested for voluntary motor activity using the climbing apparatus at 4 months and ED11-treated YAC128 mice had comparable latencies to climb, total time spent climbing and number of climbing events as saline-treated YAC128 mice (Appendix Figure S5 A-C), suggesting ED11 treatment did not have an effect on motor function as assessed by rotarod and climbing tests.

Motor learning was assessed during the training phase on the rotarod apparatus at 2 months of age. Both saline-treated and ED11-treated YAC128 mice display deficits in motor learning as they had comparable latencies to fall (Figure 4.3A) and a greater number of falls from the rotarod compared to both WT groups

(Figure 4.3B), suggesting treatment with ED11 did not confer protection against motor learning deficits.

A) Latency to Fall

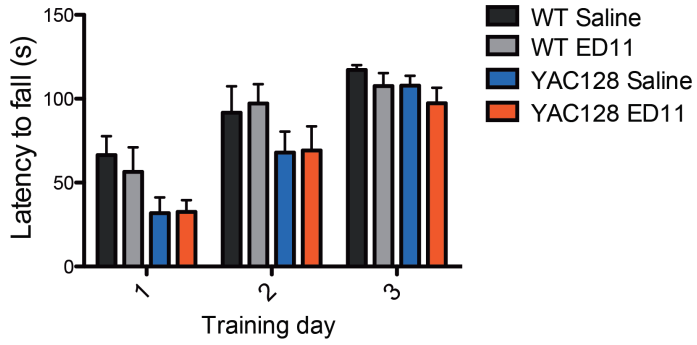

B) Number of Falls

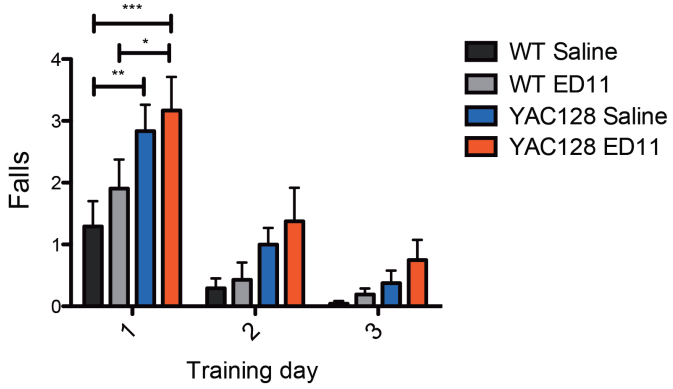

Figure 4.3: ED11-treated YAC128 mice are not protected from motor learning deficits. Saline- and ED11-treated WT and YAC128 mice were trained on a non-accelerating rotarod for 3 consecutive days at 2 months of age to assess their ability to learn a motor task and the time to fall and number of falls were recorded. ED11-treated YAC128 mice fall off the rotarod as quickly as saline-treated YAC128 mice (A, 2-way RM ANOVA: training day $F(2)=39.40$, $p<0.0001$; treatment group $F(3)=7.86$, $p=0.0981$; subjects (matching due to repeated measures on same subject) $F(27)=30.52$, $p=0.0002$; interaction $F(6)=1.77$, $p=0.5745$; N=7-9) and have comparable numbers of falls (B, 2-way RM ANOVA: training day $F(2)=38.18$, $p<0.0001$; treatment group $F(3)=12.52$, $p=0.0300$; subjects (matching due to repeated measures on same subject) $F(27)=32.52$, $p<0.0001$; interaction $F(6)=2.49$, $p=0.1629$; N=7-9). * p<0.05, ** p<0.01, *** p<0.001. Asterisks refer to significant differences following post-hoc analysis.

Cognitive learning was assessed using the novel object preference test. Mice were tested for the novel object preference test at 6 months of age, but no genotypic differences were observed at this age (Appendix Figure S6).

For psychiatric assessment, anxiety-like behaviour of mice treated with ED11 was assessed using the elevated plus maze at 6 months of age. Distances travelled within the elevated plus maze do not differ significantly between treatment groups (Figure 4.4A), suggesting all mice were active and exploring the apparatus. ED11 treatment in YAC128 mice did not result in an improvement in the number of times YAC128 mice entered the open arms (Figure 4.4B) nor did it increase the amount of time YAC128 mice dipped the heads off the edge of the platform (Figure 4.4C), suggesting that ED11 treatment did not have an effect on the anxiety-like phenotype displayed by YAC128 mice.

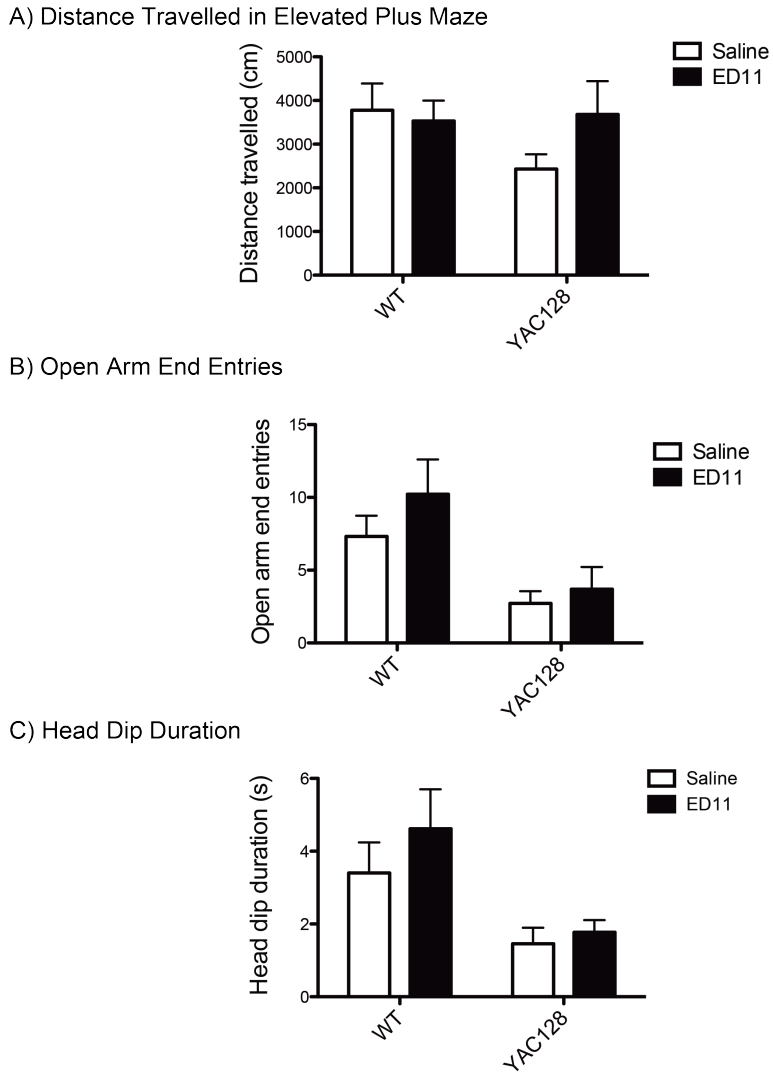

Figure 4.4: ED11 treatment does not protect YAC128 mice from anxiety-like behaviour. Mice were tested on the elevated plus maze to assess anxiety-like behaviour. While there are no statistical differences between groups in distance travelled in the apparatus (A, 2-way ANOVA: treatment $F(1)=1.23$, $p=0.4018$; genotype $F(1)=1.74$, $p=0.3196$; interaction $F(1)=2.70$, $p=0.2157$; N=14-16), YAC128 mice treated with ED11 enter the ends of the open arms less frequently than WT (B, 2-way ANOVA: treatment $F(1)=2.05$, $p=0.2390$; genotype $F(1)=16.93$, $p=0.0012$; interaction $F(1)=0.51$, $p=0.5560$; N=14-16) and spend significantly less time dipping their heads off the end of the open arm platforms than WT mice (C, 2-way ANOVA: treatment $F(1)=1.62$, $p=0.2995$; genotype $F(1)=15.86$, $p=0.0018$; interaction $F(1)=0.57$, $p=0.5377$; N=14-16), data which is comparable to the behaviour of saline-treated YAC128 mice.

BACHD mice treated with ED11 demonstrate reduced immobility time in the forced swim test, indicating an improvement in the depressive-like symptoms. In

order to discern the potential effects of ED11 on depression in YAC128 mice, the forced swim test was also carried out on treated WT and YAC128 mice at 6 months of age. While saline-treated YAC128 mice spent significantly more time immobile compared to WT animals, treatment of ED11 in YAC128 did not influence this behaviour, as ED11-treated YAC128 mice spent a comparable amount of time immobile (Figure 4.5). This finding suggests that treatment of YAC128 mice with ED11 did not protect against depressive-like behaviour.

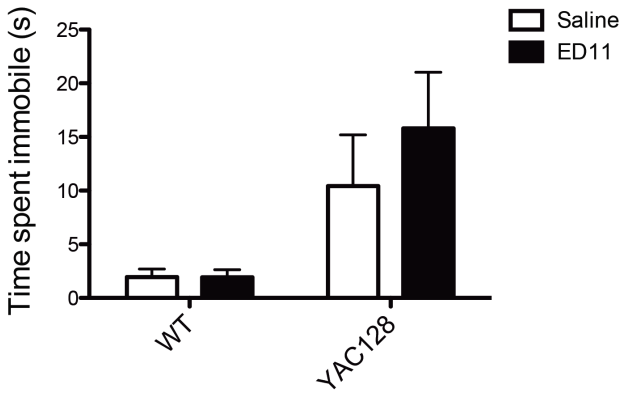

Figure 4.5: ED11 treatment in YAC128 mice is not protective against depressive-like behaviour. Saline- and ED11-treated WT and YAC128 were assessed for depressive-like behaviour using the forced swim test. Both saline- and ED11-treated YAC128 spent significantly more time immobile than both WT groups (2-way ANOVA: treatment $F(1)=0.87$, $p=0.4518$; genotype $F(1)=15.06$, $p=0.0026$; interaction $F(1)=0.87$, $p=0.4503$; N=14-16), suggesting ED11 treatment did not influence this phenotype.

Overall, behavioural assessment of ED11-treated animals using well-validated behaviour tests in YAC128 mice revealed no protection conferred by ED11 treatment against motor, psychiatric and most cognitive deficits in YAC128 mice. Motor function by rotarod test and climbing was not improved with ED11 treatment, and motor learning by rotarod fixed-speed training remained impaired in ED11-treated YAC128 mice. Psychiatric phenotypes of anxiety and depression observed in YAC128 mice were also not prevented with ED11 treatment.

4.2 TARGET ENGAGEMENT ASSESSMENT

In light of the behaviour data demonstrating a lack of benefit to YAC128 mice by treatment with ED11 and the strong discrepancy between this data and

previously published results of ED11 in BACHD mice (Aharony et al., 2015), we first wanted to confirm the blood brain barrier penetrability of the peptide. Aharony and colleagues demonstrated CNS penetration *in vivo* by subcutaneously injecting a bolus of fluorescently labeled ED11 and acutely examining fluorescent signal in the brain 40 minutes later (Aharony et al., 2015). Given that this approach is not reflective of the route of administration, time course or physical structure of ED11 used in either of our mouse studies as well as the lack of an observed effect of ED11, we decided to conduct target engagement experiments beginning with optimizing a method for detecting ED11.

4.2.1 Development of ED11 detection method

As the ED11 peptide contains a TAT tag, initial efforts to detect the peptide were developed based on identifying ED11 using a TAT antibody. The first detection method tested was western blot analysis on different concentrations of pure peptide, ED11-treated neuronal lysate as well as cortical lysate spiked with ED11. A high percentage Bis-Tris gel system was used to optimize detection of small proteins, as the small size of the ED11 peptide corresponds to approximately 2.6 kDa. Using this system, we were unable to detect a band corresponding to ED11 at the predicted size in all samples containing the peptide using the anti-TAT antibody (Figure 4.6A).

The next method tested was a dot blot, which enables detection of proteins without electrophoretic separation based on size and it was thought that this approach would provide a better chance at detecting the peptide due to its small size. While a signal was obtained in the pure peptide samples, there was also a strong signal obtained in the cortical lysates not treated with ED11. Furthermore, when comparing the signal obtained between two different batches of peptide, Batch 1 provided a much stronger signal than an equivalent concentration of Batch 3 (Figure 4.6B), hinting at the possibility of inter-batch variability as a possible contributing factor to the lack of phenotypic improvement seen in ED11-treated YAC128 mice.

Due to the non-specific signals obtained in both western and dot blots, detection of ED11 with an anti-TAT antibody was attempted using an enzyme-linked immunosorbent assay (ELISA). This method detected ED11 in samples containing ED11 and not in controls, in addition to confirming differences in TAT abundances between batches. Furthermore, two peptide samples kindly provided by Aharony and colleagues were included as controls for the ELISA (termed Offen Batch 1 and 2) and also demonstrate variability in the TAT signal (Figure 4.6C).

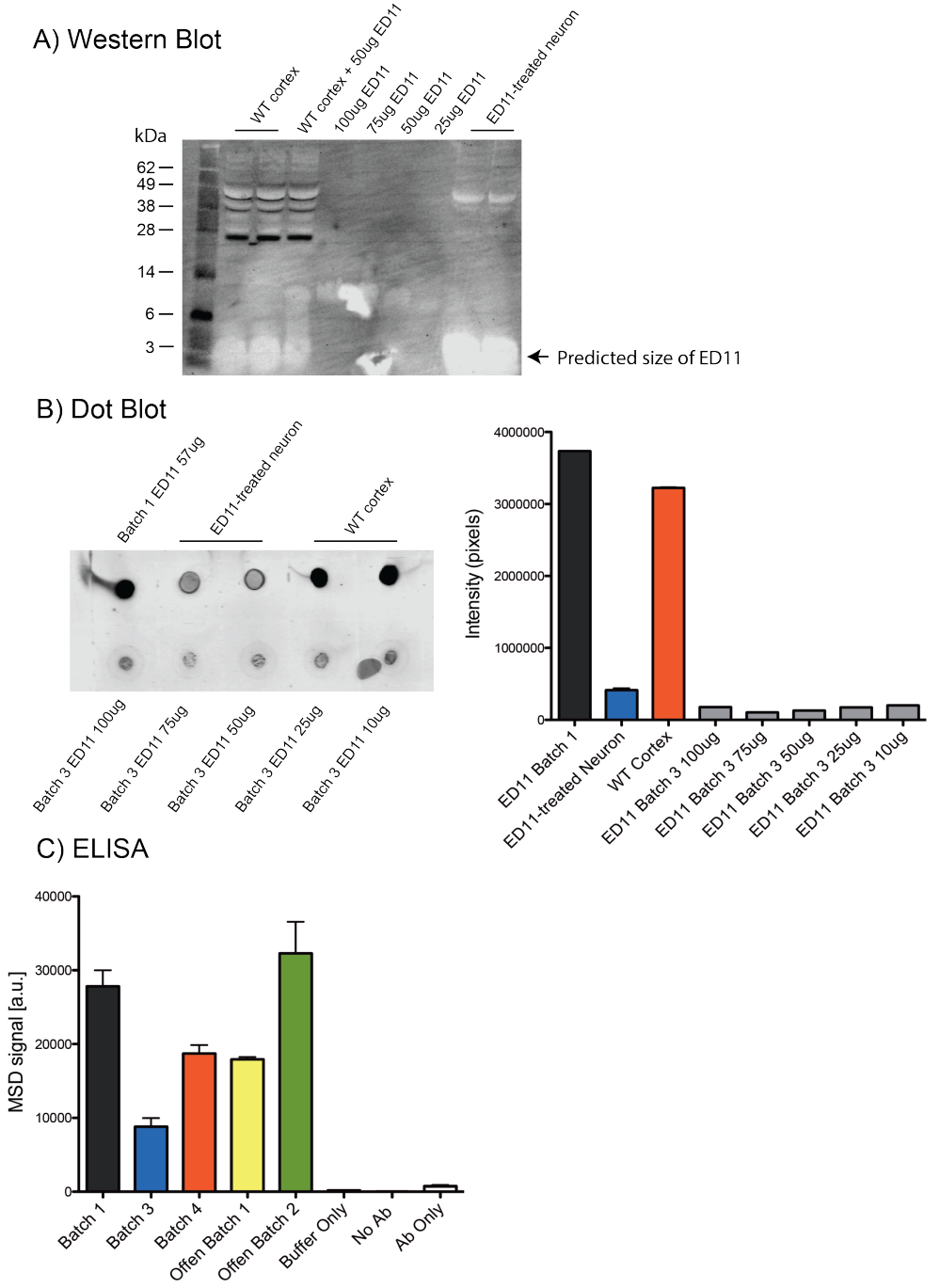

Figure 4.6: Optimization of ED11 detection assay. Detection of the ED11 peptide was attempted using three different approaches – western blot (A), dot blot (B) and ELISA (C), all using an anti-TAT antibody (Abcam, 63957). The ELISA method was chosen due to its ability to generate a signal in ED11-containing samples but not controls and the y-axis represents the luminescent signal obtained from the assay and the data is not normalized.

4.2.2 ED11 functional assessment of caspase-6 inhibition *in vitro*

Having established a detection method for ED11, it was important to address the differences in signal between the various batches of ED11 obtained from the commercial peptide company. This difference in signal represents variability in the detection of the TAT tag but does not provide any indication of the functional capacity of the ED11 peptide to inhibit C6-mediated cleavage of HTT.

To that end, an *in vitro* FRET assay was conducted on HTT-transfected COS lysate incubated with recombinant C6 enzyme and various batches of pure ED11 peptide, including an aliquot of the two peptides used by Aharony *et al*. In the absence of ED11, C6 cleaves HTT at the 586 amino acid site and is quantified by the emission of a fluorescent signal, which is reduced upon exposure to ED11. Results of the FRET assay reveal that all batches of ED11 tested were capable of inhibiting C6-mediated cleavage of HTT at the 586 site to the same or greater extent as the two control peptides received from Dr. Offen's lab, with Batch 3 appearing slightly more potent than the others (Figure 4.7). This indicates that the functional ability of the ED11 peptide to inhibit C6-mediated HTT cleavage is not impaired *in vitro* despite variability in the TAT signal observed in the ELISA.

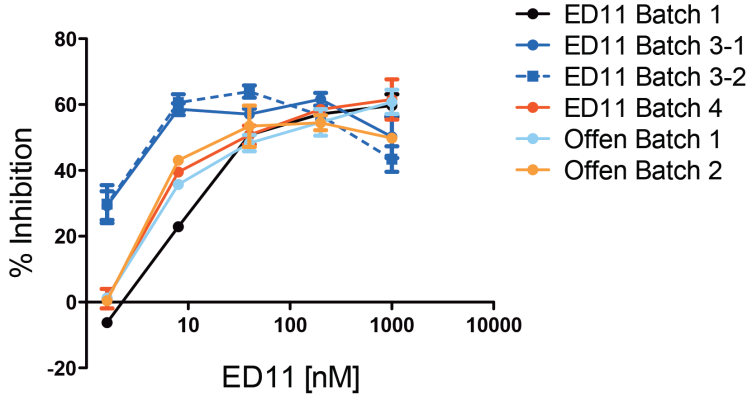

Figure 4.7: Assessment of functional capacity of ED11 peptides using a FRET assay. Various batches of pure ED11 peptide including two control batches obtained from Aharony and colleagues were incubated with recombinant C6 enzyme and HTT-transfected COS lysate. The inhibitory capacity of these peptides was determined using a FRET assay. All batches were capable of

inhibiting C6-mediated cleavage of HTT at the 586 amino acid site to the same extent as control peptides.

4.2.3 ELISA quantification of TAT *in vivo*

The ELISA method was applied to non-perfused brain lysates derived from saline- and ED11-treated WT and YAC128 animals collected at 6 months of age. Quantification of TAT revealed an increase in TAT signal following ED11 treatment in YAC128 animals but not WT animals (Figure 4.8). The absence of an increase in signal in the ED11-treated WT mice is unexpected and possibly hints at differential rates of degradation or clearance of the peptide.

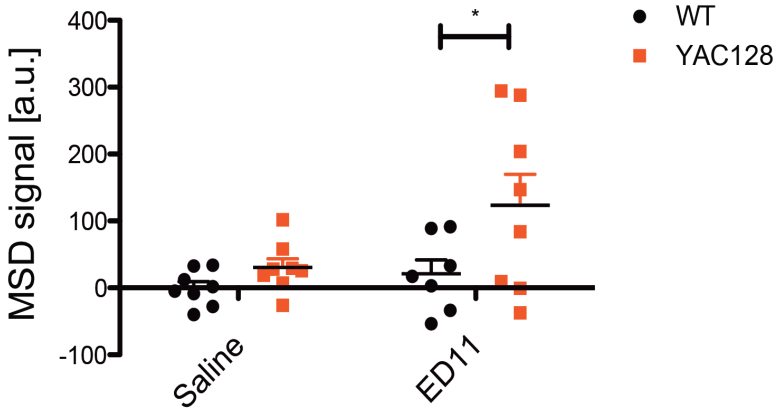

Figure 4.8: ELISA quantification of TAT in saline- and ED11-treated WT and YAC128 cortices. The TAT tag was quantified in saline- and ED11-treated WT and YAC128 cortices using an ELISA. The TAT signal was plotted as WT saline-subtracted values and revealed a significant increase in TAT signal in YAC128 but not in WT cortices following ED11 treatment (2-way ANOVA: genotype $F(1)=15.28$, $p=0.0205$; treatment $F(1)=11.24$, $p=0.0442$; interaction $F(1)=4.50$, $p=0.1930$; N=7-8). * p<0.05, ** p<0.01, *** p<0.001. Asterisks refer to significant differences following post-hoc analysis.

4.2.4 Immunohistochemical identification of ED11 *in vivo*

In addition to the quantification of TAT in cortical lysates, immunohistochemical detection of ED11 was carried out on perfused brains using a 586 neo-epitope antibody, which detects the N-terminal fragment of HTT cleaved at the 586 amino acid site, the sequence of which is also found in the ED11 peptide. Previous immunohistochemical analyses on treated BACHD brains stained with the 586 neo-epitope antibody in our hands had revealed an increase in staining in ED11-

treated brains compared to saline-treated BACHD brains, suggesting the presence of ED11 beyond (unpublished data). WT and YAC128 brains treated with ED11 were sectioned and stained with the same 586 neo-epitope antibody but no signal was obtained, despite numerous efforts at optimizing the staining protocol. As an alternative, an in-house generated 586 neo-epitope antibody was used and no differences between genotypes or treatment were detected with this antibody (Figure 4.9), suggesting that the ED11 treatment did not result in changes in the abundance of the 586 HTT sequence found in the ED11-treated brain compared to saline-treated brains. However, it is also possible that the antibody did not work as expected, that the TAT epitope may have been cleaved or that the peptide has aggregated thereby preventing antibody binding.

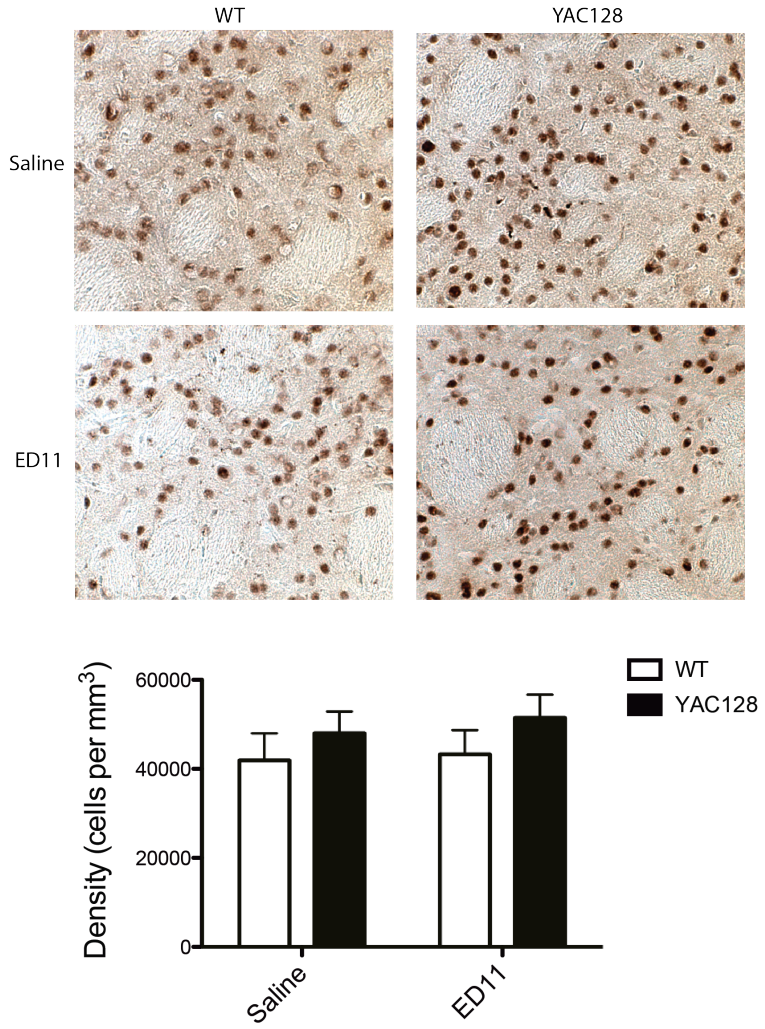

Figure 4.9: Immunohistochemical staining and quantification of ED11 in saline- and ED11-treated WT and YAC128 brains. Saline- and ED11-treated WT and YAC128 cortices were stained with a neo-epitope 586 antibody as an indicator of the presence of ED11 over and above any background 586 staining in the YAC128 brains. Quantification revealed no significant differences in signal between genotypes or treatment (2-way ANOVA: genotype $F(1)=9.74$, $p=0.2042$; treatment $F(1)=1.09$, $p=0.6639$; interaction $F(1)=0.20$, $p=0.8515$; N=5).

4.3 SUMMARY OF FINDINGS

WT and YAC128 mice were treated with a 24-amino acid peptide designed to mimic the 586 cleavage region of HTT and fused to a TAT tag for cell permeability. Continuous treatment of these mice with saline or ED11 for over 5 months did not result in any improvement in motor function or cognitive learning

in YAC128 mice. Furthermore, ED11 treatment did not prevent the anxiety and depressive-like phenotypes observed in YAC128 mice. Efforts to detect ED11 using the TAT tag were achieved using an ELISA and revealed differences in the abundance of the TAT tag between various batches of ED11. Functional assessment of ED11's ability to inhibit C6-mediated cleavage of HTT at 586 using a FRET assay demonstrated that all peptides were capable of inhibiting this cleavage event to the same extent as control peptides *in vitro*. *Ex-vivo* analysis of WT and YAC128 brains showed a modest increase in the ELISA TAT signal between saline- and ED11 treated YAC128 but not WT brains, suggesting the half-life of the peptide may differ between genotypes. Immunohistochemical staining of brain sections with a neo-epitope 586 antibody as a readout of the presence of ED11 revealed no differences in staining between genotypes or treatment. Altogether, this data suggests that while ED11 may be detectable and functional *in vitro*, its *in vivo* efficacy and ability to enter the CNS is uncertain. Furthermore, the differing sources of peptide may result in differing characteristics, all of which could account for the lack of phenotypic improvement observed in YAC128 mice.

5 INVESTIGATING THE ROLE OF CASPASE-6 IN INFLAMMATION AND ITS RELATIONSHIP TO THE INFLAMMATORY PHENOTYPE IN YAC128 MICE

The observation that partial deletion of C6 attenuates the release of IL-6 in cultured macrophages from inducible *C6* deficient mice prompted an investigation into the role of C6 in inflammation. A potential role for C6 in modulating the inflammatory response has been proposed in recent studies of immune cells in the CNS and periphery, whereby C6 has been postulated to mediate the secretion of TNF-α and the activation of macrophages and microglia (Berta et al., 2014; Kobayashi et al., 2011). Additionally, previous work suggests that C1 is capable of activating C6 in neurons (Guo et al., 2006) and that upon stress by serum deprivation or LPS treatment, neuronal inflammasomes activate C1 and subsequently C6 downstream, resulting in inflammatory IL-1β production and C6-mediated axonal degeneration (Kaushal et al., 2015).

5.1 DIFFERENCES IN INFLAMMATORY PHENOTYPES BETWEEN WT AND *C6*$^{-/-}$ MICE

We began by investigating the inflammatory state under basal, non-stimulated conditions in WT and constitutive *C6* deficient (*C6*$^{-/-}$) mice. ELISA analysis of plasma collected from these mice at 12 months of age reveals a significant decrease in circulating IL-6 levels in *C6*$^{-/-}$ mice compared to WT (Figure 5.1).

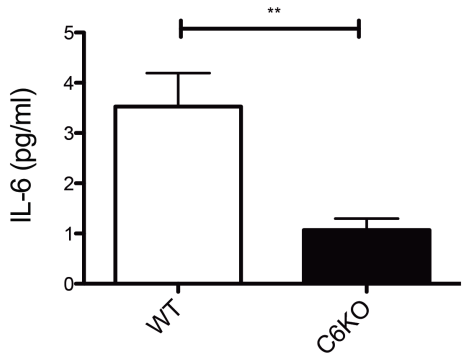

Figure 5.1: Plasma from *C6*$^{-/-}$ mice contains significantly reduced levels of circulating IL-6. ELISA quantification of plasma IL-6 levels show a significant decrease in IL-6 levels in 12-month old C6$^{-/-}$ mice (unpaired two-tailed t-test: t(15)=2.969, *p*=0.0095; N=7-10) * p<0.05, ** p<0.01, *** p<0.001.

With the observation that *C6*$^{-/-}$ mice have reduced basal circulating levels of the cytokine IL-6, we wondered if these differences would be mirrored during inflammatory stimulation. To that end, young WT and *C6*$^{-/-}$ mice 3 months of age were IP injected with 5 mg/kg of lipopolysaccharide (LPS) and the levels of cytokines IL-6 and TNF-α were measured in blood plasma prior to injection as well as 1, 3 and 6 hours following injection. The levels of both cytokines peaked at 6 hours post-injection, with TNF-α displaying a biphasic response consistent with the biphasic induction of its activator, transcription factor nuclear factor kappa-light-chain-enhancer of activated B cells (NF-κB) (Gukovsky et al., 1998; Han et al., 2002; D. F. Shen et al., 2000; Thompson et al., 1995). A trend toward reduced IL-6 release at 6 hours post-injection was observed in *C6*$^{-/-}$ mice, though this was not significant by post-hoc (Figure 5.2A). Interestingly, release of TNF-α was significantly attenuated in *C6*$^{-/-}$ mice at this time point (Figure 5.2B), consistent with the hypothesis that C6 is a regulator of TNF-α production.

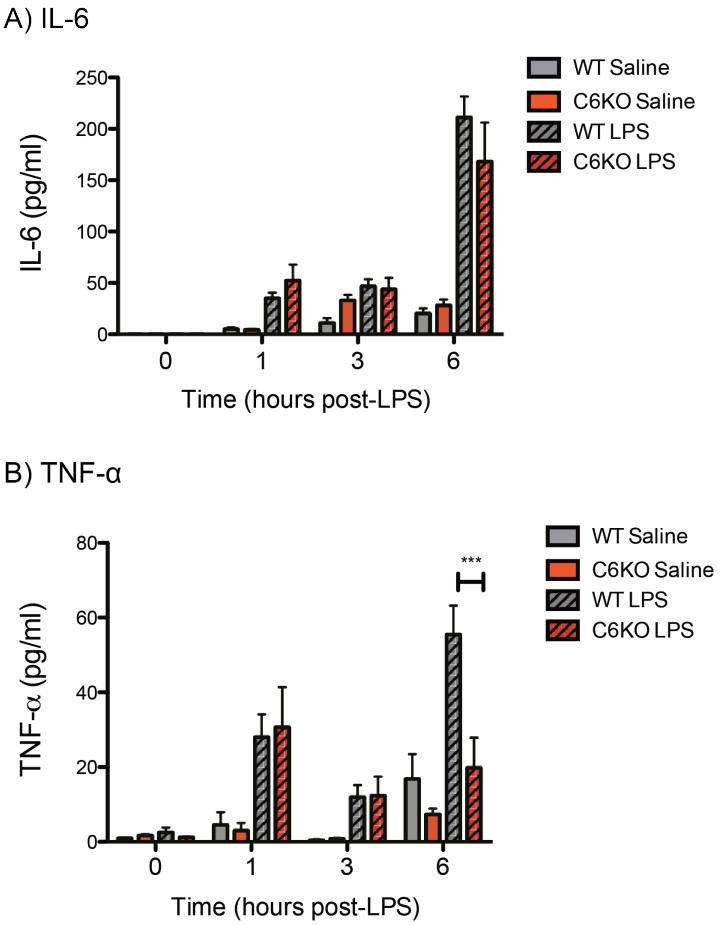

Figure 5.2: *C6*$^{-/-}$ mice secrete lower levels of plasma cytokines upon LPS stimulation. ELISA quantification of plasma cytokines prior to LPS injection and 1, 3 and 6 hours post-injection. Results show a trend toward decrease in IL-6 levels at 6 hours post-injection of LPS (A; 2-way ANOVA: treatment group $F(3)=20.40$, $p<0.0001$; time $F(3)=35.82$, $p<0.0001$; interaction $F(9)=24.94$, $p<0.0001$; N=7-10) and a significant decrease in TNF-α (B; 2-way ANOVA: treatment group $F(3)=29.40$, $p<0.0001$; time $F(3)=33.05$, $p<0.0001$; interaction $F(9)=23.74$, $p=0.0002$; N=7-10).* p<0.05, ** p<0.01, *** p<0.001. Asterisks refer to significant differences following post-hoc analysis.

Elevated cytokine levels have been linked to affective behaviours such as depression, apathy and anhedonia in both humans and mice (Anisman and Merali, 1999; Dantzer et al., 1999; Meyers, 1999; Walker et al., 1997; Yirmiya, 1996). In order to determine if the alterations in cytokine levels translate into behavioural changes, WT mice were subjected to the open field and forced swim tests following LPS injection. In this paradigm, the open field test was conducted to ensure mice had recovered from the LPS injection and that overt toxicity

symptoms affecting overall activity were not a confounding factor in the interpretation of forced swim test data, as has been previously reported (Biesmans et al., 2013). Data obtained from LPS-injected WT mice demonstrates that exploratory activity as informed by distance travelled (Figure 5.3A) and average velocity (Figure 5.3B) is unaffected by LPS treatment, confirming that mice had recovered from the injection and no longer exhibiting sickness symptoms that may confound psychiatric data. Forced swim testing on these same mice revealed a significant increase in time spent immobile in LPS-injected animals compared to saline-injected animals (Figure 5.3C), suggesting that LPS-induced inflammation results in a depressive phenotype, consistent with previous findings.

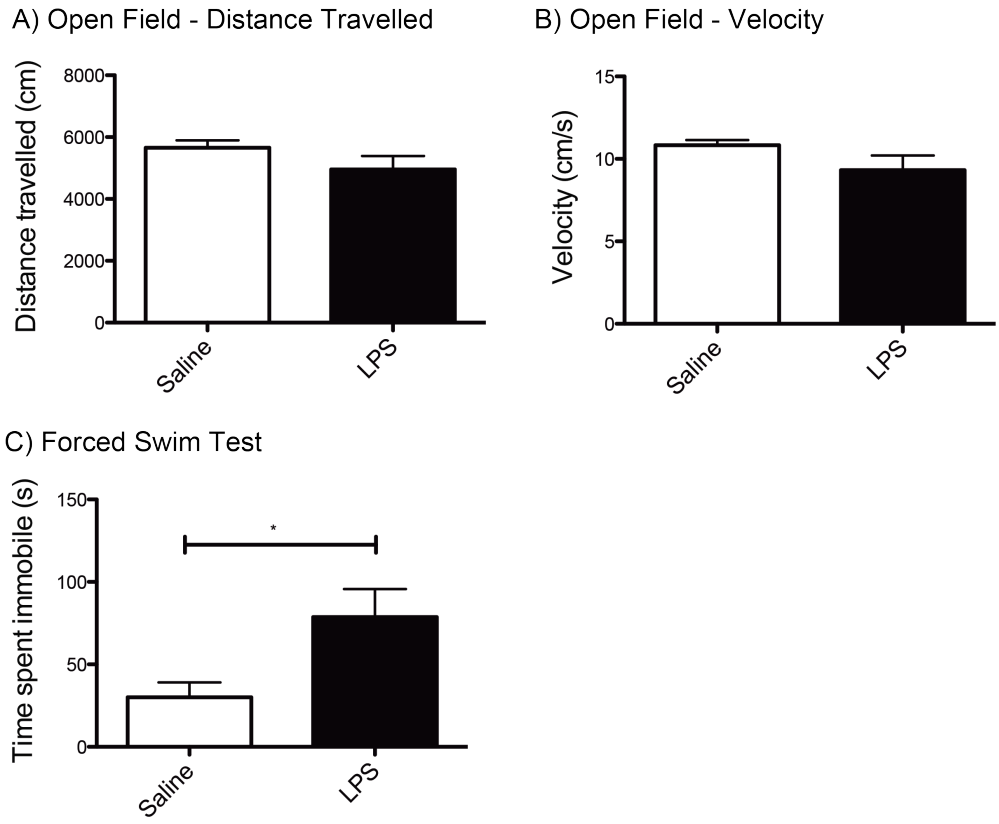

Figure 5.3: WT mice treated with LPS display depressive behaviour without changes in activity. WT mice were tested on the open field following LPS injection in order to assess basal activity and demonstrate no changes in distance travelled (A; unpaired two-tailed t-test: t(10)=1.41, *p*=0.1889; N=6) or velocity (B; unpaired two-tailed t-test: t(10)=1.60, *p*=0.1404; N=6). Forced swim testing for depressive behaviour reveals an increase in time spent immobile (C;

unpaired two-tailed t-test: t(11)=2.41, *p*=0.0349; N=6-7) indicating depression. * p<0.05, ** p<0.01, *** p<0.001.

Given the differences in inflammatory responses following system inflammatory challenge in mice lacking C6 and the possibility that these changes could translate into behavioural outcomes, we decided to examine the status of inflammation in the brain and determine if these differences might be mirrored in the CNS. To that end, microglia cultured from WT and *C6*$^{-/-}$ mice were stimulated with increasing doses of control standard endotoxin (CSE). Interestingly, IL-6 levels measured in the media following stimulation reveal no differences in the secretion of this cytokine between WT and *C6*$^{-/-}$ mice (Figure 5.4), suggesting the absence of C6 expression in microglia does not influence IL-6 activation or production. These data point to an alternative mechanism not mediated by microglia by which the loss of C6 influences the inflammatory response and results in behavioural changes.

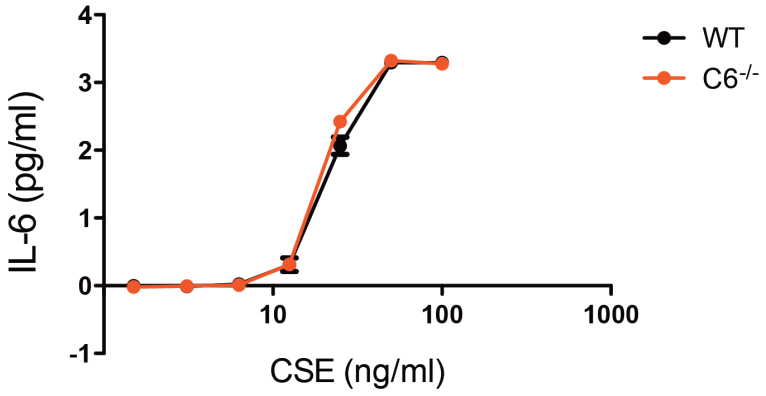

Figure 5.4: Microglia cultured from WT and *C6*$^{-/-}$ mice do not display significant differences in IL-6 secretion following CSE stimulation.
Microglia were cultured from WT and *C6*$^{-/-}$ mice and stimulated with CSE. IL-6 secreted into the media was quantified by ELISA and while a dose-dependent increase in IL-6 is observed with increasing concentrations of CSE, no genotypic differences were observed.

5.2 MECHANISM FOR DIFFERENTIAL INFLAMMATORY RESPONSE IN WT AND *C6*$^{-/-}$ MICE

The finding that WT and *C6*$^{-/-}$ microglia, the resident immune cells responsible for mounting inflammatory responses do not exhibit differences in IL-6 secretion upon stimulation led us to consider alternative mechanisms for inflammation. We postulated that perhaps neurons might play a role in mediating these responses via their interactions with microglia in the brain, which could account for the C6-specific differences observed. To simulate this scenario *in vitro*, cortical neurons from WT and *C6*$^{-/-}$ mice were cultured and treated with either NMDA or balanced salt solution (BSS) as a control. NMDA was chosen because it causes neuronal dysfunction and damage, which is a stimulus that activates microglia (Kaindl et al., 2012) and is relevant for HD. The neuronal conditioned media was then added to the media of microglia cultured from WT and *C6*$^{-/-}$ mice. The subsequent dual-conditioned media was harvested the following day and analyzed for IL-6 cytokine levels. Interestingly, the transplantation of conditioned media from NMDA-treated *C6*$^{-/-}$ neurons onto either WT or *C6*$^{-/-}$ microglia (hollow bars) resulted in a significant reduction of secreted IL-6 compared to the transplantation of conditioned media from NMDA-treated WT neurons (solid bars) (Figure 5.5). This suggests that the transplanted media from NMDA-treated WT neurons contained neuronal-derived factors that were not present in the NMDA-treated *C6*$^{-/-}$ neuronal media, which ultimately contributed to the secretion of cytokines by microglia. Furthermore, this highlights that the presence of C6 in microglia is not relevant; rather, the presence and activity of C6 in neurons influences the inflammatory response.

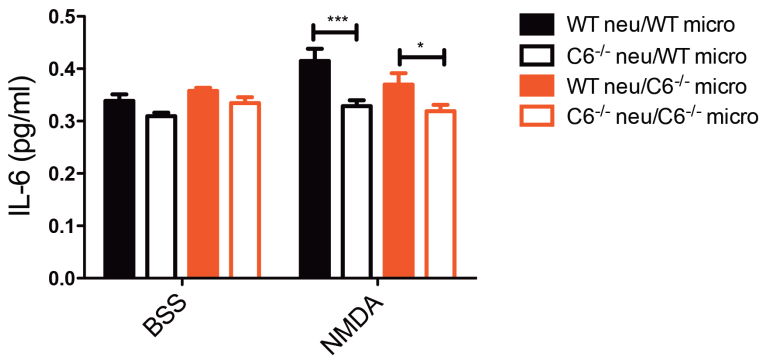

Figure 5.5: Reduced IL-6 secretion in microglia stimulated with medium from NMDA-treated *C6*$^{-/-}$ neurons. Microglia cultured from WT or *C6*$^{-/-}$ mice were treated with conditioned media from BSS- or NMDA-treated WT or *C6*$^{-/-}$ neurons. Microglia treated with NMDA-conditioned *C6*$^{-/-}$ neuronal media release significantly less IL-6 than microglia treated with NMDA-conditioned WT neuronal media (2-way ANOVA: genotype $F(3)=35.13$, $p=0.0021$; treatment $F(1)=7.40$, $p=0.0505$; interaction $F(3)=17.17$, $p=0.0390$; N=4) suggesting neuronal-derived factors found in WT and not C6 media may mediate microglial activation in response to inflammatory challenge. * p<0.05, ** p<0.01, *** p<0.001. Asterisks refer to significant differences following post-hoc analysis.

5.3 YAC128 IMMUNE CELLS ARE MORE SENSITIVE TO C6-MEDIATED INFLAMMATORY STIMULATION

It has been demonstrated that immune cells from YAC128 mice are hypersensitive to stimulation (Björkqvist et al., 2008; Träger et al., 2014b). Since previous studies have demonstrated that recombinant C6 can activate spinal microglia (Berta et al., 2014), we investigated the response of resident immune cells of the brain and periphery of WT and YAC128 to treatment with recombinant C6 enzyme *in vitro*. Treatment of microglia and alveolar macrophages isolated from both genotypes with increasing concentrations of C6 added to the media resulted in a greater increase in secreted IL-6 and TNF-α (Figure 5.6A and B respectively) in YAC128 compared to WT, suggesting that the addition of exogenous C6 stimulates the release of cytokines in brain and peripheral immune cells.

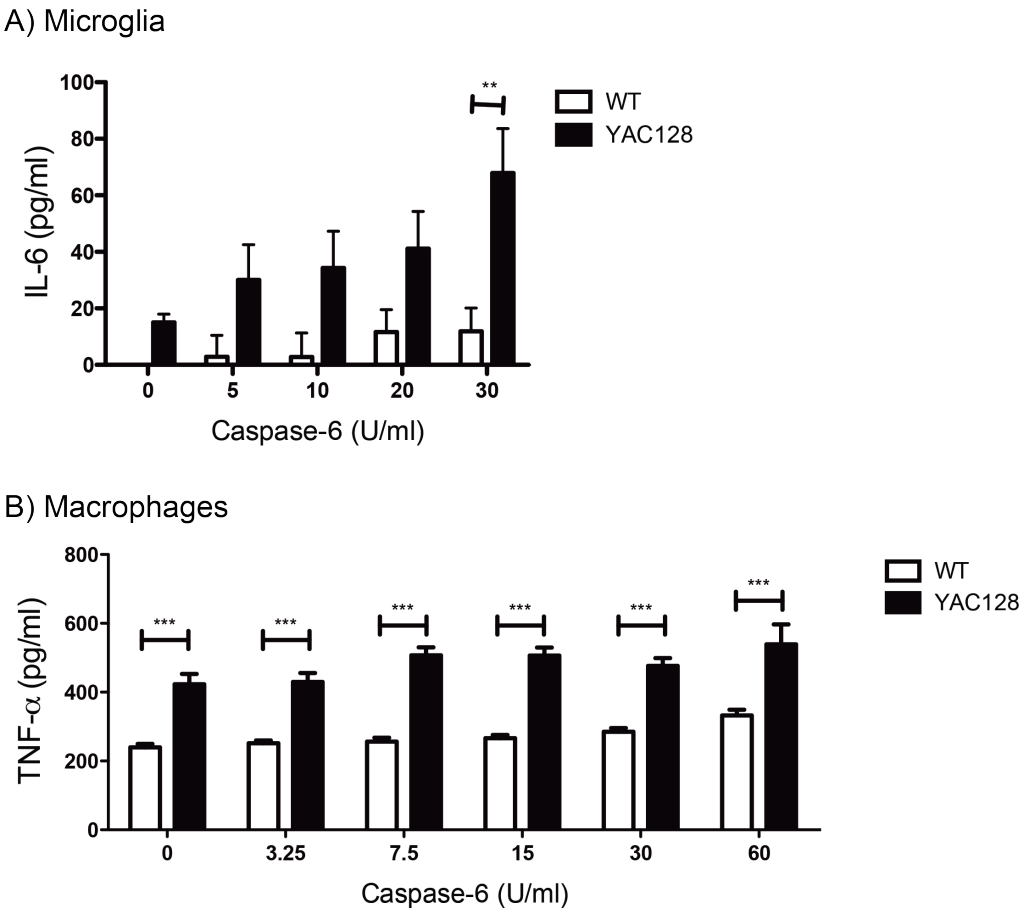

Figure 5.6: Microglia and alveolar macrophages cultured from YAC128 mice secrete higher levels of cytokines and are hypersensitive to stimulation with exogenous C6. Microglia and macrophages were cultured from WT and YAC128 mice and treated with various doses of recombinant C6. C6-treated YAC128 microglia secrete significantly more IL-6 than WT microglia (2-way ANOVA: genotype $F(1)=41.32$, $p<0.0001$; concentration $F(4)=21.06$, $p=0.0334$; interaction $F(4)=5.11$, $p=0.5477$; N=3). C6-treated YAC128 macrophages secrete significantly more TNF-α than WT macrophages (2-way ANOVA: genotype $F(1)=71.21$, $p<0.0001$; concentration $F(5)=7.63$, $p=0.0013$; interaction $F(5)=1.26$, $p=0.5806$; N=6), suggesting YAC128 immune cells are hypersensitive to C6-induced inflammation. * p<0.05, ** p<0.01, *** p<0.001. Asterisks refer to significant differences following post-hoc analysis.

5.4 SUMMARY OF FINDINGS

An analysis of basal cytokine levels in WT and *C6*$^{-/-}$ mice reveals a reduction in circulating plasma IL-6 levels in *C6*$^{-/-}$ mice compared to WT. Upon inflammatory challenge with LPS injection, *C6*$^{-/-}$ mice demonstrate a trend toward attenuated release of IL-6 and significantly reduced release of TNF-α. The influence of

elevated cytokine levels on affective behaviours was confirmed when WT mice treated with LPS displayed a significant increase in time spent immobile, indicated depressive-like behaviour and further experiments will be required to determine if this response is altered in *C6*$^{-/-}$ mice. Furthermore, depressive behaviour may also be caused by the influence of peripherally produced cytokines entering the brain from systemic inflammatory stimulants such as LPS, pointing to distinct mechanisms for mediating peripheral versus neuroinflammation.

In addition, preliminary data suggests that the inflammatory response of microglia derived from *C6*$^{-/-}$ mice may not differ significantly to that of WT microglia and media exchange experiments between neurons and microglia suggest that the differences in neuroinflammation observed between these genotypes may be mediated by neuronal-derived factors, ultimately resulting in reduced cytokine production in *C6*$^{-/-}$ microglia. Furthermore, the addition of exogenous C6 to microglia and macrophages resulted in elevated cytokine production in YAC128 compared to WT. These data suggest that neuronal-derived factors independent of C6 presence in microglia may be responsible for the underlying hyperactive inflammatory response observed in YAC128 mice.

6 DISCUSSION AND FUTURE DIRECTIONS

The overall goal of this thesis was to further characterize the role of C6 in HD and the effects of its modulation on HD phenotypes in the adult YAC128 mouse. The modulation of C6 was conducted using a tamoxifen-inducible gene deletion strategy with an optimized tamoxifen treatment protocol as well as using a peptide-based approach at the post-translational level. In addition, the role of C6 in inflammation was further characterized and its relevance to the altered inflammatory phenotypes observed in HD was assessed.

6.1 INCOMPLETE *CASPASE-6* GENE DELETION AND THRESHOLD REQUIREMENTS FOR CASPASE-6 MODULATION

The observation that most of the canonical behavioural and neuropathological phenotypes exhibited by YAC128 mice were not improved in mice with partial deletion of *C6* is most likely due to the incomplete gene deletion and moderate levels of excision observed in the brain. The selective degeneration of MSNs in the striatum of HD patients and mouse models and resultant manifestation of motor, cognitive and psychiatric symptoms points to the centrality of this region in governing these behaviours; thus it is not entirely surprising that the inability to mitigate toxic events in these neurons, including the prevention of mHTT cleavage at the 586 site through deletion of *C6* results in an unimproved diseased state.

An important distinction of this inducible C6 deletion study is that in this model, the incomplete excision results in a molecular environment whereby some cells have a complete absence of C6 due to recombination while other cells retain 100% expression of C6, or potentially greater in areas where the loxP sites influence expression. Furthermore, it is possible that some cells with reduced C6 expression may have one allele deleted; thus, a homogenate exhibiting a 50% decrease in C6 could be due to a composite of cells that are WT, hemizygous null and null for *C6.* The phenotypes altered in this model must therefore be considered with caution and may not be fully translatable to clinical strategies of C6 modulation, which may more likely be a small molecule inhibitor resulting in a

degree of inhibition consistent among all target cells. Such a strategy may still provide therapeutic benefit, as implied by recent findings. The study characterizing the constitutive C6 deficient mouse demonstrated that MSNs cultured from heterozygous deletion animals are partially protected from NMDA-induced excitotoxicity (Uribe et al., 2012), suggesting that a 50% reduction in C6 expression still confers protection against cell death. In addition, perisciatic delivery of C6 siRNA resulting in ~50% reduction in expression suppressed formalin-induced pain in mice (Berta et al., 2014). Inhibition of C6 activation also confers benefits in a stroke model (Akpan et al., 2011). These data suggest that partial inhibition resulting in reduced expression in all targeted cells can be beneficial. In contrast, a scenario in which certain cells have no C6 while others have complete expression, as is the case in the present inducible C6 deficient study, is unlikely to yield significant therapeutic benefit.

6.2 CONSIDERATIONS OF THE CRE-LOXP SYSTEM AND INDUCTION OF CRE WITH TAMOXIFEN

Conditional deletion mouse models represent a powerful way to investigate the function of a gene in a spatially and temporally controlled manner. The exploitation of the bacteriophage Cre-loxP system has enabled investigators to selectively excise a region of the genome, often with high efficiency and gain extensive insight into developmental and disease mechanisms. However, this technology is not without limitations and such caveats must be considered in the analysis and interpretation of results from inducible deletion studies.

The induction of deletion with tamoxifen in this inducible model required significant optimization and testing of multiple routes of administration, doses and post-treatment intervals in order to surmount the most significant hurdle encountered – the lack of efficient excision in the CNS. Tamoxifen induction of Cre is most commonly achieved using IP injections (Ruzankina et al., 2007; Whitfield et al., 2015) and is advantageous over other routes of administration of tamoxifen mainly due to the ability to control dose and timing (Turner et al., 2011). Evidence from other investigators in our lab using a *Hip14* inducible

deficient mouse model suggests that the use of this same *Cre-ERT2* transgene combined with the same tamoxifen protocol of 5 days of consecutive IP injections at 200 mg/kg results in near-complete excision in the CNS (Shaun Sanders, unpublished data), suggesting that the inefficiency of recombination observed in this *C6* inducible study is likely due to the design of the C6 inducible mouse itself. Support for this hypothesis comes from the observation that the excision efficiency of Cre recombinase is inversely correlated with distance between loxP sites (B. Zheng et al., 2000). This could certainly account for the reduced recombination efficiency observed, as the loxP sites in the *iC6* model are located approximately 6.5 kb apart when the recommended distance is 1-2 kb (B. Zheng et al., 2000). This obstacle necessitates a prolonged treatment period of tamoxifen, though when attempted, resulted in toxicity and lethality. Thus, a delicate balance exists between extending the treatment period and testing sufficiently high doses.

The optimization of the dosing regimen eventually resulted in efficient recombination in peripheral tissues and an overall 50% deletion level in the CNS. Future administration strategies to increase CNS penetrability and recombination efficiency could include intravenous administration of 4-OHT, as the administration of the active metabolite itself directly through the circulatory system results in the fastest CNS effect (Turner et al., 2011). However, intravenous injections require significant technical skill and the consequences of incorrect technique can be fatal. Furthermore, the high cost of 4-OHT favours the use of its precursor tamoxifen instead.

Other confounding factors to consider include the independent toxic effects of Cre and tamoxifen *in vivo* (Harno et al., 2013; Magnuson and Burlison, 2007; O'Neill et al., 2004; L. Smith, 2011; Turlo et al., 2010). The mammalian genome contains several cryptic pseudo-loxP sites that retain sufficient identity with the canonical loxP sites to allow Cre recombinase to possibly carry out unintended excision events (Thyagarajan et al., 2000). Recent studies have suggested that Cre activity is associated with chromosomal aberrations, growth inhibition and DNA damage in mammalian cells (Loonstra et al., 2001). Furthermore, there is

evidence that Cre activity alone can induce cell death and caspase activation (Y. Li et al., 2014) and glucose intolerance, a strain-dependent effect that was only observed in mice of certain genetic backgrounds (J.-Y. Lee et al., 2006). The activation of cell death pathways is also a known effect of tamoxifen, rendering it a commonly used drug for chemotherapy treatment of breast cancer (B. Fisher et al., 2004).

Contrastingly, 4-OHT has been reported to exert neuroprotective effects against β–amyloid and glutamate-induced toxicity *in vitro*, a function also attributed to endogenous estrogen (O'Neill et al., 2004). However, this benefit does not appear to extend *in vivo*, as it has been reported that tamoxifen treatment in mice abolishes the protective effects of estrogen (Gao and Dluzen, 2001). Thus, the effects of both Cre and tamoxifen on cell death mechanisms are particularly important considerations in this study especially in light of the central function of C6 in apoptosis. Alternative conditional models that do not involve the use of the tamoxifen-inducible Cre-loxP system may therefore be better suited to study the impact of the absence of C6 in adult mice.

6.3 PARTIAL GENETIC LOSS OF CASPASE-6 IN ADULTHOOD

One of the central objectives of this thesis was to determine the impact of the genetic loss of C6 in the adult mouse in the absence and presence of mHTT. Assessment of brain structures, behaviour and peripheral phenotypes revealed modest effects arising from the partial loss of C6, including changes to brain weights and volumes. In the context of mHTT, partial loss of C6 did not prevent the onset of motor or cognitive deficits and resulted in a slight improvement of some psychiatric behaviours. In peripheral tissues where a greater extent of deletion was achieved, we observed a transient delay in body weight gain, an attenuation of cytokine release in stimulated macrophages and an increase in full-length WT and mHTT levels in the liver.

The finding that the partial loss of C6 in WT mice results in a reduction of brain weight and corpus callosum volume is intriguing and slightly unexpected due to the role of C6 in mediating neuronal loss via apoptosis. Reduced whole brain

weight, forebrain weight and striatal volume was also observed in *iC6*$^{F/F}$;YAC128 controls, consistent with previous findings (Slow et al., 2003; Van Raamsdonk et al., 2005a). With the reduction in brain weights observed in both *iC6*$^{-/-}$ and *iC6*$^{F/F}$;YAC128 control mice, it is not possible to distinguish whether these changes also observed in *iC6*$^{-/-}$;YAC128 mice are due to mHTT-mediated mechanisms or to the partial loss of C6 or both. Striatal volume loss was not prevented in *iC6*$^{-/-}$;YAC128 mice, suggesting that the partial loss of C6 is not sufficient to mitigate the loss of MSNs from this region. Importantly, the expression of C6 in the striatum is increased significantly in floxed mice, thus it is conceivable that increased C6 expression may result in a greater extent of C6 activation and subsequent proteolytic cleavage of mHTT leading to pathogenesis. The partial loss of C6 in the striatum may therefore not be extensive enough to attenuate striatal atrophy.

Interestingly, a reduction in corpus callosum volume was observed in both *iC6*$^{-/-}$ and *iC6*$^{-/-}$;YAC128 mice but not in *iC6*$^{F/F}$;YAC128 control mice. Reduced corpus callosum volume has been observed previously in YAC128 mice (Carroll et al., 2011a); however, structural changes in these studies were examined using magnetic resonance imaging (MRI), a technique that offers greater sensitivity to subtle ultrastructural changes. Such changes may not be as detectable by conventional stereology methods used here. The observation that partial loss of C6 results in reduced corpus callosum volume was unexpected in light of the extensive evidence supporting a role for C6 in mediating axonal degeneration, which would argue for a preservation of white matter in the absence of C6. This could be due to compensatory mechanisms by C3 and C9, which also play a role in mediating axonal degeneration (Cusack et al., 2013). Given that decreased corpus callosum volume and brain weights were observed in *iC6*$^{-/-}$ but not in *iC6*$^{F/F}$ control mice suggests the possibility that C6 may play a role in maintaining neuronal or glial survival and its absence may be associated with cell death.

An important methodological consideration is that while *iC6*$^{-/-}$ and *iC6*$^{-/-}$;YAC128 mice share the partial loss of C6 as a feature to which phenotypes can be attributed, these two genotypic groups also have the expression of Cre in

common. It has been reported that among the documented toxic effects of Cre expression from birth is the occurrence of microcephaly due to defects in neuronal precursor proliferation and increased cell death in the embryonic brain (Forni et al., 2006; Qiu et al., 2011). It is therefore possible that the structural alterations observed here are due to Cre-mediated toxic effects on normal brain development. Such Cre-specific toxic effects could be determined by including a WT mouse only expressing Cre-ERT2 in the absence of tamoxifen or floxed alleles. This control was not included in the present study as it had been previously characterized in the *Hip14* inducible study carried out in our lab with the same Cre-ERT2 transgene in the same mouse strain and no volumetric changes were observed (Figure S7, reprinted with permission from Shaun Sanders). Additional support for the notion that this finding is not a Cre-mediated effect is the observation that constitutive *C6*$^{-/-}$ mice also demonstrate significantly reduced corpus callosum volumes compared to WT (Bibiana Wong, personal communication). However, it is still possible that the presence of Cre may exert differential toxicity mechanisms in a different inducible model despite usage of the same Cre line and mouse strain, and thus cannot be ruled out completely.

iC6$^{-/-}$*;*YAC128 mice were behaviour tested starting at 3 months of age for assessment of motor, cognitive and psychiatric function. Partial loss of C6 did not prevent the onset of motor or cognitive dysfunction as indicated by unimproved rotarod performance, climbing and motor learning, but had a mild effect on psychiatric phenotypes of anxiety and anhedonia. Numerous psychiatric behaviours including anxiety, depression and anhedonia have found causative roots in inflammatory signaling. Oxidative stress and inflammation have been described as anxiogenic triggers (Bouayed et al., 2009; Pitsavos et al., 2006) and studies in mice have shown that adenosine signaling through the A2A adenosine receptor doubles C1 activity and subsequently increases IL-1β activity, triggering the onset of anxiety phenotypes (G. S. Chiu et al., 2014). Since C6 has been implicated as a downstream target of C1 activity (Guo et al., 2006; Kaushal et al., 2015), it is plausible that expression of C6 is mechanistically linked to the manifestation of anxiety-like behaviours in mice via C1-mediated inflammatory

signaling. Furthermore, WT HTT has also been implicated in regulating anxiety-like behaviours in mice, as inducible deletion of WT HTT from cortical and hippocampal neurons resulted in an onset of anxiety-like behaviours (Pla et al., 2013). Many HD mouse models display anxiety-like behaviours and demonstrate a loss-of-function of WT HTT, possibly due to C6-mediated proteolytic cleavage. Support for a role for C6 in influencing anxiety-like behaviour also comes from the ED11-treated BACHD study, where mice treated with the ED11 peptide display an improvement in anxiety phenotypes in the open field test (Aharony et al., 2015).

iC6$^{-/-}$*;*YAC128 mice consumed a greater amount of sucrose in the sucrose preference test for anhedonia, but when this data was normalized to total fluid intake, significance was lost and only a trend toward a preference for sucrose was present. Interestingly, modulation of C6 in several paradigms has resulted in a protection from affective behaviours such as depression and anhedonia. C6R mice, constitutive *C6*$^{-/-}$*;*YAC128 mice as well as ED11-treated BACHD mice are protected from depressive-like symptoms (Aharony et al., 2015; B. K. Y. Wong et al., 2015), data that strongly points to a role for C6 in the onset of affective behaviours. Evidence linking C6 to the production of inflammatory cytokines provides a possible mechanism for this phenotype, as there is compelling evidence that the levels of cytokines during inflammation in both mice and humans correlate with depression, apathy and anhedonia (Anisman and Merali, 1999; Dantzer et al., 1999; Meyers, 1999; Walker et al., 1997; Yirmiya, 1996) (see Chapter 6.6 for further discussion).

The greater extent of deletion observed in peripheral tissues enables superior confidence in drawing conclusions on the role played by C6 in regulating phenotypes observed in these tissues. Excessive body weight gain has been observed in both YAC128 and BACHD mice (Gray et al., 2008; Pouladi et al., 2010; Southwell et al., 2013; Van Raamsdonk et al., 2006a) and is thought to be due to the modulation of the IGF-1 pathway by HTT (Pouladi et al., 2010; Van Raamsdonk et al., 2006a). Furthermore, the constitutive ablation of *C6* in YAC128 mice delays this body weight gain and results in normalized IGF-1 levels

(B. K. Y. Wong et al., 2015). The observation that *iC6*$^{-/-}$;YAC128 mice have body weights comparable to WT controls at 3 months while *iC6*$^{F/F}$;YAC128 control mice are significantly heavier than WT mice led us to the possibility that adult-onset loss of C6 may reproduce this phenotype. However, upon longitudinal examination of body weight changes including and beyond the tamoxifen injection period, it was clear that this protection of body weight gain was transient and resulted primarily from a significant loss of body weight during the injection period.

Tamoxifen treatment can induce general sickness signs in mice over the course of the treatment period including body weight loss, but mice usually recover and regain body weight with time. It has also been reported that tamoxifen directly reduces fat mass and this reduction was sustained over a period of 4-5 weeks in mice (Liu et al., 2015). Both female and male *iC6*$^{-/-}$;YAC128 mice exhibited a sharp decline in body weight during the injection period and this trend is also observed in *iC6*$^{-/-}$ mice albeit to a lesser degree. Given that a significant loss to body weight in response to tamoxifen treatment is only observed in the *iC6*$^{-/-}$ and *iC6*$^{-/-}$;YAC128 mice, it is possible that these mice are sensitized to greater body weight loss by either the presence of Cre recombinase or due to the partial loss of C6.

While all *iC6*$^{-/-}$ mice and male *iC6*$^{-/-}$;YAC128 mice are able to recover this body weight to control levels within 4-5 weeks, female *iC6*$^{-/-}$;YAC128 mice do not gain the same weight as their YAC128 counterparts despite being significantly heavier than WT mice. This sex difference could be possibly due to the presence of estrogen, which has a suppressive effect on food intake and body weight (Wallen et al., 2001). No changes in IGF-1 levels were observed in *iC6*$^{-/-}$;YAC128 mice (data not shown) suggesting that the body weight changes are unlikely to be sustained HTT-mediated effects over time.

Interestingly, alveolar macrophages cultured from *iC6*$^{-/-}$ and *iC6*$^{-/-}$;YAC128 mice display attenuated release of IL-6 upon treatment with an inflammatory stimulus, suggesting that the partial loss of C6 influences the inflammatory response. This

is consistent with previous reports suggesting that C6 is important for the release of proinflammatory cytokine TNF-α upon pneumonic challenge and in the manifestation of pain (Berta et al., 2014; Kobayashi et al., 2011). This particular finding led us to explore to role of C6 in modulating inflammation in greater detail, described in Chapter 6 and discussed in Chapter 6.6.

Finally, since previous reports characterizing the effects of constitutive genetic ablation of *C6* on various HD mouse models suggested that loss of C6 influences protein levels of HTT (Gafni et al., 2012; B. K. Y. Wong et al., 2015), both WT HTT and mHTT levels were examined in the liver, a peripheral tissue with the greatest extent of deletion (~95%). Quantification revealed that both WT HTT and mHTT levels are significantly increased compared to all other genotypes. This is in contrast to the aforementioned studies, which demonstrated a significant decrease in HTT levels in the absence of C6. This discrepancy might be in part due to the region examined – a decrease in HTT levels was detected in the striatum, while in this study an increase in HTT levels was observed in the liver and it is possible that protein clearance mechanisms are differentially regulated within these two tissues. The liver is a site of extensive protein turnover and high levels of basal autophagy (Schneider and Cuervo, 2014) and autophagy activity in the liver has been shown to decline with age (Cuervo and Dice, 2000), possibly resulting in an accumulation of proteins.

Alternatively, it is possible that this increase in WT HTT and mHTT levels could be attributed to a reduction in C6-mediated cleavage of the proteins, resulting in less fragment generation and a preservation of full-length forms of the protein. It has also been shown that cellular stress positively correlates with HTT levels independent of continual huntingtin synthesis (Leitman et al., 2013). It is quite plausible that this may be a contributing factor given that both Cre and tamoxifen can be inherently toxic and may cause hepatic stress. Further studies examining the pattern of fragments, HTT mRNA expression, intracellular localization of HTT and liver morphology would be required to investigate these possibilities.

In summary, this study examining the effects of post-natal genetic modulation of C6 revealed a reduction in the weights and volumes of several brain structures, modest changes in behavioural endpoints as well as alterations in inflammation and liver protein accumulation were observed. When examining these data in comparison to previously published effects of constitutive genetic loss of C6 in YAC128 mice, both consistencies and discrepancies are found. The prevention of depressive behaviour in the constitutive absence of C6 and the modest improvement in anxiety and anhedonic behaviours with the partial loss of C6 points to a potential role for C6 in regulating affective behaviours.

Neuropathologically, constitutive *C6*$^{-/-}$ mice demonstrate no changes in whole brain weight, an increase in striatal and cortical volumes but a decrease in corpus callosum volume, while adult-onset partial loss of C6 in mice display a reduction in brain weight, no changes to striatal and cortical volume and a decrease in corpus callosum volume compared to WT. The observation that whole brain weight is unchanged in the constitutive deficient mouse may be due to the net effect of greater striatal and cortical volume combined with reduced corpus callosum volume. Likewise, the reduced brain weight observed in the inducible deficient mice is likely reflective of the net loss of structural volumes. A comparison of phenotypes observed in YAC128 mice (Björkqvist et al., 2008; Carroll et al., 2011a; 2011b; Pouladi et al., 2009; Slow et al., 2003; Southwell et al., 2009; Träger et al., 2014b; Uribe et al., 2012; Van Raamsdonk et al., 2007a; 2005c; 2005a; Xie et al., 2010), C6R mice (Graham et al., 2006), constitutive *C6*$^{-/-}$ mice, constitutive *C6*$^{-/-}$;YAC128 mice (B. K. Y. Wong et al., 2015), inducible *iC6*$^{-/-}$ mice and inducible *iC6*$^{-/-}$;YAC128 mice is listed in Table 6.1.

Table 6.1: Comparison of phenotypes in YAC128, C6R, *C6$^{-/-}$;*YAC128 and *iC6$^{-/-}$;*YAC128 mice. Notes: -- = Not assessed and/or reported; *Not assessed due to confounding effect by Cre

Neuropathological Phenotypes	**YAC128**	**C6R**	**C6$^{-/-}$**	**C6$^{-/-}$;YAC128**	**iC6$^{-/-}$**	**iC6$^{-/-}$;YAC128**
Brain weight	Decreased - 9 months	Normalized	Unchanged	--	Decreased - 12 months	Decreased - 12 months
Striatal volume	Decreased - 3 months	Normalized	Increased - 8 months	Delayed atrophy	Unchanged	Decreased - 12 months
Cortical volume	Decreased - 12 months	--	Increased - 8 months	--	Unchanged	Unchanged
Corpus callosum volume	Decreased - 3 months	--	Decreased - 3 months	Decreased - 16 months	Decreased - 12 months	Decreased - 12 months
Striatal neuronal counts	Decreased - 12 months	Normalized	Increased - 8 months	--	--	--
Behavioural Phenotypes	**YAC128**		**C6$^{-/-}$**	**C6$^{-/-}$;YAC128**	**iC6$^{-/-}$**	**iC6$^{-/-}$;YAC128**
Motor learning	Decreased - 2 months	Normalized	--	--	Unchanged	Decreased - 3 months
Motor function - rotarod performance	Decreased - 3 months	Normalized	Unchanged	Delayed deficit	Unchanged	Decreased - 3 months
Spontaneous activity	Increased - 2 months Decreased - 8 months	Normalized	Decreased - 6 months	Decreased - 6 months	--	--
Motor function - climbing	Decreased - 7 months	--	--	--	Decreased - 6 months	Decreased - 6 months
Cognitive function - object learning	Decreased - 6-7 months	--	Decreased - 6 months	--	Unchanged	No genotypic effect
Cognitive function - spontaneous alternation	Decreased - 7 months	--	--	--	--	--
Cognitive function - sensorimotor gating by pre-pulse inhibition	Decreased - 12 months	--	--	--	--	--
Cognitive function - swimming T-maze with reversal	Decreased - 2 months	--	--	--	--	--
Psychiatric behaviour - anxiety in open field	Increased - 6-7 months	--	--	--	Unchanged	Modest improvement - 3 months
Psychiatric behaviour - anxiety in elevated plus maze	Increased - 6-7 months	--	--	--	Unchanged	Modest improvement - 9 months
Psychiatric behaviour - depression	Increased - 3 months	Normalized	--	Prevented - 6 months	Unchanged	No genotypic effect
Psychiatric behaviour - anhedonia	Increased - 3 months	Normalized	--	--	Unchanged	Modest improvement - 6 months
Peripheral Phenotypes	**YAC128**		**C6$^{-/-}$**	**C6$^{-/-}$;YAC128**	**iC6$^{-/-}$**	**iC6$^{-/-}$;YAC128**
Body weight	Increased - 2-3 months	--	Unchanged	Delayed gain	Unchanged	Delayed gain
IGF-1 levels	Increased - 3 months	--	--	Normalized - 12 months	Unchanged	Unchanged
Testes weight	Decreased - 12 months	--	--	Delayed degeneration	--*	--*
Inflammatory responses	Increased - 3 months	--	--	--	IL-6 secretion normalized	IL-6 secretion normalized
HTT levels	--	--	--	Reduced - 12 months (striatum)	Increased - 12 months (liver)	Increased - 12 months (liver)

Additionally, several caveats have been highlighted by this study that must be considered when employing inducible deletion models in the study of gene function. These include potential toxicity induced by Cre and/or tamoxifen. Furthermore, potential changes in gene expression as a result of the loxP sites indicate the possibility for undesirable changes in the regulation of gene expression. These potential confounding factors render the data obtained particularly difficult to interpret especially in light of the lack of complete and global excision observed in this mouse model and the potential toxic effects of residual C6 activity in some tissues.

6.4 INVESTIGATION OF REGULATORY REGIONS GOVERNING CASPASE-6 EXPRESSION

An unintended consequence arising from the insertion of the loxP sites was the observation that C6 protein expression patterns were altered. Most pertinent was the finding that the floxed mice displayed a significant increase in striatal C6 expression. LoxP sites as well as other genetic elements necessary for the construction of conditional mouse models have been reported to influence both flanking and distal gene expression (Meier et al., 2010). The extent of deletion observed in this region must therefore be carefully interpreted, as the observed reduction in protein levels following tamoxifen treatment may approach normal/WT levels and thus may partly explain why only modest benefits are observed in *iC6*$^{-/-}$;YAC128 mice.

Although this finding represents a potential confounding factor, it also serendipitously points to a possible novel regulatory mechanism governing C6 expression. A closer examination of the interrupted C6 sequence and subsequent analysis using two bioinformatic predictive software programs (ORCA toolkit (Portales-Casamar et al., 2009) and JASPAR analysis (Mathelier et al., 2014)) revealed several possible transcription factor (TF) binding sites interrupted by the insertion of one or both loxP sequences. Table 6.2 lists putative transcription factor binding sites that were identified in two separate analyses as lost upon the insertion of loxP sites.

Table 6.2: Putative transcription factor binding sites interrupted by the insertion of loxP sequences. A list of overlapping hits obtained in two separate bioinformatic analyses predicting possible transcription factor binding sites interrupted by either or both loxP sites. Functions obtained from NCBI Gene database.

Transcription Factor	Interrupted by loxP site 1 or 2	Function
Klf1	2	Hematopoietic-specific TF; induces expression of globin/erythroid genes
Klf4	1	Zinc finger protein required for development of barrier function of skin
NF-κB	2	Complex involved in regulating inflammation, immune function and apoptosis
Nkx2-5	Both	Regulates heart formation and development
RUNX1	2	Regulates development of normal hematopoiesis
Zfx	1	Involved in self-renewal of hematopoietic stem cells

Of particular interest is the identification of a binding site belonging to the transcription factor NF-κB potentially interrupted by the second loxP sequence inserted downstream of exon 5. NF-κB is a transcription factor that regulates a wide range of biological functions, central to which are its roles in mediating inflammation, cell death and cell survival pathways through expression of numerous target genes. These functions support the idea that C6 could be a transcriptional target of NF-κB due to its roles in cell death and possibly inflammation.

Other target genes of NF-κB include cytokines and their modulators as well as regulators of apoptosis such as IAPs. C11 has been identified as a transcriptional target of NF-κB resulting in an upregulation of C11 expression following stimulation of macrophages with LPS (Schauvliege et al., 2002). These data, taken together with the roles for C6 in mediating both apoptosis and inflammation via TNF-α release, suggest the possibility that C6 could be a transcriptional target of NF-κB, with binding of NF-κB to C6 associated with reduced expression while the interruption of this interaction results in increased C6 expression. Moreover, it has been shown that WT HTT facilitates the neuronal transport of NF-κB from the synapse to the nucleus and that this function is impaired in HD (Marcora and M. B. Kennedy, 2010). Impaired translocation to the nucleus and subsequent function of NF-κB could conceivably result in increased expression

and possible activation of C6. Further studies would be required to confirm an interaction between C6 and NF-κB and investigate the impact of inhibiting NF-κB activity on C6 expression.

6.5 PEPTIDE-MEDIATED INHIBITION OF CASPASE-6

In order to further investigate the effects of C6 modulation in the adult YAC128 mouse, a 24-amino acid peptide was employed, which was designed by Aharony and colleagues based on the HTT sequence surrounding the 586 cleavage site. Treatment with this peptide in BACHD mice resulted in reduced C6-mediated cleavage of HTT at 586, an amelioration of motor and cognitive deficits in presymptomatic mice as well as a partial recovery of motor function and an improvement in the depressive phenotype in post-symptomatic mice (Aharony et al., 2015). This data is in contrast with the findings obtained in the current study of the effects of ED11 in YAC128 mice, which resulted in no improvements in motor, cognitive or psychiatric phenotypes. Furthermore, while the ability of ED11 to inhibit C6-mediate cleavage of HTT in an *in vitro* environment were corroborated, attempts to confirm the *in vivo* presence of ED11 following a 5-month infusion period were unsuccessful.

Several possible explanations can be discussed to explain the discrepancies in results between this study and that conducted by Aharony *et al.* There are two primary differences inherent to these studies. First, our studies employed two different mouse models of HD. Second, the dose administered in the study BACHD was half (4 mg/kg/day) of that used in our study (8 mg/kg/day). Despite the use of separate mouse models, it has been reported that BACHD and YAC128 exhibit similar behavioural phenotypes, including motor learning and coordination deficits, depressive-like symptoms, impaired startle response during a test for sensorimotor gating despite differences in aggregate formation and transcriptional dysregulation (Pouladi et al., 2012). Furthermore, it is unlikely that the increased dose used in our study contributed to the lack of benefit observed, particularly in light of the fact that no overt toxicity was observed in the animals nor was the behaviour of ED11-treated WT mice significantly different from that

of saline-treated WT mice. Thus, the negative results obtained are likely due to limitations in the capacity of the peptide itself to execute its function *in vivo*.

Target engagement experiments to confirm that ED11 penetrates the blood brain barrier in the BACHD study consisted of an acute subcutaneous bolus injection of ED11 fused to a fluorescein isothiocyanate (FITC) tag at a dose of 50 mg/kg and *in vivo* fluorescence detection 40 minutes post-injection (Aharony et al., 2015). Several caveats exist with this method to validate target engagement. First, the structure of ED11 used in the target validation experiment and that used for treatment in BACHD mice differs by the presence of the FITC tag. It is not uncommon for affinity tags to exert non-specific and unintended effects on the fusion protein, resulting in unpredictable behaviour of the compound of interest (Vira et al., 2010; Weingart et al., 1999). FITC labels conjugated to antibodies have been reported to inactivate and/or alter antibody-antigen binding (Vira et al., 2010), suggesting the behaviour of the FITC-labeled ED11 molecule may differ significantly *in vivo* than that of the unlabeled version. Secondly, the acute dose used in this paradigm is more than ten times higher that used in the longitudinal study. Therefore, the observation that ED11 permeates the blood brain barrier with this acute high dose cannot necessarily be assumed to be the case in a chronic treatment of a much lower dose over a longer period of time. Moreover, no target engagement experiments were reported at the end of the longitudinal BACHD study. Lastly, the detection of FITC-labeled ED11 in the brain a short 40 minutes following injection does not ensure ED11 will remain present in the brain throughout the 28-day infusion period, nor that it remains stable in the saline solution kept within the osmotic pump throughout this time.

Independent studies conducted to determine the pharmacokinetics of ED11 *in vivo* suggest a short half-life as well as brain and plasma concentrations well below IC50 values (Ralph Laufer, personal communication). These data are not consistent with the results reported in the BACHD study and cast doubt on whether or not the benefits observed in the BACHD are indeed due to ED11. Further, this information provides a potential explanation for the lack of benefit observed in ED11-treated YAC128 mice.

Our efforts to investigate the functional validity and target engagement of the peptide suggest that it could indeed act as an inhibitor of cleavage at the 586 site in *in vitro* environments. Indeed, *in vitro* ELISA results confirm the presence of the TAT tag in pure ED11 batches, albeit with different abundances. Furthermore, an *in vitro* FRET assay conducted in order to confirm the ability of ED11 to inhibit C6-mediated cleavage of HTT at 586 revealed all batches were capable of inhibiting this cleavage event to the same degree as or greater than control peptides used in the study by Aharony and colleagues. Taken together, this suggests that ED11 is detectable and functional *in vitro*; however, these experiments do not preclude the possibility that ED11 may not cross the blood brain barrier, may be degraded/removed prior to carrying out its function or that the TAT tag and adjoining HTT sequence may not remain conjugated together in an *in vivo* setting.

Under the assumption that ED11 is entirely responsible for the protective effects observed in the BACHD study, differences in blood brain barrier integrity between BACHD and YAC128 models may account for the discrepancies observed. It has been reported that under normal conditions, YAC128 mice do not have a compromised blood brain barrier (Franciosi et al., 2012). However, studies investigating the status of the blood brain barrier in BACHD have not been conducted. It is plausible that the blood brain barrier in BACHD mice may be compromised, thus allowing the entry of ED11 into the brain and a subsequent amelioration of behavioural phenotypes. Further studies investigating the integrity of the blood brain barrier in BACHD mice as well as the half-life of ED11 observed *in vivo* under the same conditions of dosing and route of administration are required to ensure the continued presence of ED11 in the brain and to be able to confidently attribute the positive findings in the BACHD study to ED11.

6.6 CASPASE-6 AS A MODULATOR OF INFLAMMATION

Though C6 has been traditionally considered an executioner apoptotic caspase, several non-apoptotic functions have been recently described, including a

potential role for regulating the production of pro-inflammatory cytokine TNF-α (Berta et al., 2014; Kobayashi et al., 2011). The finding that partial loss of C6 in the inducible deficiency study resulted in attenuated cytokine secretion in alveolar macrophages lacking C6 led us to further investigate the role of C6 in inflammation, particularly as aberrant inflammatory responses have been well documented in HD.

We find that basal levels of circulating pro-inflammatory cytokine IL-6 is reduced in *C6*$^{-/-}$ mice, while the secretion of TNF-α is significantly reduced and a trend towards reduction in IL-6 levels exists in *C6*$^{-/-}$ mice following systemic administration of LPS, consistent with previous reports associating the loss of C6 with blunted inflammatory responses. We also observed that depressive-like symptoms could be induced in mice with the treatment of low doses of LPS independent of sickness phenotypes in WT mice. Additional experiments investigating the role of C6 in mediating the onset of affective behaviours such as depression and anhedonia are required to determine if the differences in cytokine secretion in *C6*$^{-/-}$ mice translate to behavioural outcomes. Mechanistically, we show data to support the hypothesis that the differential inflammatory response in *C6*$^{-/-}$ mice may not due to autonomous microglial differences but potentially rather to neuronal-mediated secretion of C6 and resultant stimulation of microglial production of pro-inflammatory cytokines.

Is C6 an inflammatory caspase? Is it capable of promoting inflammation through direct cleavage and activation of proinflammatory cytokines similar to C1-mediated activation of IL-1β? Assessment of putative proteolytic cleavage sites using prediction software PROSPER (protease specificity prediction server) within the proinflammatory cytokines TNF-α, IL-6 and IL-1β cytokines did not reveal any predicted C6 cleavage sites, suggesting that C6 may exert its effects indirectly via other caspases. The finding that C6 activation is not always associated with cell death renders further merit to this postulation. Interestingly, C8 is also capable of cleaving IL-1β at the same site as C1, leading to its maturation (Maelfait et al., 2008). The compensatory role observed by C8 in cleaving mHTT at the 586 site in the absence of C6 suggests possible

overlapping functions between the two proteases. C8 and C6 both play dual roles in mediating apoptotic and necroptotic pathways (Mocarski et al., 2012; van Raam et al., 2013), and it is plausible that C6 may be involved in mediating both inflammatory and apoptotic mechanisms.

Intriguingly, links have been suggested connecting the excitotoxic and inflammatory pathways. These two pathways have been thought to converge upon TNF-α as TNF-α has been shown to potentiate glutamate-induced toxicity (Tolosa et al., 2011) while also mediating inflammation following its release from microglia (Olmos and Lladó, 2014). Given the well-established role for C6 in facilitating excitotoxicity and the finding that excitotoxicity can lead to NMDA receptor activation on microglia and downstream inflammatory signaling (Kaindl et al., 2012), it is quite possible that C6 plays a previously underappreciated role in mediating inflammation. Furthermore, while C6 is structurally different from inflammatory caspases-1 and -4 in its lack of possession of a DED domain, C6 and C1/4 do share a similar substrate preference for hydrophobic residues at the P4 position, which is not the case for its fellow executioner caspases-3 and -7 (Talanian et al., 1997). This finding hints at the possibility that C6, C1 and C4 may overlap in their cleavage of certain substrates involved in common cellular pathways such as inflammation.

6.7 FUTURE DIRECTIONS FOR CASPASE-6 MODULATION IN HD

In light of the pathogenic role for C6 in mediating mHTT cleavage at the 586 site as well as its participation in mediating the pathogenesis of other neurological conditions, C6 has been aggressively studied as a potential therapeutic candidate. However, the mounting evidence supporting diverse non-apoptotic roles for C6 suggests that therapeutic approaches targeting C6 should be considered with caution. As additional important physiological functions of C6 come to light, it may be necessary to preserve some level of C6 activity and thus developing therapeutic compounds that downregulate rather than entirely inhibit C6 activity may offer the best strategy.

In the context of HD, the most significant concern when assessing C6 as a therapeutic target is the possibility for compensatory mechanisms that result in 586 cleavage in the absence of C6. While compensation within the caspase family has been shown to result from the constitutive absence of one member from conception, one cannot rule out the possibility that alternate caspases may be upregulated during the transient inhibition of C6 potentially offered by a small molecular inhibitor during adulthood. Such an inhibitor, assuming it does not inhibit C6 with 100% efficacy, could still provide therapeutic benefit as evidenced by gene dosage studies.

Small molecule chemical inhibitors can be developed to target the active site of the C6 enzyme, an allosteric site that regulates enzymatic activity or an exosite of the enzyme that interferes with the cleavage of specific substrates. This latter approach is likely the ideal strategy in HD, as it enables the targeted disruption of a specific enzyme-substrate interaction. Such an exosite has been discovered for the cleavage of poly(ADP) ribose polymerase 1 by C7, whereby binding of the substrate in the exosite increases proteolytic efficiency of that particular substrate (Boucher et al., 2012). Thus, identifying possible exosites in C6 relevant for HTT cleavage and subsequently targeting this region may be an ideal strategy for specific C6 inhibition of HTT cleavage.

Mimicking the C6R mutation in humans with the goal of preventing the generation of the 586 fragment regardless of the candidate protease could also be a selective strategy. At present, the potential for genome editing with tools such as CRISPR render this concept a potentially viable therapeutic in the near future and the genomic context surrounding the cleavage site may offer greater flexibility for targeting over the polyQ expansion itself.

Indirect strategies to modulate C6 activity offer an alternative for therapeutic development and can be devised based on the activation mechanisms discovered to date for C6. Within the caspase cascade, several caspases lead to the downstream activation of C6 and their modulation can thus be targeted as indirect C6 inhibitors. Recent work by Leblanc and colleagues has revealed that

neuronal inflammasome activation via C1 following treatment with an inflammatory stimulus activates C6 downstream, resulting in concomitant IL-1β-mediated neuroinflammation and C6-associated axonal degeneration (Kaushal et al., 2015). C1 is thus a particularly attractive therapeutic target in HD, offering the potential advantage of mitigating both overactive inflammatory phenotypes as well as axonal loss, features often found in tandem in neurodegenerative conditions.

C9 has also been shown to influence C6 activation, particularly in studies of stroke. A study conducted by Akpan and colleagues demonstrated that intranasal treatment of mice with a C9 inhibitor attenuated C6 activation and provided protection against axon loss and neuronal cell death during ischemia (Akpan et al., 2011). The efficacy observed with the intranasal route of administration in this study is promising for therapeutic delivery in humans and the existence of an endogenous inhibitor of C9, XIAP, also provides an alternative target for C9/C6 modulation. Not only can inhibitor compounds be designed and modeled after XIAP, but since XIAP itself is subject to regulation, upstream activators of XIAP can also serve as therapeutic targets for the ultimate modulation of C6 activity.

Combinatorial approaches to targeting caspase activity could also prove to be viable therapeutic interventions. The discovery that C8 and C10 are both capable of cleaving at the 586 site (B. K. Y. Wong et al., 2015) ensures that the generation of the 586 fragment cannot be entirely abolished without the simultaneous inhibition of enzymatic function of all three proteases. However, such a blanket approach targeting multiple caspases should be approached with caution as they may exhibit a net negative effect, given the central role that caspases play in regulating critical cellular processes.

The discovery that phosphorylation at the Ser257 residue of C6 by ARK5 inhibits the autoactivation of C6 and C3-processed C6 (Cao et al., 2012; Suzuki et al., 2004; Velázquez-Delgado and Hardy, 2012) offers an additional point of regulation at the post-translational level. Enhancers of ARK5 kinase activity could potentially be employed to modulate C6 activity; however, this strategy may have

unintended effects on the activity of other substrates of ARK5. Similarly, p53 has been shown to contribute to C6 activation (Ehrnhoefer et al., 2014; MacLachlan and El-Deiry, 2002); however, inhibition of p53 is likely a suboptimal strategy for the modulation of C6 given its critical role as a tumour suppressor protein. Additional studies aimed at investigating upstream activation mechanisms of C6 will be critical for the development of therapeutic compounds centered around C6.

Further experiments interrogating the role for C6 in mediating the inflammatory response in the presence of mHTT will be critical for extending our knowledge of the non-apoptotic functions of C6, particularly in the context of HD. Follow-up studies investigating the impact of the loss of C6 in HD could most easily be conducted using the existing constitutive *C6*$^{-/-}$;YAC128 mouse model. It would be interesting to investigate whether or not the hyperactive inflammatory responses observed in YAC128 mice are mitigated by the genetic loss of C6 and if any amelioration in inflammatory phenotypes can be reproduced by modulating C6 in adulthood. Moreover, the link between C6 activity, cytokine production and the onset of affective behaviours can be confirmed by administering proinflammatory cytokines to *C6*$^{-/-}$;YAC128 mice and observing the possible recurrence of depressive-like symptoms, a phenotype that had been rescued with the constitutive deletion of C6 (B. K. Y. Wong et al., 2015). This work would further validate the role of C6 in inflammation.

Delineating the contributions of peripheral versus neuroinflammation to HD pathogenesis is also of importance, as well as investigating the potential crosstalk that exists between the two. In light of the observation that peripheral interventions, including those that cause inflammation, can translate into changes with the CNS and affect CNS-related outcomes, it will be important to assess inflammatory profiles *in vivo* where both systems coexist.

Therapeutic compounds being tested in other neurodegenerative conditions may also prove to be beneficial for HD. The identification of convergent pathogenic pathways such as synaptic dysfunction, aberrant apoptotic mechanisms and

altered protein clearance pathways shared by multiple neurodegenerative diseases (Ehrnhoefer et al., 2011c) offers the unique opportunity for developing drugs that may provide clinical benefit to a heterogenous group of conditions. One such example is laquinimod, a drug currently being tested in a Phase III clinical trial for multiple sclerosis. Numerous studies are underway to determine the effects of laquinimod treatment on HD phenotypes. Importantly, preliminary data suggests that laquinimod decreases C6 activation in neurons and partially protects axons from degeneration following growth factor withdrawal (Dagmar Ehrnhoefer, personal communication). Additional experiments are ongoing to fully characterize the impact of laquinimod on C6 activity and HD-related phenotypes. Thus, the repurposing of compounds already being tested for other neurodegenerative diseases that share common pathways may prove to be of therapeutic benefit in HD.

REFERENCES

Aharony, I., Ehrnhoefer, D.E., Shruster, A., Qiu, X., Franciosi, S., Hayden, M.R., Offen, D., 2015. A Huntingtin-based peptide inhibitor of caspase-6 provides protection from mutant Huntingtin-induced motor and behavioral deficits. Hum. Mol. Genet. ddv023. doi:10.1093/hmg/ddv023

Akpan, N., Serrano-Saiz, E., Zacharia, B.E., Otten, M.L., Ducruet, A.F., Snipas, S.J., Liu, W., Velloza, J., Cohen, G., Sosunov, S.A., Frey, W.H., Salvesen, G.S., Connolly, E.S., Troy, C.M., 2011. Intranasal delivery of caspase-9 inhibitor reduces caspase-6-dependent axon/neuron loss and improves neurological function after stroke. J. Neurosci. 31, 8894–8904. doi:10.1523/JNEUROSCI.0698-11.2011

Albin, R.L., Young, A.B., Penney, J.B., 1989. The functional anatomy of basal ganglia disorders. Trends Neurosci. 12, 366–375.

Albrecht, S., Bogdanovic, N., Ghetti, B., Winblad, B., LeBlanc, A.C., 2009. Caspase-6 activation in familial alzheimer disease brains carrying amyloid precursor protein or presenilin i or presenilin II mutations. J. Neuropathol. Exp. Neurol. 68, 1282–1293. doi:10.1097/NEN.0b013e3181c1da10

Albrecht, S., Bourdeau, M., Bennett, D., Mufson, E.J., Bhattacharjee, M., LeBlanc, A.C., 2007. Activation of caspase-6 in aging and mild cognitive impairment. Am. J. Pathol. 170, 1200–1209. doi:10.2353/ajpath.2007.060974

Alnemri, E.S., Livingston, D.J., Nicholson, D.W., Salvesen, G., Thornberry, N.A., Wong, W.W., Yuan, J., 1996. Human ICE/CED-3 protease nomenclature. Cell 87, 171.

Andersson, K.B., Winer, L.H., Mørk, H.K., Molkentin, J.D., Jaisser, F., 2010. Tamoxifen administration routes and dosage for inducible Cre-mediated gene disruption in mouse hearts. Transgenic Res. 19, 715–725. doi:10.1007/s11248-009-9342-4

Andrade, M.A., Bork, P., 1995. HEAT repeats in the Huntington's disease protein. Nat. Genet. 11, 115–116. doi:10.1038/ng1095-115

Andrew, S.E., Goldberg, Y.P., Kremer, B., Telenius, H., Theilmann, J., Adam, S., Starr, E., Squitieri, F., Lin, B., Kalchman, M.A., 1993. The relationship between trinucleotide (CAG) repeat length and clinical features of Huntington's disease. Nat. Genet. 4, 398–403. doi:10.1038/ng0893-398

Anisman, H., Merali, Z., 1999. Anhedonic and anxiogenic effects of cytokine exposure. Adv. Exp. Med. Biol. 461, 199–233. doi:10.1007/978-0-585-37970-8_12

Arrasate, M., Mitra, S., Schweitzer, E.S., Segal, M.R., Finkbeiner, S., 2004. Inclusion body formation reduces levels of mutant huntingtin and the risk of neuronal death. Nature 431, 805–810. doi:10.1038/nature02998

Aylward, E.H., Sparks, B.F., Field, K.M., Yallapragada, V., Shpritz, B.D., Rosenblatt, A., Brandt, J., Gourley, L.M., Liang, K., Zhou, H., Margolis, R.L., Ross, C.A., 2004. Onset and rate of striatal atrophy in preclinical Huntington disease. Neurology 63, 66–72.

Aziz, N.A., Swaab, D.F., Pijl, H., Roos, R.A.C., 2007. Hypothalamic dysfunction and neuroendocrine and metabolic alterations in Huntington's disease:

clinical consequences and therapeutic implications. Rev Neurosci 18, 223–251.
Baburamani, A.A., Miyakuni, Y., Vontell, R., Supramaniam, V.G., Svedin, P., Rutherford, M., Gressens, P., Mallard, C., Takeda, S., Thornton, C., Hagberg, H., 2015. Does Caspase-6 Have a Role in Perinatal Brain Injury? Dev. Neurosci. 0. doi:10.1159/000375368
Bär, K.J., Boettger, M.K., Andrich, J., Epplen, J.T., Fischer, F., Cordes, J., Koschke, M., Agelink, M.W., 2008. Cardiovagal modulation upon postural change is altered in Huntington's disease. Eur. J. Neurol. 15, 869–871. doi:10.1111/j.1468-1331.2008.02173.x
Beal, M.F., 2004. Excitotoxicity in Huntington's Disease, in: Excitotoxicity in Neurological Diseases. Springer US, Boston, MA, pp. 243–249. doi:10.1007/978-1-4419-8959-8_13
Becker, N., Munhoz, R.P., Raskin, S., Werneck, L.C., Teive, H.A.G., 2007. Non-choreic movement disorders as initial manifestations of Huntington's disease. Arq Neuropsiquiatr 65, 402–405.
Berta, T., Park, C.-K., Xu, Z.-Z., Xie, R.-G., Liu, T., Lü, N., Liu, Y.-C., Ji, R.-R., 2014. Extracellular caspase-6 drives murine inflammatory pain via microglial TNF-α secretion. J. Clin. Invest. 124, 1173–1186. doi:10.1172/JCI72230
Bezprozvanny, I., 2007. Inositol 1,4,5-tripshosphate receptor, calcium signalling and Huntington's disease. Subcell. Biochem. 45, 323–335.
Bezprozvanny, I., Hayden, M.R., 2004. Deranged neuronal calcium signaling and Huntington disease. Biochem. Biophys. Res. Commun. 322, 1310–1317. doi:10.1016/j.bbrc.2004.08.035
Bi, X., 2010. Alzheimer disease: update on basic mechanisms. J Am Osteopath Assoc 110, S3–9.
Biesmans, S., Meert, T.F., Bouwknecht, J.A., Acton, P.D., Davoodi, N., De Haes, P., Kuijlaars, J., Langlois, X., Matthews, L.J.R., Ver Donck, L., Hellings, N., Nuydens, R., 2013. Systemic immune activation leads to neuroinflammation and sickness behavior in mice. Mediators Inflamm. 2013, 271359. doi:10.1155/2013/271359
Bingol, B., Sheng, M., 2011. Deconstruction for reconstruction: the role of proteolysis in neural plasticity and disease. Neuron 69, 22–32. doi:10.1016/j.neuron.2010.11.006
Björkqvist, M., Wild, E.J., Thiele, J., Silvestroni, A., Andre, R., Lahiri, N., Raibon, E., Lee, R.V., Benn, C.L., Soulet, D., Magnusson, A., Woodman, B., Landles, C., Pouladi, M.A., Hayden, M.R., Khalili-Shirazi, A., Lowdell, M.W., Brundin, P., Bates, G.P., Leavitt, B.R., Möller, T., Tabrizi, S.J., 2008. A novel pathogenic pathway of immune activation detectable before clinical onset in Huntington's disease. J. Exp. Med. 205, 1869–1877. doi:10.1084/jem.20080178
Boatright, K.M., Salvesen, G.S., 2003. Mechanisms of caspase activation. Curr. Opin. Cell Biol. doi:10.1016/j.ceb.2003.10.009
Bouayed, J., Rammal, H., Soulimani, R., 2009. Oxidative stress and anxiety: relationship and cellular pathways. Oxid Med Cell Longev 2, 63–67.
Boucher, D., Blais, V., Denault, J.-B., 2012. Caspase-7 uses an exosite to

promote poly(ADP ribose) polymerase 1 proteolysis. Proc. Natl. Acad. Sci. U.S.A. 109, 5669–5674. doi:10.1073/pnas.1200934109
Bouchier-Hayes, L., Martin, S.J., 2002. CARD games in apoptosis and immunity. EMBO Rep. 3, 616–621. doi:10.1093/embo-reports/kvf139
Bradford, J., Shin, J.-Y., Roberts, M., Wang, C.-E., Li, X.-J., Li, S., 2009. Expression of mutant huntingtin in mouse brain astrocytes causes age-dependent neurological symptoms. Proc. Natl. Acad. Sci. U.S.A. 106, 22480–22485. doi:10.1073/pnas.0911503106
Butters, N., Wolfe, J., Granholm, E., Martone, M., 1986. An assessment of verbal recall, recognition and fluency abilities in patients with Huntington's disease. Cortex 22, 11–32.
Cain, K., Bratton, S.B., Cohen, G.M., 2002. The Apaf-1 apoptosome: a large caspase-activating complex. Biochimie 84, 203–214.
Caine, E.D., Ebert, M.H., Weingartner, H., 1977. An outline for the analysis of dementia. The memory disorder of Huntingtons disease. Neurology 27, 1087–1092.
Cao, Q., Wang, X.-J., Liu, C.-W., Liu, D.-F., Li, L.-F., Gao, Y.-Q., Su, X.-D., 2012. Inhibitory mechanism of caspase-6 phosphorylation revealed by crystal structures, molecular dynamics simulations, and biochemical assays. J. Biol. Chem. 287, 15371–15379. doi:10.1074/jbc.M112.351213
Carroll, J.B., Bates, G.P., Steffan, J., Saft, C., Tabrizi, S.J., 2015. Treating the whole body in Huntington's disease. Lancet Neurol 14, 1135–1142. doi:10.1016/S1474-4422(15)00177-5
Carroll, J.B., Lerch, J.P., Franciosi, S., Spreeuw, A., Bissada, N., Henkelman, R.M., Hayden, M.R., 2011a. Natural history of disease in the YAC128 mouse reveals a discrete signature of pathology in Huntington disease. Neurobiol. Dis. 43, 257–265. doi:10.1016/j.nbd.2011.03.018
Carroll, J.B., Southwell, A.L., Graham, R.K., Lerch, J.P., Ehrnhoefer, D.E., Cao, L.-P., Zhang, W.-N., Deng, Y., Bissada, N., Henkelman, R.M., Hayden, M.R., 2011b. Mice lacking caspase-2 are protected from behavioral changes, but not pathology, in the YAC128 model of Huntington disease. Mol Neurodegener 6, 59. doi:10.1186/1750-1326-6-59
Cattaneo, E., 2003. Dysfunction of wild-type huntingtin in Huntington disease. News Physiol. Sci. 18, 34–37.
Cattaneo, E., Zuccato, C., Tartari, M., 2005. Normal huntingtin function: an alternative approach to Huntington's disease. Nat. Rev. Neurosci. 6, 919–930. doi:10.1038/nrn1806
Cha, J.-H.J., 2007. Transcriptional signatures in Huntington's disease. Prog. Neurobiol. 83, 228–248. doi:10.1016/j.pneurobio.2007.03.004
Chiang, M.-C., Chern, Y., Juo, C.-G., 2011. The dysfunction of hepatic transcriptional factors in mice with Huntington's Disease. Biochim. Biophys. Acta 1812, 1111–1120. doi:10.1016/j.bbadis.2011.05.006
Chiu, E., Alexander, L., 1982. Causes of death in Huntington's disease. Med. J. Aust. 1, 153.
Chiu, G.S., Darmody, P.T., Walsh, J.P., Moon, M.L., Kwakwa, K.A., Bray, J.K., McCusker, R.H., Freund, G.G., 2014. Adenosine through the A2A adenosine

receptor increases IL-1β in the brain contributing to anxiety. Brain Behav. Immun. 41, 218–231. doi:10.1016/j.bbi.2014.05.018
Cookson, B.T., Brennan, M.A., 2001. Pro-inflammatory programmed cell death. Trends Microbiol. 9, 113–114.
Coppoolse, E.R., de Vroomen, M.J., van Gennip, F., Hersmus, B.J.M., van Haaren, M.J.J., 2005. Size does matter: cre-mediated somatic deletion efficiency depends on the distance between the target lox-sites. Plant Mol. Biol. 58, 687–698. doi:10.1007/s11103-005-7705-7
Couette, M., Bachoud-Levi, A.-C., Brugieres, P., Sieroff, E., Bartolomeo, P., 2008. Orienting of spatial attention in Huntington's Disease. Neuropsychologia 46, 1391–1400. doi:10.1016/j.neuropsychologia.2007.12.017
Cowling, V., Downward, J., 2002. Caspase-6 is the direct activator of caspase-8 in the cytochrome c-induced apoptosis pathway: absolute requirement for removal of caspase-6 prodomain. Cell Death Differ. 9, 1046–1056. doi:10.1038/sj.cdd.4401065
Cuervo, A.M., Dice, J.F., 2000. Age-related decline in chaperone-mediated autophagy. J. Biol. Chem. 275, 31505–31513. doi:10.1074/jbc.M002102200
Cusack, C.L., Swahari, V., Hampton Henley, W., Michael Ramsey, J., Deshmukh, M., 2013. Distinct pathways mediate axon degeneration during apoptosis and axon-specific pruning. Nat Commun 4, 1876. doi:10.1038/ncomms2910
Dale, M., van Duijn, E., 2015. Anxiety in Huntington's Disease. J Neuropsychiatry Clin Neurosci 27, 262–271. doi:10.1176/appi.neuropsych.14100265
Dalrymple, A., Wild, E.J., Joubert, R., Sathasivam, K., Björkqvist, M., Petersén, Å., Jackson, G.S., Isaacs, J.D., Kristiansen, M., Bates, G.P., Leavitt, B.R., Keir, G., Ward, M., Tabrizi, S.J., 2007. Proteomic profiling of plasma in Huntington's disease reveals neuroinflammatory activation and biomarker candidates. J. Proteome Res. 6, 2833–2840. doi:10.1021/pr0700753
Dantzer, R., Wollman, E., Vitkovic, L., Yirmiya, R., 1999. Cytokines and depression: fortuitous or causative association? Mol. Psychiatry 4, 328–332.
Dau, A., Gladding, C.M., Sepers, M.D., Raymond, L.A., 2014. Chronic blockade of extrasynaptic NMDA receptors ameliorates synaptic dysfunction and pro-death signaling in Huntington disease transgenic mice. Neurobiol. Dis. 62, 533–542. doi:10.1016/j.nbd.2013.11.013
Davies, S.W., Turmaine, M., Cozens, B.A., DiFiglia, M., Sharp, A.H., Ross, C.A., Scherzinger, E., Wanker, E.E., Mangiarini, L., Bates, G.P., 1997. Formation of neuronal intranuclear inclusions underlies the neurological dysfunction in mice transgenic for the HD mutation. Cell 90, 537–548.
Davis, B.K., Wen, H., Ting, J.P.-Y., 2011. The inflammasome NLRs in immunity, inflammation, and associated diseases. Annu. Rev. Immunol. 29, 707–735. doi:10.1146/annurev-immunol-031210-101405
de Calignon, A., Fox, L.M., Pitstick, R., Carlson, G.A., Bacskai, B.J., Spires-Jones, T.L., Hyman, B.T., 2010. Caspase activation precedes and leads to tangles. Nature 464, 1201–1204. doi:10.1038/nature08890
DiFiglia, M., 1990. Excitotoxic injury of the neostriatum: a model for Huntington's

disease. Trends Neurosci. 13, 286–289.
DiFiglia, M., Sapp, E., Chase, K.O., Davies, S.W., Bates, G.P., Vonsattel, J.P., Aronin, N., 1997. Aggregation of huntingtin in neuronal intranuclear inclusions and dystrophic neurites in brain. Science 277, 1990–1993.
Donovan, S.L., Schweers, B., Martins, R., Johnson, D., Dyer, M.A., 2006. Compensation by tumor suppressor genes during retinal development in mice and humans. BMC Biol. 4, 14. doi:10.1186/1741-7007-4-14
Du, C., Fang, M., Li, Y., Li, L., Wang, X., 2000. Smac, a mitochondrial protein that promotes cytochrome c-dependent caspase activation by eliminating IAP inhibition. Cell 102, 33–42. doi:10.1038/35036027
Duff, K., Paulsen, J.S., Beglinger, L.J., Langbehn, D.R., Stout, J.C., Predict-HD Investigators of the Huntington Study Group, 2007. Psychiatric symptoms in Huntington's disease before diagnosis: the predict-HD study. Biol. Psychiatry 62, 1341–1346. doi:10.1016/j.biopsych.2006.11.034
Duyao, M.P., Auerbach, A.B., Ryan, A., Persichetti, F., Barnes, G.T., McNeil, S.M., Ge, P., Vonsattel, J.P., Gusella, J.F., Joyner, A.L., 1995. Inactivation of the mouse Huntington's disease gene homolog Hdh. Science 269, 407–410.
Duyckaerts, C., Delatour, B., Potier, M.-C., 2009. Classification and basic pathology of Alzheimer disease. Acta Neuropathol. 118, 5–36. doi:10.1007/s00401-009-0532-1
Eckelman, B.P., Salvesen, G.S., 2006. The human anti-apoptotic proteins cIAP1 and cIAP2 bind but do not inhibit caspases. J. Biol. Chem. 281, 3254–3260. doi:10.1074/jbc.M510863200
Eckelman, B.P., Salvesen, G.S., Scott, F.L., 2006. Human inhibitor of apoptosis proteins: why XIAP is the black sheep of the family. EMBO Rep. 7, 988–994. doi:10.1038/sj.embor.7400795
Eckhart, L., Ban, J., Fischer, H., Tschachler, E., 2000. Caspase-14: analysis of gene structure and mRNA expression during keratinocyte differentiation. Biochem. Biophys. Res. Commun. 277, 655–659. doi:10.1006/bbrc.2000.3698
Ehrnhoefer, D.E., Butland, S.L., Pouladi, M.A., Hayden, M.R., 2009. Mouse models of Huntington disease: variations on a theme. Dis Model Mech 2, 123–129. doi:10.1242/dmm.002451
Ehrnhoefer, D.E., Skotte, N.H., Ladha, S., Nguyen, Y.T.N., Qiu, X., Deng, Y., Huynh, K.T., Engemann, S., Nielsen, S.M., Becanovic, K., Leavitt, B.R., Hasholt, L., Hayden, M.R., 2014. p53 increases caspase-6 expression and activation in muscle tissue expressing mutant huntingtin. Hum. Mol. Genet. 23, 717–729. doi:10.1093/hmg/ddt458
Ehrnhoefer, D.E., Skotte, N.H., Savill, J., Nguyen, Y.T.N., Ladha, S., Cao, L.-P., Dullaghan, E., Hayden, M.R., 2011a. A quantitative method for the specific assessment of caspase-6 activity in cell culture. PLoS ONE 6, e27680. doi:10.1371/journal.pone.0027680
Ehrnhoefer, D.E., Sutton, L., Hayden, M.R., 2011b. Small changes, big impact: posttranslational modifications and function of huntingtin in Huntington disease. Neuroscientist 17, 475–492. doi:10.1177/1073858410390378
Ehrnhoefer, D.E., Wong, B.K.Y., Hayden, M.R., 2011c. Convergent pathogenic

pathways in Alzheimer“s and Huntington”s diseases: shared targets for drug development. Nat Rev Drug Discov 10, 853–867. doi:10.1038/nrd3556
El-Daher, M.-T., Hangen, E., Bruyère, J., Poizat, G., Al-Ramahi, I., Pardo, R., Bourg, N., Souquere, S., Mayet, C., Pierron, G., Lévêque-Fort, S., Botas, J., Humbert, S., Saudou, F., 2015. Huntingtin proteolysis releases non-polyQ fragments that cause toxicity through dynamin 1 dysregulation. EMBO J. doi:10.15252/embj.201490808
Everett, K.D., Barghouthi, S., Speert, D.P., 1996. In vitro culture of murine peritoneal and alveolar macrophages modulates phagocytosis of Pseudomonas aeruginosa and glucose transport. J. Leukoc. Biol. 59, 539–544.
Faideau, M., Kim, J., Cormier, K., Gilmore, R., Welch, M., Auregan, G., Dufour, N., Guillermier, M., Brouillet, E., Hantraye, P., Déglon, N., Ferrante, R.J., Bonvento, G., 2010. In vivo expression of polyglutamine-expanded huntingtin by mouse striatal astrocytes impairs glutamate transport: a correlation with Huntington's disease subjects. Hum. Mol. Genet. 19, 3053–3067. doi:10.1093/hmg/ddq212
Fan, M.M.Y., Raymond, L.A., 2007. N-methyl-D-aspartate (NMDA) receptor function and excitotoxicity in Huntington's disease. Prog. Neurobiol. 81, 272–293. doi:10.1016/j.pneurobio.2006.11.003
Feil, S., Valtcheva, N., Feil, R., 2009. Inducible Cre mice. Methods Mol. Biol. 530, 343–363. doi:10.1007/978-1-59745-471-1_18
Filloux, F., Wagster, M.V., Folstein, S., Price, D.L., Hedreen, J.C., Dawson, T.M., Wamsley, J.K., 1990. Nigral dopamine type-1 receptors are reduced in Huntington's disease: a postmortem autoradiographic study using [3H]SCH 23390 and correlation with [3H]forskolin binding. Exp. Neurol. 110, 219–227.
Fink, S.L., Cookson, B.T., 2006. Caspase-1-dependent pore formation during pyroptosis leads to osmotic lysis of infected host macrophages. Cell. Microbiol. 8, 1812–1825. doi:10.1111/j.1462-5822.2006.00751.x
Finke, K., Bublak, P., Dose, M., Müller, H.J., Schneider, W.X., 2006. Parameter-based assessment of spatial and non-spatial attentional deficits in Huntington's disease. Brain 129, 1137–1151. doi:10.1093/brain/awl040
Finlay, B.L., Darlington, R.B., 1995. Linked regularities in the development and evolution of mammalian brains. Science 268, 1578–1584.
Fisher, B., Jeong, J.-H., Bryant, J., Anderson, S., Dignam, J., Fisher, E.R., Wolmark, N., National Surgical Adjuvant Breast and Bowel Project randomised clinical trials, 2004. Treatment of lymph-node-negative, oestrogen-receptor-positive breast cancer: long-term findings from National Surgical Adjuvant Breast and Bowel Project randomised clinical trials. Lancet 364, 858–868. doi:10.1016/S0140-6736(04)16981-X
Fisher, E.R., Hayden, M.R., 2014. Multisource ascertainment of Huntington disease in Canada: prevalence and population at risk. Mov. Disord. 29, 105–114. doi:10.1002/mds.25717
Forni, P.E., Scuoppo, C., Imayoshi, I., Taulli, R., Dastrù, W., Sala, V., Betz, U.A.K., Muzzi, P., Martinuzzi, D., Vercelli, A.E., Kageyama, R., Ponzetto, C., 2006. High levels of Cre expression in neuronal progenitors cause defects in

brain development leading to microencephaly and hydrocephaly. J. Neurosci. 26, 9593–9602. doi:10.1523/JNEUROSCI.2815-06.2006
Franciosi, S., Ryu, J.K., Shim, Y., Hill, A., Connolly, C., Hayden, M.R., McLarnon, J.G., Leavitt, B.R., 2012. Age-dependent neurovascular abnormalities and altered microglial morphology in the YAC128 mouse model of Huntington disease. Neurobiol. Dis. 45, 438–449. doi:10.1016/j.nbd.2011.09.003
Fuentes-Prior, P., Salvesen, G.S., 2004. The protein structures that shape caspase activity, specificity, activation and inhibition. Biochemical Journal 384, 201–232. doi:10.1042/BJ20041142
Gafni, J., Ellerby, L.M., 2002. Calpain activation in Huntington's disease. J. Neurosci. 22, 4842–4849.
Gafni, J., Papanikolaou, T., DeGiacomo, F., Holcomb, J., Chen, S., Menalled, L., Kudwa, A., Fitzpatrick, J., Miller, S., Ramboz, S., Tuunanen, P.I., Lehtimäki, K.K., Yang, X.W., Park, L., Kwak, S., Howland, D., Park, H., Ellerby, L.M., 2012. Caspase-6 activity in a BACHD mouse modulates steady-state levels of mutant huntingtin protein but is not necessary for production of a 586 amino acid proteolytic fragment. J. Neurosci. 32, 7454–7465. doi:10.1523/JNEUROSCI.6379-11.2012
Galvan, V., Chen, S., Lu, D., Logvinova, A., Goldsmith, P., Koo, E.H., Bredesen, D.E., 2002. Caspase cleavage of members of the amyloid precursor family of proteins. J. Neurochem. 82, 283–294.
Gamblin, T.C., Chen, F., Zambrano, A., Abraha, A., Lagalwar, S., Guillozet, A.L., Lu, M., Fu, Y., Garcia-Sierra, F., LaPointe, N., Miller, R., Berry, R.W., Binder, L.I., Cryns, V.L., 2003. Caspase cleavage of tau: linking amyloid and neurofibrillary tangles in Alzheimer's disease. Proc. Natl. Acad. Sci. U.S.A. 100, 10032–10037. doi:10.1073/pnas.1630428100
Gao, X., Dluzen, D.E., 2001. Tamoxifen abolishes estrogen's neuroprotective effect upon methamphetamine neurotoxicity of the nigrostriatal dopaminergic system. Neuroscience 103, 385–394.
Garcia-Calvo, M., Peterson, E.P., Leiting, B., Ruel, R., Nicholson, D.W., Thornberry, N.A., 1998. Inhibition of human caspases by peptide-based and macromolecular inhibitors. J. Biol. Chem. 273, 32608–32613.
Gatchel, J.R., Zoghbi, H.Y., 2005. Diseases of unstable repeat expansion: mechanisms and common principles. Nat. Rev. Genet. 6, 743–755. doi:10.1038/nrg1691
Gilliam, T.C., Bucan, M., MacDonald, M.E., Zimmer, M., Haines, J.L., Cheng, S.V., Pohl, T.M., Meyers, R.H., Whaley, W.L., Allitto, B.A., 1987. A DNA segment encoding two genes very tightly linked to Huntington's disease. Science 238, 950–952.
Godefroy, N., Foveau, B., Albrecht, S., Goodyer, C.G., LeBlanc, A.C., 2013. Expression and activation of caspase-6 in human fetal and adult tissues. PLoS ONE 8, e79313. doi:10.1371/journal.pone.0079313
Goldberg, Y.P., Nicholson, D.W., Rasper, D.M., Kalchman, M.A., Koide, H.B., Graham, R.K., Bromm, M., Kazemi-Esfarjani, P., Thornberry, N.A., Vaillancourt, J.P., Hayden, M.R., 1996. Cleavage of huntingtin by apopain, a proapoptotic cysteine protease, is modulated by the polyglutamine tract. Nat.

Genet. 13, 442–449. doi:10.1038/ng0896-442
Graham, R.K., Deng, Y., Carroll, J., Vaid, K., Cowan, C., Pouladi, M.A., Metzler, M., Bissada, N., Wang, L., Faull, R.L.M., Gray, M., Yang, X.W., Raymond, L.A., Hayden, M.R., 2010. Cleavage at the 586 amino acid caspase-6 site in mutant huntingtin influences caspase-6 activation in vivo. J. Neurosci. 30, 15019–15029. doi:10.1523/JNEUROSCI.2071-10.2010
Graham, R.K., Deng, Y., Slow, E.J., Haigh, B., Bissada, N., Lu, G., Pearson, J., Shehadeh, J., Bertram, L., Murphy, Z., Warby, S.C., Doty, C.N., Roy, S., Wellington, C.L., Leavitt, B.R., Raymond, L.A., Nicholson, D.W., Hayden, M.R., 2006. Cleavage at the caspase-6 site is required for neuronal dysfunction and degeneration due to mutant huntingtin. Cell 125, 1179–1191. doi:10.1016/j.cell.2006.04.026
Graham, R.K., Ehrnhoefer, D.E., Hayden, M.R., 2011. Caspase-6 and neurodegeneration. Trends Neurosci. 34, 646–656. doi:10.1016/j.tins.2011.09.001
Gray, M., Shirasaki, D.I., Cepeda, C., André, V.M., Wilburn, B., Lu, X.-H., Tao, J., Yamazaki, I., Li, S.-H., Sun, Y.E., Li, X.-J., Levine, M.S., Yang, X.W., 2008. Full-length human mutant huntingtin with a stable polyglutamine repeat can elicit progressive and selective neuropathogenesis in BACHD mice. J. Neurosci. 28, 6182–6195. doi:10.1523/JNEUROSCI.0857-08.2008
Grether, G.F., 2005. Environmental change, phenotypic plasticity, and genetic compensation. Am. Nat. 166, E115–23. doi:10.1086/432023
Group, 1993. A novel gene containing a trinucleotide repeat that is expanded and unstable on Huntington“s disease chromosomes. The Huntington”s Disease Collaborative Research Group. Cell 72, 971–983.
Gukovsky, I., Gukovskaya, A.S., Blinman, T.A., Zaninovic, V., Pandol, S.J., 1998. Early NF-kappaB activation is associated with hormone-induced pancreatitis. Am. J. Physiol. 275, G1402–14.
Guo, H., Albrecht, S., Bourdeau, M., Petzke, T., 2004. Active caspase-6 and caspase-6-cleaved tau in neuropil threads, neuritic plaques, and neurofibrillary tangles of Alzheimer's disease. The American journal of …. doi:10.1016/S0002-9440(10)63317-2
Guo, H., Pétrin, D., Zhang, Y., Bergeron, C., Goodyer, C.G., LeBlanc, A.C., 2006. Caspase-1 activation of caspase-6 in human apoptotic neurons. Cell Death Differ. 13, 285–292. doi:10.1038/sj.cdd.4401753
Gusella, J.F., Wexler, N.S., Conneally, P.M., Naylor, S.L., Anderson, M.A., Tanzi, R.E., Watkins, P.C., Ottina, K., Wallace, M.R., Sakaguchi, A.Y., 1983. A polymorphic DNA marker genetically linked to Huntington's disease. Nature 306, 234–238.
Halawani, D., Tessier, S., Anzellotti, D., Bennett, D.A., Latterich, M., LeBlanc, A.C., 2010. Identification of Caspase-6-mediated processing of the valosin containing protein (p97) in Alzheimer's disease: a novel link to dysfunction in ubiquitin proteasome system-mediated protein degradation. J. Neurosci. 30, 6132–6142. doi:10.1523/JNEUROSCI.5874-09.2010
Han, S.-J., Ko, H.-M., Choi, J.-H., Seo, K.H., Lee, H.-S., Choi, E.-K., Choi, I.-W., Lee, H.-K., Im, S.-Y., 2002. Molecular mechanisms for lipopolysaccharide-

induced biphasic activation of nuclear factor-kappa B (NF-kappa B). J. Biol. Chem. 277, 44715–44721. doi:10.1074/jbc.M202524200
Hardingham, G.E., Bading, H., 2010. Synaptic versus extrasynaptic NMDA receptor signalling: implications for neurodegenerative disorders. Nat. Rev. Neurosci. 11, 682–696. doi:10.1038/nrn2911
Hardingham, G.E., Bading, H., 2003. The Yin and Yang of NMDA receptor signalling. Trends Neurosci. 26, 81–89. doi:10.1016/S0166-2236(02)00040-1
Hardingham, G.E., Fukunaga, Y., Bading, H., 2002. Extrasynaptic NMDARs oppose synaptic NMDARs by triggering CREB shut-off and cell death pathways. Nat. Neurosci. 5, 405–414. doi:10.1038/nn835
Harjes, P., Wanker, E.E., 2003. The hunt for huntingtin function: interaction partners tell many different stories. Trends Biochem. Sci. 28, 425–433. doi:10.1016/S0968-0004(03)00168-3
Harno, E., Cottrell, E.C., White, A., 2013. Metabolic pitfalls of CNS Cre-based technology. Cell Metab. 18, 21–28. doi:10.1016/j.cmet.2013.05.019
Harper, P.S., 2014. Huntington's Disease in a Historical Context, in: Bates, G.P., Tabrizi, S.J., Jones, L. (Eds.), Huntingtons Disease. New York, pp. 3–24.
Harrison, D.C., Davis, R.P., Bond, B.C., Campbell, C.A., James, M.F., Parsons, A.A., Philpott, K.L., 2001. Caspase mRNA expression in a rat model of focal cerebral ischemia. Brain Res. Mol. Brain Res. 89, 133–146.
Hayashi, S., McMahon, A.P., 2002. Efficient recombination in diverse tissues by a tamoxifen-inducible form of Cre: a tool for temporally regulated gene activation/inactivation in the mouse. Dev. Biol. 244, 305–318. doi:10.1006/dbio.2002.0597
Hayden, M.R., Bloch, M., Fahy, M., 1988a. Predictive testing for Huntington's disease using linked DNA markers. N. Engl. J. Med. 319, 583–584. doi:10.1056/NEJM198809013190916
Hayden, M.R., Hewitt, J., Kastelein, J.J., Langlois, S., Wilson, R.D., Fox, S., Hilbert, C., Bloch, M., 1987. First-trimester prenatal diagnosis for Huntington's disease with DNA probes. Lancet 1, 1284–1285.
Hayden, M.R., Hewitt, J., Wasmuth, J.J., Kastelein, J.J., Langlois, S., Conneally, M., Haines, J., Smith, B., Hilbert, C., Allard, D., 1988b. A polymorphic DNA marker that represents a conserved expressed sequence in the region of the Huntington disease gene. Am. J. Hum. Genet. 42, 125–131.
Hägglund, J., Aquilonius, S.M., Eckernäs, S.A., Hartvig, P., Lundquist, H., Gullberg, P., Långström, B., 1987. Dopamine receptor properties in Parkinson“s disease and Huntington”s chorea evaluated by positron emission tomography using 11C-N-methyl-spiperone. Acta Neurol. Scand. 75, 87–94.
Hegde, R., Srinivasula, S.M., Zhang, Z., Wassell, R., Mukattash, R., Cilenti, L., DuBois, G., Lazebnik, Y., Zervos, A.S., Fernandes-Alnemri, T., Alnemri, E.S., 2002. Identification of Omi/HtrA2 as a mitochondrial apoptotic serine protease that disrupts inhibitor of apoptosis protein-caspase interaction. J. Biol. Chem. 277, 432–438. doi:10.1074/jbc.M109721200
Heise, C.E., Murray, J., Augustyn, K.E., Bravo, B., Chugha, P., Cohen, F., Giannetti, A.M., Gibbons, P., Hannoush, R.N., Hearn, B.R., Jaishankar, P., Ly, C.Q., Shah, K., Stanger, K., Steffek, M., Tang, Y., Zhao, X., Lewcock,

J.W., Renslo, A.R., Flygare, J., Arkin, M.R., 2012. Mechanistic and structural understanding of uncompetitive inhibitors of caspase-6. PLoS ONE 7, e50864. doi:10.1371/journal.pone.0050864
Hermel, E., Gafni, J., Propp, S.S., Leavitt, B.R., Wellington, C.L., Young, J.E., Hackam, A.S., Logvinova, A.V., Peel, A.L., Chen, S.F., Hook, V., Singaraja, R., Krajewski, S., Goldsmith, P.C., Ellerby, H.M., Hayden, M.R., Bredesen, D.E., Ellerby, L.M., 2004. Specific caspase interactions and amplification are involved in selective neuronal vulnerability in Huntington's disease. Cell Death Differ. 11, 424–438. doi:10.1038/sj.cdd.4401358
Hébert, J.M., McConnell, S.K., 2000. Targeting of cre to the Foxg1 (BF-1) locus mediates loxP recombination in the telencephalon and other developing head structures. Dev. Biol. 222, 296–306. doi:10.1006/dbio.2000.9732
Hickey, M.A., Kosmalska, A., Enayati, J., Cohen, R., Zeitlin, S., Levine, M.S., Chesselet, M.-F., 2008. Extensive early motor and non-motor behavioral deficits are followed by striatal neuronal loss in knock-in Huntington's disease mice. Neuroscience 157, 280–295. doi:10.1016/j.neuroscience.2008.08.041
Hirata, H., Takahashi, A., Kobayashi, S., Yonehara, S., Sawai, H., Okazaki, T., Yamamoto, K., Sasada, M., 1998. Caspases are activated in a branched protease cascade and control distinct downstream processes in Fas-induced apoptosis. J. Exp. Med. 187, 587–600.
Ho, L.W., Brown, R., Maxwell, M., Wyttenbach, A., Rubinsztein, D.C., 2001. Wild type Huntingtin reduces the cellular toxicity of mutant Huntingtin in mammalian cell models of Huntington's disease. J. Med. Genet. 38, 450–452. doi:10.1136/jmg.38.7.450
Hodgson, J.G., Agopyan, N., Gutekunst, C.-A., Leavitt, B.R., LePiane, F., Singaraja, R., Smith, D.J., Bissada, N., McCutcheon, K., Nasir, J., Jamot, L., Li, X.-J., Stevens, M.E., Rosemond, E., Roder, J.C., Phillips, A.G., Rubin, E.M., Hersch, S.M., Hayden, M.R., 1999. A YAC Mouse Model for Huntington’s Disease with Full-Length Mutant Huntingtin, Cytoplasmic Toxicity, and Selective Striatal Neurodegeneration. Neuron 23, 181–192. doi:10.1016/S0896-6273(00)80764-3
Holmes, C., Boche, D., Wilkinson, D., Yadegarfar, G., Hopkins, V., Bayer, A., Jones, R.W., Bullock, R., Love, S., Neal, J.W., Zotova, E., Nicoll, J.A.R., 2008. Long-term effects of Abeta42 immunisation in Alzheimer's disease: follow-up of a randomised, placebo-controlled phase I trial. Lancet 372, 216–223. doi:10.1016/S0140-6736(08)61075-2
Hoogeveen, A.T., Willemsen, R., Meyer, N., de Rooij, K.E., Roos, R.A., van Ommen, G.J., Galjaard, H., 1993. Characterization and localization of the Huntington disease gene product. Hum. Mol. Genet. 2, 2069–2073.
Hou, Y.C.C., Hannigan, A.M., Gorski, S.M., 2009. An executioner caspase regulates autophagy. Autophagy 5, 530–533.
Houde, C., Banks, K.G., Coulombe, N., Rasper, D., Grimm, E., Roy, S., Simpson, E.M., Nicholson, D.W., 2004. Caspase-7 expanded function and intrinsic expression level underlies strain-specific brain phenotype of caspase-3-null mice. J. Neurosci. 24, 9977–9984. doi:10.1523/JNEUROSCI.3356-04.2004

Hsiao, H.-Y., Chen, Y.-C., Chen, H.-M., Tu, P.-H., Chern, Y., 2013. A critical role of astrocyte-mediated nuclear factor-κB-dependent inflammation in Huntington's disease. Hum. Mol. Genet. 22, 1826–1842. doi:10.1093/hmg/ddt036
Hsiao, H.-Y., Chiu, F.-L., Chen, C.-M., Wu, Y.-R., Chen, H.-M., Chen, Y.-C., Kuo, H.-C., Chern, Y., 2014. Inhibition of soluble tumor necrosis factor is therapeutic in Huntington's disease. Hum. Mol. Genet. 23, 4328–4344. doi:10.1093/hmg/ddu151
Huesmann, G.R., Clayton, D.F., 2006. Dynamic role of postsynaptic caspase-3 and BIRC4 in zebra finch song-response habituation. Neuron 52, 1061–1072. doi:10.1016/j.neuron.2006.10.033
Huntington, G., 1872. On chorea. The Medical and Surgical Reporter 26, 317–321.
Hyman, B.T., Yuan, J., 2012. Apoptotic and non-apoptotic roles of caspases in neuronal physiology and pathophysiology. Nat. Rev. Neurosci. 13, 395–406. doi:10.1038/nrn3228
Irmler, M., Thome, M., Hahne, M., Schneider, P., Hofmann, K., Steiner, V., Bodmer, J.L., Schröter, M., Burns, K., Mattmann, C., Rimoldi, D., French, L.E., Tschopp, J., 1997. Inhibition of death receptor signals by cellular FLIP. Nature 388, 190–195. doi:10.1038/40657
Kaindl, A.M., Degos, V., Peineau, S., Gouadon, E., Chhor, V., Loron, G., Le Charpentier, T., Josserand, J., Ali, C., Vivien, D., Collingridge, G.L., Lombet, A., Issa, L., Rene, F., Loeffler, J.-P., Kavelaars, A., Verney, C., Mantz, J., Gressens, P., 2012. Activation of microglial N-methyl-D-aspartate receptors triggers inflammation and neuronal cell death in the developing and mature brain. Ann. Neurol. 72, 536–549. doi:10.1002/ana.23626
Karam, A., Tebbe, L., Weber, C., Messaddeq, N., Morlé, L., Kessler, P., Wolfrum, U., Trottier, Y., 2015. A novel function of Huntingtin in the cilium and retinal ciliopathy in Huntington's disease mice. Neurobiol. Dis. 80, 15–28. doi:10.1016/j.nbd.2015.05.008
Karch, C.M., Goate, A.M., 2015. Alzheimer's disease risk genes and mechanisms of disease pathogenesis. Biol. Psychiatry 77, 43–51. doi:10.1016/j.biopsych.2014.05.006
Kaushal, V., Dye, R., Pakavathkumar, P., Foveau, B., Flores, J., Hyman, B., Ghetti, B., Koller, B.H., LeBlanc, A.C., 2015. Neuronal NLRP1 inflammasome activation of Caspase-1 coordinately regulates inflammatory interleukin-1-beta production and axonal degeneration-associated Caspase-6 activation. Cell Death Differ. doi:10.1038/cdd.2015.16
Kay, C., Fisher, E.M.C., Hayden, M.R., 2014. Epidemiology, in: Bates, G.P., Tabrizi, S.J., Jones, L. (Eds.), Huntington's Disease. New York, pp. 131–164.
Kegel, K.B., Kim, M., Sapp, E., McIntyre, C., Castaño, J.G., Aronin, N., DiFiglia, M., 2000. Huntingtin expression stimulates endosomal-lysosomal activity, endosome tubulation, and autophagy. J. Neurosci. 20, 7268–7278.
Kennedy, N.J., Kataoka, T., Tschopp, J., Budd, R.C., 1999. Caspase activation is required for T cell proliferation. J. Exp. Med. 190, 1891–1896.
Kiermayer, C., Conrad, M., Schneider, M., Schmidt, J., Brielmeier, M., 2007.

Optimization of spatiotemporal gene inactivation in mouse heart by oral application of tamoxifen citrate. Genesis 45, 11–16. doi:10.1002/dvg.20244
Kim, Y.J., Yi, Y., Sapp, E., Wang, Y., Ben Cuiffo, Kegel, K.B., Qin, Z.-H., Aronin, N., DiFiglia, M., 2001. Caspase 3-cleaved N-terminal fragments of wild-type and mutant huntingtin are present in normal and Huntington's disease brains, associate with membranes, and undergo calpain-dependent proteolysis. Proc. Natl. Acad. Sci. U.S.A. 98, 12784–12789. doi:10.1073/pnas.221451398
Kitamura, Y., Shimohama, S., Kamoshima, W., Matsuoka, Y., Nomura, Y., Taniguchi, T., 1997. Changes of p53 in the brains of patients with Alzheimer's disease. Biochem. Biophys. Res. Commun. 232, 418–421. doi:10.1006/bbrc.1997.6301
Klaiman, G., Champagne, N., LeBlanc, A.C., 2009. Self-activation of Caspase-6 in vitro and in vivo: Caspase-6 activation does not induce cell death in HEK293T cells. Biochim. Biophys. Acta 1793, 592–601. doi:10.1016/j.bbamcr.2008.12.004
Kobayashi, H., Nolan, A., Naveed, B., Hoshino, Y., Segal, L.N., Fujita, Y., Rom, W.N., Weiden, M.D., 2011. Neutrophils activate alveolar macrophages by producing caspase-6-mediated cleavage of IL-1 receptor-associated kinase-M. J. Immunol. 186, 403–410. doi:10.4049/jimmunol.1001906
Kremer, B., Goldberg, P., Andrew, S.E., Theilmann, J., Telenius, H., Zeisler, J., Squitieri, F., Lin, B., Bassett, A., Almqvist, E., 1994. A worldwide study of the Huntington's disease mutation. The sensitivity and specificity of measuring CAG repeats. N. Engl. J. Med. 330, 1401–1406. doi:10.1056/NEJM199405193302001
Kwan, W., Magnusson, A., Chou, A., Adame, A., Carson, M.J., Kohsaka, S., Masliah, E., Möller, T., Ransohoff, R., Tabrizi, S.J., Björkqvist, M., Muchowski, P.J., 2012a. Bone marrow transplantation confers modest benefits in mouse models of Huntington's disease. J. Neurosci. 32, 133–142. doi:10.1523/JNEUROSCI.4846-11.2012
Kwan, W., Träger, U., Davalos, D., Chou, A., Bouchard, J., Andre, R., Miller, A., Weiss, A., Giorgini, F., Cheah, C., Möller, T., Stella, N., Akassoglou, K., Tabrizi, S.J., Muchowski, P.J., 2012b. Mutant huntingtin impairs immune cell migration in Huntington disease. J. Clin. Invest. 122, 4737–4747. doi:10.1172/JCI64484
Labadorf, A., Hoss, A.G., Lagomarsino, V., Latourelle, J.C., Hadzi, T.C., Bregu, J., MacDonald, M.E., Gusella, J.F., Chen, J.-F., Akbarian, S., Weng, Z., Myers, R.H., 2015. RNA Sequence Analysis of Human Huntington Disease Brain Reveals an Extensive Increase in Inflammatory and Developmental Gene Expression. PLoS ONE 10, e0143563. doi:10.1371/journal.pone.0143563
Landles, C., Sathasivam, K., Weiss, A., Woodman, B., Moffitt, H., Finkbeiner, S., Sun, B., Gafni, J., Ellerby, L.M., Trottier, Y., Richards, W.G., Osmand, A., Paganetti, P., Bates, G.P., 2010. Proteolysis of mutant huntingtin produces an exon 1 fragment that accumulates as an aggregated protein in neuronal nuclei in Huntington disease. J. Biol. Chem. 285, 8808–8823. doi:10.1074/jbc.M109.075028

Landles, C., Weiss, A., Franklin, S., Howland, D., Bates, G., 2012. Caspase-6 does not contribute to the proteolysis of mutant huntingtin in the HdhQ150 knock-in mouse model of Huntington's disease. PLoS Curr 4, e4fd085bfc9973. doi:10.1371/4fd085bfc9973

Lawrence, A.D., Sahakian, B.J., Hodges, J.R., Rosser, A.E., Lange, K.W., Robbins, T.W., 1996. Executive and mnemonic functions in early Huntington's disease. Brain 119 (Pt 5), 1633–1645.

Leavitt, B.R., Guttman, J.A., Hodgson, J.G., Kimel, G.H., Singaraja, R., Vogl, A.W., Hayden, M.R., 2001. Wild-type huntingtin reduces the cellular toxicity of mutant huntingtin in vivo. Am. J. Hum. Genet. 68, 313–324. doi:10.1086/318207

Leavitt, B.R., Van Raamsdonk, J.M., Shehadeh, J., Fernandes, H., Murphy, Z., Graham, R.K., Wellington, C.L., Raymond, L.A., Hayden, M.R., 2006. Wild-type huntingtin protects neurons from excitotoxicity. J. Neurochem. 96, 1121–1129. doi:10.1111/j.1471-4159.2005.03605.x

LeBlanc, A., Liu, H., Goodyer, C., Bergeron, C., Hammond, J., 1999. Caspase-6 role in apoptosis of human neurons, amyloidogenesis, and Alzheimer's disease. J. Biol. Chem. 274, 23426–23436.

LeBlanc, A.C., Ramcharitar, J., Afonso, V., Hamel, E., Bennett, D.A., Pakavathkumar, P., Albrecht, S., 2014. Caspase-6 activity in the CA1 region of the hippocampus induces age-dependent memory impairment. Cell Death Differ. 21, 696–706. doi:10.1038/cdd.2013.194

Lee, J.-Y., Ristow, M., Lin, X., White, M.F., Magnuson, M.A., Hennighausen, L., 2006. RIP-Cre revisited, evidence for impairments of pancreatic beta-cell function. J. Biol. Chem. 281, 2649–2653. doi:10.1074/jbc.M512373200

Lee, J.W., Kim, M.R., Soung, Y.H., Nam, S.W., Kim, S.H., Lee, J.Y., Yoo, N.J., Lee, S.H., 2006. Mutational analysis of the CASP6 gene in colorectal and gastric carcinomas. APMIS 114, 646–650. doi:10.1111/j.1600-0463.2006.apm_417.x

Leitman, J., Ulrich Hartl, F., Lederkremer, G.Z., 2013. Soluble forms of polyQ-expanded huntingtin rather than large aggregates cause endoplasmic reticulum stress. Nat Commun 4, 2753. doi:10.1038/ncomms3753

Lens, S.M.A., Kataoka, T., Fortner, K.A., Tinel, A., Ferrero, I., MacDonald, R.H., Hahne, M., Beermann, F., Attinger, A., Orbea, H.-A., Budd, R.C., Tschopp, J., 2002. The caspase 8 inhibitor c-FLIP(L) modulates T-cell receptor-induced proliferation but not activation-induced cell death of lymphocytes. Molecular and Cellular Biology 22, 5419–5433. doi:10.1128/MCB.22.15.5419-5433.2002

Lerch, J.P., Carroll, J.B., Dorr, A., Spring, S., Evans, A.C., Hayden, M.R., Sled, J.G., Henkelman, R.M., 2008. Cortical thickness measured from MRI in the YAC128 mouse model of Huntington's disease. NeuroImage 41, 243–251. doi:10.1016/j.neuroimage.2008.02.019

Lerner, R.P., Trejo Martinez, L.D.C.G., Zhu, C., Chesselet, M.-F., Hickey, M.A., 2012. Striatal atrophy and dendritic alterations in a knock-in mouse model of Huntington's disease. Brain Res. Bull. 87, 571–578. doi:10.1016/j.brainresbull.2012.01.012

Li, S.H., Lam, S., Cheng, A.L., Li, X.J., 2000. Intranuclear huntingtin increases the expression of caspase-1 and induces apoptosis. Hum. Mol. Genet. 9, 2859–2867.
Li, Y., Choi, P.S., Casey, S.C., Felsher, D.W., 2014. Activation of Cre recombinase alone can induce complete tumor regression. PLoS ONE 9, e107589. doi:10.1371/journal.pone.0107589
Li, Z., Jo, J., Jia, J.-M., Lo, S.-C., Whitcomb, D.J., Jiao, S., Cho, K., Sheng, M., 2010. Caspase-3 activation via mitochondria is required for long-term depression and AMPA receptor internalization. Cell 141, 859–871. doi:10.1016/j.cell.2010.03.053
Li, Z., Sheng, M., 2012. Caspases in synaptic plasticity. Mol Brain 5, 15. doi:10.1186/1756-6606-5-15
Liu, L., Zou, P., Zheng, L., Linarelli, L.E., Amarell, S., Passaro, A., Liu, D., Cheng, Z., 2015. Tamoxifen reduces fat mass by boosting reactive oxygen species. Cell Death Dis 6, e1586. doi:10.1038/cddis.2014.553
Loonstra, A., Vooijs, M., Beverloo, H.B., Allak, B.A., van Drunen, E., Kanaar, R., Berns, A., Jonkers, J., 2001. Growth inhibition and DNA damage induced by Cre recombinase in mammalian cells. Proc. Natl. Acad. Sci. U.S.A. 98, 9209–9214. doi:10.1073/pnas.161269798
Louis, E.D., Lee, P., Quinn, L., Marder, K., 1999. Dystonia in Huntington's disease: prevalence and clinical characteristics. Mov. Disord. 14, 95–101.
Mace, P.D., Riedl, S.J., Salvesen, G.S., 2014. Caspase enzymology and activation mechanisms. Meth. Enzymol. 544, 161–178. doi:10.1016/B978-0-12-417158-9.00007-8
MacLachlan, T.K., El-Deiry, W.S., 2002. Apoptotic threshold is lowered by p53 transactivation of caspase-6. Proc. Natl. Acad. Sci. U.S.A. 99, 9492–9497. doi:10.1073/pnas.132241599
Maelfait, J., Vercammen, E., Janssens, S., Schotte, P., Haegman, M., Magez, S., Beyaert, R., 2008. Stimulation of Toll-like receptor 3 and 4 induces interleukin-1beta maturation by caspase-8. J. Exp. Med. 205, 1967–1973. doi:10.1084/jem.20071632
Magnuson, M.A., Burlison, J.S., 2007. Caveats and considerations for performing pancreas-specific gene manipulations in the mouse. Diabetes Obes Metab 9 Suppl 2, 5–13. doi:10.1111/j.1463-1326.2007.00771.x
Magnusson-Lind, A., Davidsson, M., Silajdžić, E., Hansen, C., McCourt, A.C., Tabrizi, S.J., Björkqvist, M., 2014. Skeletal muscle atrophy in R6/2 mice - altered circulating skeletal muscle markers and gene expression profile changes. J Huntingtons Dis 3, 13–24. doi:10.3233/JHD-130075
Maiuri, M.C., Zalckvar, E., Kimchi, A., Kroemer, G., 2007. Self-eating and self-killing: crosstalk between autophagy and apoptosis. Nat. Rev. Mol. Cell Biol. 8, 741–752. doi:10.1038/nrm2239
Mangiarini, L., Sathasivam, K., Seller, M., Cozens, B., Harper, A., Hetherington, C., Lawton, M., Trottier, Y., Lehrach, H., Davies, S.W., Bates, G.P., 1996. Exon 1 of the HD gene with an expanded CAG repeat is sufficient to cause a progressive neurological phenotype in transgenic mice. Cell 87, 493–506.
Marcora, E., Kennedy, M.B., 2010. The Huntington“s disease mutation impairs

Huntingtin”s role in the transport of NF-κB from the synapse to the nucleus. Hum. Mol. Genet. 19, 4373–4384. doi:10.1093/hmg/ddq358
Martin, D.D.O., Hayden, M.R., 2015. Post-translational myristoylation at the cross roads of cell death, autophagy and neurodegeneration. Biochem. Soc. Trans. 43, 229–234. doi:10.1042/BST20140281
Martin, D.D.O., Heit, R.J., Yap, M.C., Davidson, M.W., Hayden, M.R., Berthiaume, L.G., 2014. Identification of a post-translationally myristoylated autophagy-inducing domain released by caspase cleavage of huntingtin. Hum. Mol. Genet. 23, 3166–3179. doi:10.1093/hmg/ddu027
Martin, D.D.O., Ladha, S., Ehrnhoefer, D.E., Hayden, M.R., 2015. Autophagy in Huntington disease and huntingtin in autophagy. Trends Neurosci. 38, 26–35. doi:10.1016/j.tins.2014.09.003
Martinon, F., Burns, K., Tschopp, J., 2002. The inflammasome: a molecular platform triggering activation of inflammatory caspases and processing of proIL-beta. Mol. Cell 10, 417–426.
Mathelier, A., Zhao, X., Zhang, A.W., Parcy, F., Worsley-Hunt, R., Arenillas, D.J., Buchman, S., Chen, C.-Y., Chou, A., Ienasescu, H., Lim, J., Shyr, C., Tan, G., Zhou, M., Lenhard, B., Sandelin, A., Wasserman, W.W., 2014. JASPAR 2014: an extensively expanded and updated open-access database of transcription factor binding profiles. Nucleic Acids Res. 42, D142–7. doi:10.1093/nar/gkt997
McIlwain, D.R., Berger, T., Mak, T.W., 2015. Caspase functions in cell death and disease. Cold Spring Harb Perspect Biol 7, a026716. doi:10.1101/cshperspect.a026716
McNeil, S.M., Novelletto, A., Srinidhi, J., Barnes, G., Kornbluth, I., Altherr, M.R., Wasmuth, J.J., Gusella, J.F., MacDonald, M.E., Myers, R.H., 1997. Reduced penetrance of the Huntington's disease mutation. Hum. Mol. Genet. 6, 775–779.
McStay, G.P., Salvesen, G.S., Green, D.R., 2008. Overlapping cleavage motif selectivity of caspases: implications for analysis of apoptotic pathways. Cell Death Differ. 15, 322–331. doi:10.1038/sj.cdd.4402260
Meier, I.D., Bernreuther, C., Tilling, T., Neidhardt, J., Wong, Y.W., Schulze, C., Streichert, T., Schachner, M., 2010. Short DNA sequences inserted for gene targeting can accidentally interfere with off-target gene expression. FASEB J. 24, 1714–1724. doi:10.1096/fj.09-140749
Melik, Z., Kobal, J., Cankar, K., Strucl, M., 2012. Microcirculation response to local cooling in patients with Huntington's disease. J. Neurol. 259, 921–928. doi:10.1007/s00415-011-6279-3
Menalled, L., El-Khodor, B.F., Patry, M., Suárez-Fariñas, M., Orenstein, S.J., Zahasky, B., Leahy, C., Wheeler, V., Yang, X.W., MacDonald, M., Morton, A.J., Bates, G., Leeds, J., Park, L., Howland, D., Signer, E., Tobin, A., Brunner, D., 2009. Systematic behavioral evaluation of Huntington's disease transgenic and knock-in mouse models. Neurobiol. Dis. 35, 319–336. doi:10.1016/j.nbd.2009.05.007
Menalled, L., Lutz, C., Ramboz, S., Brunner, D., Lager, B., Noble, S., Park, L., Howland, D., 2014. A Field Guide to Working with Mouse Models of

Huntington’s Disease 1–52.
Menalled, L.B., Chesselet, M.-F., 2002. Mouse models of Huntington's disease. Trends Pharmacol. Sci. 23, 32–39.
Mende-Mueller, L.M., Toneff, T., Hwang, S.R., Chesselet, M.-F., Hook, V.Y., 2001. Tissue-specific proteolysis of Huntingtin (htt) in human brain: evidence of enhanced levels of N- and C-terminal htt fragments in Huntington's disease striatum. J. Neurosci. 21, 1830–1837.
Metzler, M., Gan, L., Mazarei, G., Graham, R.K., Liu, L., Bissada, N., Lu, G., Leavitt, B.R., Hayden, M.R., 2010. Phosphorylation of huntingtin at Ser421 in YAC128 neurons is associated with protection of YAC128 neurons from NMDA-mediated excitotoxicity and is modulated by PP1 and PP2A. J. Neurosci. 30, 14318–14329. doi:10.1523/JNEUROSCI.1589-10.2010
Metzler, M., Gan, L., Wong, T.P., Liu, L., Helm, J., Liu, L., Georgiou, J., Wang, Y., Bissada, N., Cheng, K., Roder, J.C., Wang, Y.T., Hayden, M.R., 2007. NMDA receptor function and NMDA receptor-dependent phosphorylation of huntingtin is altered by the endocytic protein HIP1. J. Neurosci. 27, 2298–2308. doi:10.1523/JNEUROSCI.5175-06.2007
Meyers, C.A., 1999. Mood and cognitive disorders in cancer patients receiving cytokine therapy. Adv. Exp. Med. Biol. 461, 75–81. doi:10.1007/978-0-585-37970-8_5
Miller, J.P., Holcomb, J., Al-Ramahi, I., de Haro, M., Gafni, J., Zhang, N., Kim, E., Sanhueza, M., Torcassi, C., Kwak, S., Botas, J., Hughes, R.E., Ellerby, L.M., 2010. Matrix metalloproteinases are modifiers of huntingtin proteolysis and toxicity in Huntington's disease. Neuron 67, 199–212. doi:10.1016/j.neuron.2010.06.021
Milnerwood, A.J., Gladding, C.M., Pouladi, M.A., Kaufman, A.M., Hines, R.M., Boyd, J.D., Ko, R.W.Y., Vasuta, O.C., Graham, R.K., Hayden, M.R., Murphy, T.H., Raymond, L.A., 2010. Early increase in extrasynaptic NMDA receptor signaling and expression contributes to phenotype onset in Huntington's disease mice. Neuron 65, 178–190. doi:10.1016/j.neuron.2010.01.008
Mocarski, E.S., Upton, J.W., Kaiser, W.J., 2012. Viral infection and the evolution of caspase 8-regulated apoptotic and necrotic death pathways. Nat. Rev. Immunol. 12, 79–88. doi:10.1038/nri3131
Narkilahti, S., Pitkänen, A., 2005. Caspase 6 expression in the rat hippocampus during epileptogenesis and epilepsy. Neuroscience 131, 887–897. doi:10.1016/j.neuroscience.2004.12.013
Nasir, J., Floresco, S.B., O'Kusky, J.R., Diewert, V.M., Richman, J.M., Zeisler, J., Borowski, A., Marth, J.D., Phillips, A.G., Hayden, M.R., 1995. Targeted disruption of the Huntington's disease gene results in embryonic lethality and behavioral and morphological changes in heterozygotes. Cell 81, 811–823.
Neuwald, A.F., Hirano, T., 2000. HEAT repeats associated with condensins, cohesins, and other complexes involved in chromosome-related functions. Genome Res. 10, 1445–1452. doi:10.1101/gr.147400
Nicholson, D.W., Ali, A., Thornberry, N.A., Vaillancourt, J.P., Ding, C.K., Gallant, M., Gareau, Y., Griffin, P.R., Labelle, M., Lazebnik, Y.A., 1995. Identification and inhibition of the ICE/CED-3 protease necessary for mammalian

apoptosis. Nature 376, 37–43. doi:10.1038/376037a0
Nikolaev, A., McLaughlin, T., O'Leary, D.D.M., Tessier-Lavigne, M., 2009. APP binds DR6 to trigger axon pruning and neuron death via distinct caspases. Nature 457, 981–989. doi:10.1038/nature07767
Norman, J.M., Cohen, G.M., Bampton, E.T.W., 2010. The in vitro cleavage of the hAtg proteins by cell death proteases. Autophagy 6, 1042–1056.
O'Neill, K., Chen, S., Diaz Brinton, R., 2004. Impact of the selective estrogen receptor modulator, tamoxifen, on neuronal outgrowth and survival following toxic insults associated with aging and Alzheimer's disease. Exp. Neurol. 188, 268–278. doi:10.1016/j.expneurol.2004.01.014
Ochaba, J., Lukacsovich, T., Csikos, G., Zheng, S., Margulis, J., Salazar, L., Mao, K., Lau, A.L., Yeung, S.Y., Humbert, S., Saudou, F., Klionsky, D.J., Finkbeiner, S., Zeitlin, S.O., Marsh, J.L., Housman, D.E., Thompson, L.M., Steffan, J.S., 2014. Potential function for the Huntingtin protein as a scaffold for selective autophagy. Proc. Natl. Acad. Sci. U.S.A. 111, 16889–16894. doi:10.1073/pnas.1420103111
Olmos, G., Lladó, J., 2014. Tumor necrosis factor alpha: a link between neuroinflammation and excitotoxicity. Mediators Inflamm. 2014, 861231–12. doi:10.1155/2014/861231
Olson, N.E., Graves, J.D., Shu, G.L., Ryan, E.J., Clark, E.A., 2003. Caspase activity is required for stimulated B lymphocytes to enter the cell cycle. J. Immunol. 170, 6065–6072.
Ona, V.O., Li, M., Vonsattel, J.P., Andrews, L.J., Khan, S.Q., Chung, W.M., Frey, A.S., Menon, A.S., Li, X.J., Stieg, P.E., Yuan, J., Penney, J.B., Young, A.B., Cha, J.H., Friedlander, R.M., 1999. Inhibition of caspase-1 slows disease progression in a mouse model of Huntington's disease. Nature 399, 263–267. doi:10.1038/20446
Orth, K., Chinnaiyan, A.M., Garg, M., Froelich, C.J., Dixit, V.M., 1996. The CED-3/ICE-like protease Mch2 is activated during apoptosis and cleaves the death substrate lamin A. J. Biol. Chem. 271, 16443–16446. doi:10.1080/13557858.2014.907388
Orvoen, S., Pla, P., Gardier, A.M., Saudou, F., David, D.J., 2012. Huntington's disease knock-in male mice show specific anxiety-like behaviour and altered neuronal maturation. Neurosci. Lett. 507, 127–132. doi:10.1016/j.neulet.2011.11.063
Panov, A.V., Gutekunst, C.-A., Leavitt, B.R., Hayden, M.R., Burke, J.R., Strittmatter, W.J., Greenamyre, J.T., 2002. Early mitochondrial calcium defects in Huntington's disease are a direct effect of polyglutamines. Nat. Neurosci. 5, 731–736. doi:10.1038/nn884
Park, K.J., Grosso, C.A., Aubert, I., Kaplan, D.R., Miller, F.D., 2010. p75NTR-dependent, myelin-mediated axonal degeneration regulates neural connectivity in the adult brain. Nat. Neurosci. 13, 559–566. doi:10.1038/nn.2513
Parsons, M.P., Raymond, L.A., 2014. Extrasynaptic NMDA receptor involvement in central nervous system disorders. Neuron 82, 279–293. doi:10.1016/j.neuron.2014.03.030

Paulsen, J.S., 2011. Cognitive impairment in Huntington disease: diagnosis and treatment. Curr Neurol Neurosci Rep 11, 474–483. doi:10.1007/s11910-011-0215-x
Paulsen, J.S., Ready, R.E., Hamilton, J.M., Mega, M.S., Cummings, J.L., 2001. Neuropsychiatric aspects of Huntington's disease. J. Neurol. Neurosurg. Psychiatr. 71, 310–314. doi:10.1136/jnnp.71.3.310
Petersén, Å., Björkqvist, M., 2006. Hypothalamic-endocrine aspects in Huntington's disease. Eur. J. Neurosci. 24, 961–967. doi:10.1111/j.1460-9568.2006.04985.x
Pitsavos, C., Panagiotakos, D.B., Papageorgiou, C., Tsetsekou, E., Soldatos, C., Stefanadis, C., 2006. Anxiety in relation to inflammation and coagulation markers, among healthy adults: the ATTICA study. Atherosclerosis 185, 320–326. doi:10.1016/j.atherosclerosis.2005.06.001
Pla, P., Orvoen, S., Benstaali, C., Dodier, S., Gardier, A.M., David, D.J., Humbert, S., Saudou, F., 2013. Huntingtin acts non cell-autonomously on hippocampal neurogenesis and controls anxiety-related behaviors in adult mouse. PLoS ONE 8, e73902. doi:10.1371/journal.pone.0073902
Pla, P., Orvoen, S., Saudou, F., David, D.J., Humbert, S., 2014. Mood disorders in Huntington's disease: from behavior to cellular and molecular mechanisms. Front Behav Neurosci 8, 135. doi:10.3389/fnbeh.2014.00135
Politis, M., Lahiri, N., Niccolini, F., Su, P., Wu, K., Giannetti, P., Scahill, R.I., Turkheimer, F.E., Tabrizi, S.J., Piccini, P., 2015. Increased central microglial activation associated with peripheral cytokine levels in premanifest Huntington's disease gene carriers. Neurobiol. Dis. 83, 115–121. doi:10.1016/j.nbd.2015.08.011
Pompl, P.N., Yemul, S., Xiang, Z., Ho, L., Haroutunian, V., Purohit, D., Mohs, R., Pasinetti, G.M., 2003. Caspase gene expression in the brain as a function of the clinical progression of Alzheimer disease. Arch. Neurol. 60, 369–376.
Pop, C., Salvesen, G.S., 2009. Human caspases: activation, specificity, and regulation. J. Biol. Chem. 284, 21777–21781. doi:10.1074/jbc.R800084200
Porsolt, R.D., Bertin, A., Jalfre, M., 1977. Behavioral despair in mice: a primary screening test for antidepressants. Arch Int Pharmacodyn Ther 229, 327–336.
Portales-Casamar, E., Arenillas, D., Lim, J., Swanson, M.I., Jiang, S., McCallum, A., Kirov, S., Wasserman, W.W., 2009. The PAZAR database of gene regulatory information coupled to the ORCA toolkit for the study of regulatory sequences. Nucleic Acids Res. 37, D54–60. doi:10.1093/nar/gkn783
Pouladi, M.A., Graham, R.K., Karasinska, J.M., Xie, Y., Santos, R.D., Petersén, Å., Hayden, M.R., 2009. Prevention of depressive behaviour in the YAC128 mouse model of Huntington disease by mutation at residue 586 of huntingtin. Brain 132, 919–932. doi:10.1093/brain/awp006
Pouladi, M.A., Morton, A.J., Hayden, M.R., 2013. Choosing an animal model for the study of Huntington's disease. Nat. Rev. Neurosci. 14, 708–721. doi:10.1038/nrn3570
Pouladi, M.A., Stanek, L.M., Xie, Y., Franciosi, S., Southwell, A.L., Deng, Y., Butland, S., Zhang, W., Cheng, S.H., Shihabuddin, L.S., Hayden, M.R., 2012.

Marked differences in neurochemistry and aggregates despite similar behavioural and neuropathological features of Huntington disease in the full-length BACHD and YAC128 mice. Hum. Mol. Genet. 21, 2219–2232. doi:10.1093/hmg/dds037

Pouladi, M.A., Xie, Y., Skotte, N.H., Ehrnhoefer, D.E., Graham, R.K., Kim, J.E., Bissada, N., Yang, X.W., Paganetti, P., Friedlander, R.M., Leavitt, B.R., Hayden, M.R., 2010. Full-length huntingtin levels modulate body weight by influencing insulin-like growth factor 1 expression. Hum. Mol. Genet. 19, 1528–1538. doi:10.1093/hmg/ddq026

Qiu, L., Rivera-Pérez, J.A., Xu, Z., 2011. A non-specific effect associated with conditional transgene expression based on Cre-loxP strategy in mice. PLoS ONE 6, e18778. doi:10.1371/journal.pone.0018778

Quarrell, O.W.J., 2014. Juvenile Huntington's Disease, in: Bates, G.P., Tabrizi, S.J., Jones, L. (Eds.), Huntingtons Disease. New York, pp. 66–85.

Ramcharitar, J., Afonso, V.M., Albrecht, S., Bennett, D.A., LeBlanc, A.C., 2013a. Caspase-6 activity predicts lower episodic memory ability in aged individuals. Neurobiol. Aging 34, 1815–1824. doi:10.1016/j.neurobiolaging.2013.01.007

Ramcharitar, J., Albrecht, S., Afonso, V.M., Kaushal, V., Bennett, D.A., LeBlanc, A.C., 2013b. Cerebrospinal fluid tau cleaved by caspase-6 reflects brain levels and cognition in aging and Alzheimer disease. J. Neuropathol. Exp. Neurol. 72, 824–832. doi:10.1097/NEN.0b013e3182a0a39f

Reinert, R.B., Kantz, J., Misfeldt, A.A., Poffenberger, G., Gannon, M., Brissova, M., Powers, A.C., 2012. Tamoxifen-Induced Cre-loxP Recombination Is Prolonged in Pancreatic Islets of Adult Mice. PLoS ONE 7, e33529. doi:10.1371/journal.pone.0033529

Ribchester, R.R., Thomson, D., Wood, N.I., Hinks, T., Gillingwater, T.H., Wishart, T.M., Court, F.A., Morton, A.J., 2004. Progressive abnormalities in skeletal muscle and neuromuscular junctions of transgenic mice expressing the Huntington's disease mutation. Eur. J. Neurosci. 20, 3092–3114. doi:10.1111/j.1460-9568.2004.03783.x

Richfield, E.K., O'Brien, C.F., Eskin, T., Shoulson, I., 1991. Heterogeneous dopamine receptor changes in early and late Huntington's disease. Neurosci. Lett. 132, 121–126.

Ridley, R.M., Frith, C.D., Crow, T.J., Conneally, P.M., 1988. Anticipation in Huntington's disease is inherited through the male line but may originate in the female. J. Med. Genet. 25, 589–595.

Rigamonti, D., Bauer, J.H., De-Fraja, C., Conti, L., Sipione, S., Sciorati, C., Clementi, E., Hackam, A., Hayden, M.R., Li, Y., Cooper, J.K., Ross, C.A., Govoni, S., Vincenz, C., Cattaneo, E., 2000. Wild-type huntingtin protects from apoptosis upstream of caspase-3. J. Neurosci. 20, 3705–3713.

Rissman, R.A., Poon, W.W., Blurton-Jones, M., Oddo, S., Torp, R., Vitek, M.P., LaFerla, F.M., Rohn, T.T., Cotman, C.W., 2004. Caspase-cleavage of tau is an early event in Alzheimer disease tangle pathology. J. Clin. Invest. 114, 121–130. doi:10.1172/JCI20640

Rogers, S., Wells, R., Rechsteiner, M., 1986. Amino acid sequences common to rapidly degraded proteins: the PEST hypothesis. Science 234, 364–368.

Rosas, H.D., Koroshetz, W.J., Chen, Y.I., Skeuse, C., Vangel, M., Cudkowicz, M.E., Caplan, K., Marek, K., Seidman, L.J., Makris, N., Jenkins, B.G., Goldstein, J.M., 2003. Evidence for more widespread cerebral pathology in early HD: an MRI-based morphometric analysis. Neurology 60, 1615–1620.
Rui, Y.-N., Xu, Z., Patel, B., Chen, Z., Chen, D., Tito, A., David, G., Sun, Y., Stimming, E.F., Bellen, H.J., Cuervo, A.M., Zhang, S., 2015. Huntingtin functions as a scaffold for selective macroautophagy. Nat. Cell Biol. doi:10.1038/ncb3101
Runne, H., Kuhn, A., Wild, E.J., Pratyaksha, W., Kristiansen, M., Isaacs, J.D., Régulier, E., Delorenzi, M., Tabrizi, S.J., Luthi-Carter, R., 2007. Analysis of potential transcriptomic biomarkers for Huntington's disease in peripheral blood. Proc. Natl. Acad. Sci. U.S.A. 104, 14424–14429. doi:10.1073/pnas.0703652104
Rust, C., Wild, N., Bernt, C., Vennegeerts, T., Wimmer, R., Beuers, U., 2009. Bile acid-induced apoptosis in hepatocytes is caspase-6-dependent. J. Biol. Chem. 284, 2908–2916. doi:10.1074/jbc.M804585200
Ruzankina, Y., Pinzon-Guzman, C., Asare, A., Ong, T., Pontano, L., Cotsarelis, G., Zediak, V.P., Velez, M., Bhandoola, A., Brown, E.J., 2007. Deletion of the developmentally essential gene ATR in adult mice leads to age-related phenotypes and stem cell loss. Cell Stem Cell 1, 113–126. doi:10.1016/j.stem.2007.03.002
Salvesen, G.S., Duckett, C.S., 2002. IAP proteins: blocking the road to death's door. Nat. Rev. Mol. Cell Biol. 3, 401–410. doi:10.1038/nrm830
Sassone, J., Colciago, C., Cislaghi, G., Silani, V., Ciammola, A., 2009. Huntington's disease: the current state of research with peripheral tissues. Exp. Neurol. 219, 385–397. doi:10.1016/j.expneurol.2009.05.012
Schauvliege, R., Vanrobaeys, J., Schotte, P., Beyaert, R., 2002. Caspase-11 gene expression in response to lipopolysaccharide and interferon-gamma requires nuclear factor-kappa B and signal transducer and activator of transcription (STAT) 1. J. Biol. Chem. 277, 41624–41630. doi:10.1074/jbc.M207852200
Schmidt-Supprian, M., Rajewsky, K., 2007. Vagaries of conditional gene targeting. Nat. Immunol. 8, 665–668. doi:10.1038/ni0707-665
Schneider, J.L., Cuervo, A.M., 2014. Liver autophagy: much more than just taking out the trash. Nat Rev Gastroenterol Hepatol 11, 187–200. doi:10.1038/nrgastro.2013.211
Schoenmann, Z., Assa-Kunik, E., Tiomny, S., Minis, A., Haklai-Topper, L., Arama, E., Yaron, A., 2010. Axonal degeneration is regulated by the apoptotic machinery or a NAD+-sensitive pathway in insects and mammals. J. Neurosci. 30, 6375–6386. doi:10.1523/JNEUROSCI.0922-10.2010
Sedvall, G., Karlsson, P., Lundin, A., Anvret, M., Suhara, T., Halldin, C., Farde, L., 1994. Dopamine D1 receptor number--a sensitive PET marker for early brain degeneration in Huntington's disease. Eur Arch Psychiatry Clin Neurosci 243, 249–255.
Semaka, A., Kay, C., Doty, C.N., Collins, J.A., Tam, N., Hayden, M.R., 2013. High frequency of intermediate alleles on Huntington disease-associated

haplotypes in British Columbia's general population. Am. J. Med. Genet. B Neuropsychiatr. Genet. 162B, 864–871. doi:10.1002/ajmg.b.32193
Sepers, M.D., Raymond, L.A., 2014. Mechanisms of synaptic dysfunction and excitotoxicity in Huntington's disease. Drug Discov. Today 19, 990–996. doi:10.1016/j.drudis.2014.02.006
Shabanzadeh, A.P., D'Onofrio, P.M., Monnier, P.P., Koeberle, P.D., 2015. Targeting caspase-6 and caspase-8 to promote neuronal survival following ischemic stroke. Cell Death Dis 6, e1967. doi:10.1038/cddis.2015.272
Shalini, S., Dorstyn, L., Dawar, S., Kumar, S., 2014. Old, new and emerging functions of caspases. Cell Death Differ. doi:10.1038/cdd.2014.216
Shehadeh, J., Fernandes, H.B., Zeron Mullins, M.M., Graham, R.K., Leavitt, B.R., Hayden, M.R., Raymond, L.A., 2006. Striatal neuronal apoptosis is preferentially enhanced by NMDA receptor activation in YAC transgenic mouse model of Huntington disease. Neurobiol. Dis. 21, 392–403. doi:10.1016/j.nbd.2005.08.001
Shen, C., Xiong, W.C., Mei, L., 2014. Caspase-3, shears for synapse pruning. Dev. Cell 28, 604–606. doi:10.1016/j.devcel.2014.03.010
Shen, D.F., Chang, M.A., Matteson, D.M., Buggage, R., Kozhich, A.T., Chan, C.C., 2000. Biphasic ocular inflammatory response to endotoxin-induced uveitis in the mouse. Arch. Ophthalmol. 118, 521–527.
Shi, J., Zhao, Y., Wang, Y., Gao, W., Ding, J., Li, P., Hu, L., Shao, F., 2014. Inflammatory caspases are innate immune receptors for intracellular LPS. Nature 514, 187–192. doi:10.1038/nature13683
Shiotsuki, H., Yoshimi, K., Shimo, Y., Funayama, M., Takamatsu, Y., Ikeda, K., Takahashi, R., Kitazawa, S., Hattori, N., 2010. A rotarod test for evaluation of motor skill learning. J. Neurosci. Methods 189, 180–185. doi:10.1016/j.jneumeth.2010.03.026
Simon, D.J., Weimer, R.M., McLaughlin, T., Kallop, D., Stanger, K., Yang, J., O'Leary, D.D.M., Hannoush, R.N., Tessier-Lavigne, M., 2012. A caspase cascade regulating developmental axon degeneration. J. Neurosci. 32, 17540–17553. doi:10.1523/JNEUROSCI.3012-12.2012
Singh, A.B., Kaushal, V., Megyesi, J.K., Shah, S.V., Kaushal, G.P., 2002. Cloning and expression of rat caspase-6 and its localization in renal ischemia/reperfusion injury. Kidney Int. 62, 106–115. doi:10.1046/j.1523-1755.2002.00427.x
Skraastad, M.I., Van de Vosse, E., Belfroid, R., Höld, K., Vegter-van der Vlis, M., Sandkuijl, L.A., Bakker, E., van Ommen, G.J., 1992. Significant linkage disequilibrium between the Huntington disease gene and the loci D4S10 and D4S95 in the Dutch population. Am. J. Hum. Genet. 51, 730–735.
Slee, E.A., Harte, M.T., Kluck, R.M., Wolf, B.B., Casiano, C.A., Newmeyer, D.D., Wang, H.G., Reed, J.C., Nicholson, D.W., Alnemri, E.S., Green, D.R., Martin, S.J., 1999. Ordering the cytochrome c-initiated caspase cascade: hierarchical activation of caspases-2, -3, -6, -7, -8, and -10 in a caspase-9-dependent manner. J. Cell Biol. 144, 281–292.
Slow, E.J., Graham, R.K., Osmand, A.P., Devon, R.S., Lu, G., Deng, Y., Pearson, J., Vaid, K., Bissada, N., Wetzel, R., Leavitt, B.R., Hayden, M.R.,

2005. Absence of behavioral abnormalities and neurodegeneration in vivo despite widespread neuronal huntingtin inclusions. Proc. Natl. Acad. Sci. U.S.A. 102, 11402–11407. doi:10.1073/pnas.0503634102
Slow, E.J., van Raamsdonk, J., Rogers, D., Coleman, S.H., Graham, R.K., Deng, Y., Oh, R., Bissada, N., Hossain, S.M., Yang, Y.-Z., Li, X.-J., Simpson, E.M., Gutekunst, C.-A., Leavitt, B.R., Hayden, M.R., 2003. Selective striatal neuronal loss in a YAC128 mouse model of Huntington disease. Hum. Mol. Genet. 12, 1555–1567. doi:10.1093/hmg/ddg169
Smith, A.J., De Sousa, M.A., Kwabi-Addo, B., Heppell-Parton, A., Impey, H., Rabbitts, P., 1995. A site-directed chromosomal translocation induced in embryonic stem cells by Cre-loxP recombination. Nat. Genet. 9, 376–385. doi:10.1038/ng0495-376
Smith, L., 2011. Good planning and serendipity: exploiting the Cre/Lox system in the testis. Reproduction 141, 151–161. doi:10.1530/REP-10-0404
Smith, R., Brundin, P., Li, J.-Y., 2005. Synaptic dysfunction in Huntington's disease: a new perspective. Cell. Mol. Life Sci. 62, 1901–1912. doi:10.1007/s00018-005-5084-5
Southwell, A.L., Ko, J., Patterson, P.H., 2009. Intrabody gene therapy ameliorates motor, cognitive, and neuropathological symptoms in multiple mouse models of Huntington's disease. J. Neurosci. 29, 13589–13602. doi:10.1523/JNEUROSCI.4286-09.2009
Southwell, A.L., Warby, S.C., Carroll, J.B., Doty, C.N., Skotte, N.H., Zhang, W., Villanueva, E.B., Kovalik, V., Xie, Y., Pouladi, M.A., Collins, J.A., Yang, X.W., Franciosi, S., Hayden, M.R., 2013. A fully humanized transgenic mouse model of Huntington disease. Hum. Mol. Genet. 22, 18–34. doi:10.1093/hmg/dds397
Suzuki, A., Kusakai, G.-I., Kishimoto, A., Shimojo, Y., Miyamoto, S., Ogura, T., Ochiai, A., Esumi, H., 2004. Regulation of caspase-6 and FLIP by the AMPK family member ARK5. Oncogene 23, 7067–7075. doi:10.1038/sj.onc.1207963
Swerdlow, N.R., Paulsen, J., Braff, D.L., Butters, N., Geyer, M.A., Swenson, M.R., 1995. Impaired prepulse inhibition of acoustic and tactile startle response in patients with Huntington's disease. J. Neurol. Neurosurg. Psychiatr. 58, 192–200.
Tabrizi, S.J., Cleeter, M.W., Xuereb, J., Taanman, J.W., Cooper, J.M., Schapira, A.H., 1999. Biochemical abnormalities and excitotoxicity in Huntington's disease brain. Ann. Neurol. 45, 25–32.
Tai, Y.F., Pavese, N., Gerhard, A., Tabrizi, S.J., Barker, R.A., Brooks, D.J., Piccini, P., 2007. Microglial activation in presymptomatic Huntington's disease gene carriers. Brain 130, 1759–1766. doi:10.1093/brain/awm044
Talanian, R.V., Quinlan, C., Trautz, S., Hackett, M.C., Mankovich, J.A., Banach, D., Ghayur, T., Brady, K.D., Wong, W.W., 1997. Substrate specificities of caspase family proteases. J. Biol. Chem. 272, 9677–9682.
Tebbenkamp, A.T.N., Green, C., Xu, G., Denovan-Wright, E.M., Rising, A.C., Fromholt, S.E., Brown, H.H., Swing, D., Mandel, R.J., Tessarollo, L., Borchelt, D.R., 2011. Transgenic mice expressing caspase-6-derived N-

terminal fragments of mutant huntingtin develop neurologic abnormalities with predominant cytoplasmic inclusion pathology composed largely of a smaller proteolytic derivative. Hum. Mol. Genet. 20, 2770–2782. doi:10.1093/hmg/ddr176

Telenius, H., Kremer, H.P., Theilmann, J., Andrew, S.E., Almqvist, E., Anvret, M., Greenberg, C., Greenberg, J., Lucotte, G., Squitieri, F., 1993. Molecular analysis of juvenile Huntington disease: the major influence on (CAG)n repeat length is the sex of the affected parent. Hum. Mol. Genet. 2, 1535–1540.

Thompson, J.E., Phillips, R.J., Erdjument-Bromage, H., Tempst, P., Ghosh, S., 1995. I kappa B-beta regulates the persistent response in a biphasic activation of NF-kappa B. Cell 80, 573–582.

Thornberry, N.A., Rano, T.A., Peterson, E.P., Rasper, D.M., Timkey, T., Garcia-Calvo, M., Houtzager, V.M., Nordstrom, P.A., Roy, S., Vaillancourt, J.P., Chapman, K.T., Nicholson, D.W., 1997. A combinatorial approach defines specificities of members of the caspase family and granzyme B. Functional relationships established for key mediators of apoptosis. J. Biol. Chem. 272, 17907–17911.

Thyagarajan, B., Guimarães, M.J., Groth, A.C., Calos, M.P., 2000. Mammalian genomes contain active recombinase recognition sites. Gene 244, 47–54.

Tiwari, M., Sharma, L.K., Vanegas, D., Callaway, D.A., Bai, Y., Lechleiter, J.D., Herman, B., 2014. A nonapoptotic role for CASP2/caspase 2: modulation of autophagy. Autophagy 10, 1054–1070. doi:10.4161/auto.28528

Tolosa, L., Caraballo-Miralles, V., Olmos, G., Lladó, J., 2011. TNF-α potentiates glutamate-induced spinal cord motoneuron death via NF-κB. Mol. Cell. Neurosci. 46, 176–186. doi:10.1016/j.mcn.2010.09.001

Träger, U., Andre, R., Lahiri, N., Magnusson-Lind, A., Weiss, A., Grueninger, S., McKinnon, C., Sirinathsinghji, E., Kahlon, S., Pfister, E.L., Moser, R., Hummerich, H., Antoniou, M., Bates, G.P., Luthi-Carter, R., Lowdell, M.W., Björkqvist, M., Ostroff, G.R., Aronin, N., Tabrizi, S.J., 2014a. HTT-lowering reverses Huntington's disease immune dysfunction caused by NFκB pathway dysregulation. Brain 137, 819–833. doi:10.1093/brain/awt355

Träger, U., Andre, R., Magnusson-Lind, A., Miller, J.R.C., Connolly, C., Weiss, A., Grueninger, S., Silajdžić, E., Smith, D.L., Leavitt, B.R., Bates, G.P., Björkqvist, M., Tabrizi, S.J., 2014b. Characterisation of immune cell function in fragment and full-length Huntington's disease mouse models. Neurobiol. Dis. 73C, 388–398. doi:10.1016/j.nbd.2014.10.012

Trottier, Y., Lutz, Y., Stevanin, G., Imbert, G., Devys, D., Cancel, G., Saudou, F., Weber, C., David, G., Tora, L., 1995. Polyglutamine expansion as a pathological epitope in Huntington's disease and four dominant cerebellar ataxias. Nature 378, 403–406. doi:10.1038/378403a0

Troy, C.M., Jean, Y.Y., 2015. Caspases: therapeutic targets in neurologic disease. Neurotherapeutics 12, 42–48. doi:10.1007/s13311-014-0307-9

Turlo, K.A., Gallaher, S.D., Vora, R., Laski, F.A., Iruela-Arispe, M.L., 2010. When Cre-mediated recombination in mice does not result in protein loss. Genetics 186, 959–967. doi:10.1534/genetics.110.121608

Turner, P.V., Brabb, T., Pekow, C., Vasbinder, M.A., 2011. Administration of substances to laboratory animals: routes of administration and factors to consider. J. Am. Assoc. Lab. Anim. Sci. 50, 600–613.
Uribe, V., Wong, B.K.Y., Graham, R.K., Cusack, C.L., Skotte, N.H., Pouladi, M.A., Xie, Y., Feinberg, K., Ou, Y., Ouyang, Y., Deng, Y., Franciosi, S., Bissada, N., Spreeuw, A., Zhang, W., Ehrnhoefer, D.E., Vaid, K., Miller, F.D., Deshmukh, M., Howland, D., Hayden, M.R., 2012. Rescue from excitotoxicity and axonal degeneration accompanied by age-dependent behavioral and neuroanatomical alterations in caspase-6-deficient mice. Hum. Mol. Genet. 21, 1954–1967. doi:10.1093/hmg/dds005
Valmiki, M.G., Ramos, J.W., 2009. Death effector domain-containing proteins. Cell. Mol. Life Sci. 66, 814–830. doi:10.1007/s00018-008-8489-0
Van de Craen, M., Declercq, W., Van den brande, I., Fiers, W., Vandenabeele, P., 1999. The proteolytic procaspase activation network: an in vitro analysis. Cell Death Differ. 6, 1117–1124. doi:10.1038/sj.cdd.4400589
van der Burg, J.M.M., Björkqvist, M., Brundin, P., 2009. Beyond the brain: widespread pathology in Huntington's disease. Lancet Neurol 8, 765–774. doi:10.1016/S1474-4422(09)70178-4
van Dijk, J.G., van der Velde, E.A., Roos, R.A., Bruyn, G.W., 1986. Juvenile Huntington disease. Hum. Genet. 73, 235–239.
van Raam, B.J., Ehrnhoefer, D.E., Hayden, M.R., Salvesen, G.S., 2013. Intrinsic cleavage of receptor-interacting protein kinase-1 by caspase-6. Cell Death Differ. 20, 86–96. doi:10.1038/cdd.2012.98
Van Raamsdonk, J.M., Gibson, W.T., Pearson, J., Murphy, Z., Lu, G., Leavitt, B.R., Hayden, M.R., 2006a. Body weight is modulated by levels of full-length huntingtin. Hum. Mol. Genet. 15, 1513–1523. doi:10.1093/hmg/ddl072
Van Raamsdonk, J.M., Metzler, M., Slow, E., Pearson, J., Schwab, C., Carroll, J., Graham, R.K., Leavitt, B.R., Hayden, M.R., 2007a. Phenotypic abnormalities in the YAC128 mouse model of Huntington disease are penetrant on multiple genetic backgrounds and modulated by strain. Neurobiol. Dis. 26, 189–200. doi:10.1016/j.nbd.2006.12.010
Van Raamsdonk, J.M., Murphy, Z., Selva, D.M., Hamidizadeh, R., Pearson, J., Petersén, Å., Björkqvist, M., Muir, C., Mackenzie, I.R., Hammond, G.L., Vogl, A.W., Hayden, M.R., Leavitt, B.R., 2007b. Testicular degeneration in Huntington disease. Neurobiol. Dis. 26, 512–520. doi:10.1016/j.nbd.2007.01.006
Van Raamsdonk, J.M., Murphy, Z., Slow, E.J., Leavitt, B.R., Hayden, M.R., 2005a. Selective degeneration and nuclear localization of mutant huntingtin in the YAC128 mouse model of Huntington disease. Hum. Mol. Genet. 14, 3823–3835. doi:10.1093/hmg/ddi407
Van Raamsdonk, J.M., Pearson, J., Murphy, Z., Hayden, M.R., Leavitt, B.R., 2006b. Wild-type huntingtin ameliorates striatal neuronal atrophy but does not prevent other abnormalities in the YAC128 mouse model of Huntington disease. BMC Neurosci 7, 80. doi:10.1186/1471-2202-7-80
Van Raamsdonk, J.M., Pearson, J., Rogers, D.A., Bissada, N., Vogl, A.W., Hayden, M.R., Leavitt, B.R., 2005b. Loss of wild-type huntingtin influences

motor dysfunction and survival in the YAC128 mouse model of Huntington disease. Hum. Mol. Genet. 14, 1379–1392. doi:10.1093/hmg/ddi147
Van Raamsdonk, J.M., Pearson, J., Slow, E.J., Hossain, S.M., Leavitt, B.R., Hayden, M.R., 2005c. Cognitive dysfunction precedes neuropathology and motor abnormalities in the YAC128 mouse model of Huntington's disease. J. Neurosci. 25, 4169–4180. doi:10.1523/JNEUROSCI.0590-05.2005
Van Raamsdonk, J.M., Warby, S.C., Hayden, M.R., 2007c. Selective degeneration in YAC mouse models of Huntington disease. Brain Res. Bull. 72, 124–131. doi:10.1016/j.brainresbull.2006.10.018
van Vugt, J.P., van Hilten, B.J., Roos, R.A., 1996. Hypokinesia in Huntington's disease. Mov. Disord. 11, 384–388. doi:10.1002/mds.870110406
Vandenabeele, P., Galluzzi, L., Vanden Berghe, T., Kroemer, G., 2010. Molecular mechanisms of necroptosis: an ordered cellular explosion. Nat. Rev. Mol. Cell Biol. 11, 700–714. doi:10.1038/nrm2970
Velázquez-Delgado, E.M., Hardy, J.A., 2012. Phosphorylation regulates assembly of the caspase-6 substrate-binding groove. Structure 20, 742–751. doi:10.1016/j.str.2012.02.003
Verhagen, A.M., Ekert, P.G., Pakusch, M., Silke, J., Connolly, L.M., Reid, G.E., Moritz, R.L., Simpson, R.J., Vaux, D.L., 2000. Identification of DIABLO, a mammalian protein that promotes apoptosis by binding to and antagonizing IAP proteins. Cell 102, 43–53. doi:10.1038/35036027
Vira, S., Mekhedov, E., Humphrey, G., Blank, P.S., 2010. Fluorescent-labeled antibodies: Balancing functionality and degree of labeling. Anal. Biochem. 402, 146–150. doi:10.1016/j.ab.2010.03.036
Vogel, C.M., Drury, I., Terry, L.C., Young, A.B., 1991. Myoclonus in adult Huntington's disease. Ann. Neurol. 29, 213–215. doi:10.1002/ana.410290217
Vonsattel, J.P., Myers, R.H., Stevens, T.J., Ferrante, R.J., Bird, E.D., Richardson, E.P., 1985. Neuropathological classification of Huntington's disease. J. Neuropathol. Exp. Neurol. 44, 559–577.
Waldron-Roby, E., Hoerauf, J., Arbez, N., Zhu, S., Kulcsar, K., Ross, C.A., 2015. Sox11 Reduces Caspase-6 Cleavage and Activity. PLoS ONE 10, e0141439. doi:10.1371/journal.pone.0141439
Waldron-Roby, E., Ratovitski, T., Wang, X., Jiang, M., Watkin, E., Arbez, N., Graham, R.K., Hayden, M.R., Hou, Z., Mori, S., Swing, D., Pletnikov, M., Duan, W., Tessarollo, L., Ross, C.A., 2012. Transgenic mouse model expressing the caspase 6 fragment of mutant huntingtin. J. Neurosci. 32, 183–193. doi:10.1523/JNEUROSCI.1305-11.2012
Waldvogel, H.J., Kim, E.H., Tippett, L.J., Vonsattel, J.P., Faull, R.L.M., 2014. Neuropathology in the Human Brain, in: Bates, G.P., Tabrizi, S.J., Jones, L. (Eds.), Huntingtons Disease. New York, pp. 185–217.
Walker, L.G., Walker, M.B., Heys, S.D., Lolley, J., Wesnes, K., Eremin, O., 1997. The psychological and psychiatric effects of rIL-2 therapy: a controlled clinical trial. Psychooncology 6, 290–301. doi:10.1002/(SICI)1099-1611(199712)6:4<290::AID-PON283>3.0.CO;2-G
Wallen, W.J., Belanger, M.P., Wittnich, C., 2001. Sex hormones and the selective estrogen receptor modulator tamoxifen modulate weekly body

weights and food intakes in adolescent and adult rats. J. Nutr. 131, 2351–2357.
Wang, H., Yu, S.-W., Koh, D.W., Lew, J., Coombs, C., Bowers, W., Federoff, H.J., Poirier, G.G., Dawson, T.M., Dawson, V.L., 2004. Apoptosis-inducing factor substitutes for caspase executioners in NMDA-triggered excitotoxic neuronal death. J. Neurosci. 24, 10963–10973. doi:10.1523/JNEUROSCI.3461-04.2004
Wang, S.-Z., Liu, B.-H., Tao, H.W., Xia, K., Zhang, L.I., 2009. A genetic strategy for stochastic gene activation with regulated sparseness (STARS). PLoS ONE 4, e4200. doi:10.1371/journal.pone.0004200
Wang, X.-J., Cao, Q., Liu, X., Wang, K.-T., Mi, W., Zhang, Y., Li, L.-F., LeBlanc, A.C., Su, X.-D., 2010. Crystal structures of human caspase 6 reveal a new mechanism for intramolecular cleavage self-activation. EMBO Rep. 11, 841–847. doi:10.1038/embor.2010.141
Wang, X.-J., Cao, Q., Zhang, Y., Su, X.-D., 2015. Activation and regulation of caspase-6 and its role in neurodegenerative diseases. Annu. Rev. Pharmacol. Toxicol. 55, 553–572. doi:10.1146/annurev-pharmtox-010814-124414
Warby, S.C., Doty, C.N., Graham, R.K., Carroll, J.B., Yang, Y.-Z., Singaraja, R.R., Overall, C.M., Hayden, M.R., 2008. Activated caspase-6 and caspase-6-cleaved fragments of huntingtin specifically colocalize in the nucleus. Hum. Mol. Genet. 17, 2390–2404. doi:10.1093/hmg/ddn139
Wasmuth, J.J., Hewitt, J., Smith, B., Allard, D., Haines, J.L., Skarecky, D., Partlow, E., Hayden, M.R., 1988. A highly polymorphic locus very tightly linked to the Huntington's disease gene. Nature 332, 734–736. doi:10.1038/332734a0
Watanabe, C., Shu, G.L., Zheng, T.S., Flavell, R.A., Clark, E.A., 2008. Caspase 6 regulates B cell activation and differentiation into plasma cells. J. Immunol. 181, 6810–6819.
Weingart, C.L., Broitman-Maduro, G., Dean, G., Newman, S., Peppler, M., Weiss, A.A., 1999. Fluorescent labels influence phagocytosis of Bordetella pertussis by human neutrophils. Infect. Immun. 67, 4264–4267.
Wellington, C.L., 2000. Inhibiting Caspase Cleavage of Huntingtin Reduces Toxicity and Aggregate Formation in Neuronal and Nonneuronal Cells. Journal of Biological Chemistry 275, 19831–19838. doi:10.1074/jbc.M001475200
Wellington, C.L., Ellerby, L.M., Gutekunst, C.A., Rogers, D., Warby, S., Graham, R.K., Loubser, O., van Raamsdonk, J., Singaraja, R., Yang, Y.Z., Gafni, J., Bredesen, D., Hersch, S.M., Leavitt, B.R., Roy, S., Nicholson, D.W., Hayden, M.R., 2002. Caspase cleavage of mutant huntingtin precedes neurodegeneration in Huntington's disease. J. Neurosci. 22, 7862–7872.
Wellington, C.L., Ellerby, L.M., Hackam, A.S., Margolis, R.L., Trifiro, M.A., Singaraja, R., McCutcheon, K., Salvesen, G.S., Propp, S.S., Bromm, M., Rowland, K.J., Zhang, T., Rasper, D., Roy, S., Thornberry, N., Pinsky, L., Kakizuka, A., Ross, C.A., Nicholson, D.W., Bredesen, D.E., Hayden, M.R., 1998. Caspase cleavage of gene products associated with triplet expansion

disorders generates truncated fragments containing the polyglutamine tract. J. Biol. Chem. 273, 9158–9167.
Wellington, C.L., Ellerby, L.M., Leavitt, B.R., Roy, S., Nicholson, D.W., Hayden, M.R., 2003. Huntingtin proteolysis in Huntington disease. Clinical Neuroscience Research 3, 129–139. doi:10.1016/S1566-2772(03)00055-0
Wexler, N.S., Lorimer, J., Porter, J., Gomez, F., Moskowitz, C., Shackell, E., Marder, K., Penchaszadeh, G., Roberts, S.A., Gayán, J., Brocklebank, D., Cherny, S.S., Cardon, L.R., Gray, J., Dlouhy, S.R., Wiktorski, S., Hodes, M.E., Conneally, P.M., Penney, J.B., Gusella, J., Cha, J.-H., Irizarry, M., Rosas, D., Hersch, S., Hollingsworth, Z., MacDonald, M., Young, A.B., Andresen, J.M., Housman, D.E., De Young, M.M., Bonilla, E., Stillings, T., Negrette, A., Snodgrass, S.R., Martinez-Jaurrieta, M.D., Ramos-Arroyo, M.A., Bickham, J., Ramos, J.S., Marshall, F., Shoulson, I., Rey, G.J., Feigin, A., Arnheim, N., Acevedo-Cruz, A., Acosta, L., Alvir, J., Fischbeck, K., Thompson, L.M., Young, A., Dure, L., O'Brien, C.J., Paulsen, J., Brickman, A., Krch, D., Peery, S., Hogarth, P., Higgins, D.S., Landwehrmeyer, B., U.S.-Venezuela Collaborative Research Project, 2004. Venezuelan kindreds reveal that genetic and environmental factors modulate Huntington's disease age of onset. Proc. Natl. Acad. Sci. U.S.A. 101, 3498–3503. doi:10.1073/pnas.0308679101
Wexler, N.S., Young, A.B., Tanzi, R.E., Travers, H., Starosta-Rubinstein, S., Penney, J.B., Snodgrass, S.R., Shoulson, I., Gomez, F., Ramos Arroyo, M.A., 1987. Homozygotes for Huntington's disease. Nature 326, 194–197. doi:10.1038/326194a0
Whitfield, J., Littlewood, T., Soucek, L., 2015. Tamoxifen administration to mice. Cold Spring Harb Protoc 2015, 269–271. doi:10.1101/pdb.prot077966
Wild, E., Magnusson, A., Lahiri, N., Krus, U., Orth, M., Tabrizi, S.J., Björkqvist, M., 2011. Abnormal peripheral chemokine profile in Huntington's disease. PLoS Curr 3, RRN1231. doi:10.1371/currents.RRN1231
Wirawan, E., Vande Walle, L., Kersse, K., Cornelis, S., Claerhout, S., Vanoverberghe, I., Roelandt, R., De Rycke, R., Verspurten, J., Declercq, W., Agostinis, P., Vanden Berghe, T., Lippens, S., Vandenabeele, P., 2010. Caspase-mediated cleavage of Beclin-1 inactivates Beclin-1-induced autophagy and enhances apoptosis by promoting the release of proapoptotic factors from mitochondria. Cell Death Dis 1, e18. doi:10.1038/cddis.2009.16
Wong, B.K.Y., Ehrnhoefer, D.E., Graham, R.K., Martin, D.D.O., Ladha, S., Uribe, V., Stanek, L.M., Franciosi, S., Qiu, X., Deng, Y., Kovalik, V., Zhang, W., Pouladi, M.A., Shihabuddin, L.S., Hayden, M.R., 2015. Partial rescue of some features of Huntington Disease in the genetic absence of caspase-6 in YAC128 mice. Neurobiol. Dis. 76, 24–36. doi:10.1016/j.nbd.2014.12.030
Wong, Y.C., Holzbaur, E.L.F., 2015. Autophagosome dynamics in neurodegeneration at a glance. J. Cell. Sci. 128, 1259–1267. doi:10.1242/jcs.161216
Woo, M., Hakem, R., Furlonger, C., Hakem, A., Duncan, G.S., Sasaki, T., Bouchard, D., Lu, L., Wu, G.E., Paige, C.J., Mak, T.W., 2003. Caspase-3 regulates cell cycle in B cells: a consequence of substrate specificity. Nat.

Immunol. 4, 1016–1022. doi:10.1038/ni976
Wu, H., Che, X., Zheng, Q., Wu, A., Pan, K., Shao, A., Wu, Q., Zhang, J., Hong, Y., 2014. Caspases: a molecular switch node in the crosstalk between autophagy and apoptosis. Int. J. Biol. Sci. 10, 1072–1083. doi:10.7150/ijbs.9719
Xie, Y., Hayden, M.R., Xu, B., 2010. BDNF overexpression in the forebrain rescues Huntington's disease phenotypes in YAC128 mice. J. Neurosci. 30, 14708–14718. doi:10.1523/JNEUROSCI.1637-10.2010
Xu, G., Cirilli, M., Huang, Y., Rich, R.L., Myszka, D.G., Wu, H., 2001. Covalent inhibition revealed by the crystal structure of the caspase-8/p35 complex. Nature 410, 494–497. doi:10.1038/35068604
Yang, C., Kaushal, V., Haun, R.S., Seth, R., Shah, S.V., Kaushal, G.P., 2008. Transcriptional activation of caspase-6 and -7 genes by cisplatin-induced p53 and its functional significance in cisplatin nephrotoxicity. Cell Death Differ. 15, 530–544. doi:10.1038/sj.cdd.4402287
Ye, Y.-C., Wang, H.-J., Chen, L., Liu, W.-W., Tashiro, S.-I., Onodera, S., Xia, M.-Y., Ikejima, T., 2013. Negatively-regulated necroptosis by autophagy required caspase-6 activation in TNFα-treated murine fibrosarcoma L929 cells. Int. Immunopharmacol. 17, 548–555. doi:10.1016/j.intimp.2013.05.009
Yirmiya, R., 1996. Endotoxin produces a depressive-like episode in rats. Brain Res. 711, 163–174.
Yoo, N.J., Lee, J.W., Kim, Y.J., Soung, Y.H., Kim, S.Y., Nam, S.W., Park, W.S., Lee, J.Y., Lee, S.H., 2004. Loss of caspase-2, -6 and -7 expression in gastric cancers. APMIS 112, 330–335. doi:10.1111/j.1600-0463.2004.apm1120602.x
Yu, L., Lenardo, M.J., Baehrecke, E.H., 2004. Autophagy and caspases - A new cell death program. Cell Cycle 3, 1124–1126.
Zeitlin, S., Liu, J.P., Chapman, D.L., Papaioannou, V.E., Efstratiadis, A., 1995. Increased apoptosis and early embryonic lethality in mice nullizygous for the Huntington's disease gene homologue. Nat. Genet. 11, 155–163. doi:10.1038/ng1095-155
Zeron, M.M., Chen, N., Moshaver, A., Lee, A.T., Wellington, C.L., Hayden, M.R., Raymond, L.A., 2001. Mutant huntingtin enhances excitotoxic cell death. Mol. Cell. Neurosci. 17, 41–53. doi:10.1006/mcne.2000.0909
Zeron, M.M., Hansson, O., Chen, N., Wellington, C.L., Leavitt, B.R., Brundin, P., Hayden, M.R., Raymond, L.A., 2002. Increased sensitivity to N-methyl-D-aspartate receptor-mediated excitotoxicity in a mouse model of Huntington's disease. Neuron 33, 849–860.
Zhao, H., Zhao, W., Lok, K., Wang, Z., Yin, M., 2014. A synergic role of caspase-6 and caspase-3 in Tau truncation at D421 induced by H2O 2. Cell. Mol. Neurobiol. 34, 369–378. doi:10.1007/s10571-013-0021-x
Zhao, M., Su, J., Head, E., Cotman, C.W., 2003. Accumulation of caspase cleaved amyloid precursor protein represents an early neurodegenerative event in aging and in Alzheimer's disease. Neurobiol. Dis. 14, 391–403.
Zheng, B., Sage, M., Sheppeard, E.A., Jurecic, V., Bradley, A., 2000. Engineering Mouse Chromosomes with Cre-loxP: Range, Efficiency, and Somatic Applications. Molecular and Cellular Biology 20, 648–655.

doi:10.1128/MCB.20.2.648-655.2000
Zheng, T.S., Hunot, S., Kuida, K., Momoi, T., Srinivasan, A., Nicholson, D.W., Lazebnik, Y., Flavell, R.A., 2000. Deficiency in caspase-9 or caspase-3 induces compensatory caspase activation. Nat. Med. 6, 1241–1247. doi:10.1038/81343
Zielonka, D., Piotrowska, I., Marcinkowski, J.T., Mielcarek, M., 2014. Skeletal muscle pathology in Huntington's disease. Front Physiol 5, 380. doi:10.3389/fphys.2014.00380
Zuccato, C., Ciammola, A., Rigamonti, D., Leavitt, B.R., Goffredo, D., Conti, L., MacDonald, M.E., Friedlander, R.M., Silani, V., Hayden, M.R., Timmusk, T., Sipione, S., Cattaneo, E., 2001. Loss of huntingtin-mediated BDNF gene transcription in Huntington's disease. Science 293, 493–498. doi:10.1126/science.1059581
Zuccato, C., Valenza, M., Cattaneo, E., 2010. Molecular mechanisms and potential therapeutical targets in Huntington's disease. Physiol. Rev. 90, 905–981. doi:10.1152/physrev.00041.2009

APPENDIX: SUPPLEMENTARY DATA

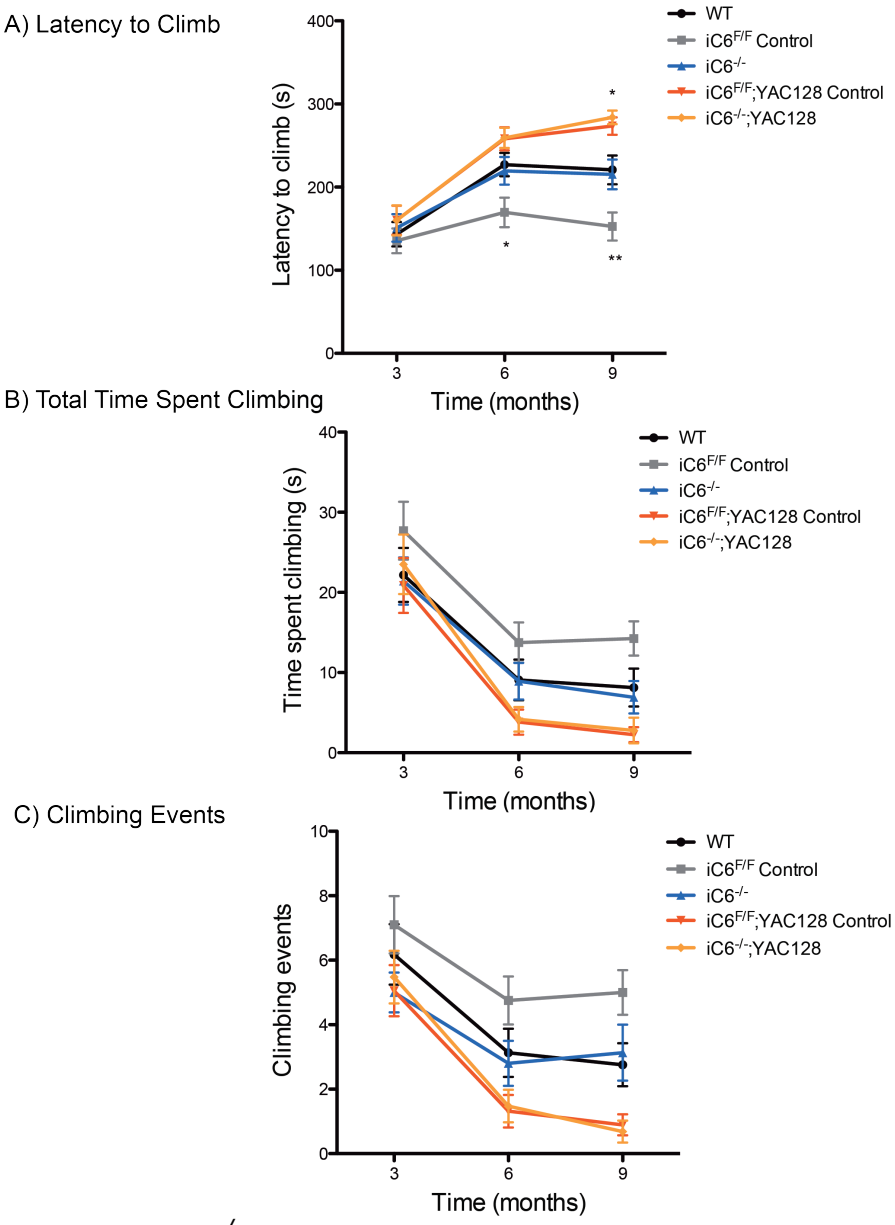

Figure S1: *iC6$^{-/-}$;YAC128* mice are not protected from climbing deficits. Inducible C6 deficient mice were tested for spontaneous motor function using the climbing test. YAC128 mice partially lacking C6 display increased latency to climb (A, 2-way ANOVA: genotype $F(4)=7.63$, $p<0.0001$; time $F(2)=11.80$, $p<0.0001$; interaction $F(8)=2.17$, $p=0.0458$; N=38-42), reduced time spent climbing (B, 2-way ANOVA: genotype $F(4)=3.39$, $p<0.0001$; time $F(2)=17.01$, $p<0.0001$; interaction $F(8)=0.55$, $p=0.8544$; N=38-42), and reduced climbing events (C, 2-way ANOVA: genotype $F(4)=5.28$, $p<0.0001$; time $F(2)=9.90$, $p<0.0001$; interaction $F(8)=0.99$, $p=0.5490$; N=38-42) no different from iC6$^{F/F}$;YAC128 mice. * p<0.05, ** p<0.01, *** p<0.001, compared to WT unless otherwise indicated.

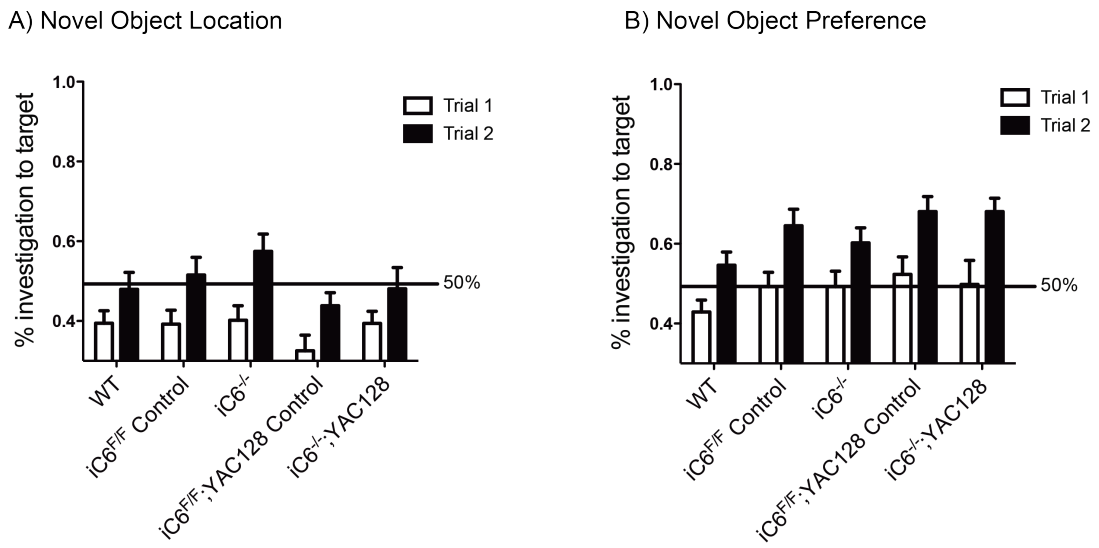

Figure S2: No genotypic differences observed in novel object location and novel object preference tests. Inducible C6 deficient mice were tested for cognitive learning using the novel object location and novel object preference tests. No genotypic differences were observed in the novel object location test (A, 2-way ANOVA: trial $F(1)=11.60$, $p<0.0001$; genotype $F(4)=4.20$, $p=0.097$; interaction $F(4)=0.91$, $p=0.7828$; N=18-20) nor in the novel object preference test (B, 2-way ANOVA: trial $F(1)=15.42$, $p<0.0001$; genotype $F(4)=4.75$, $p=0.0539$; interaction $F(4)=0.55$, $p=0.8946$; N=18-20). * p<0.05, ** p<0.01, *** p<0.001, compared to WT unless otherwise indicated.

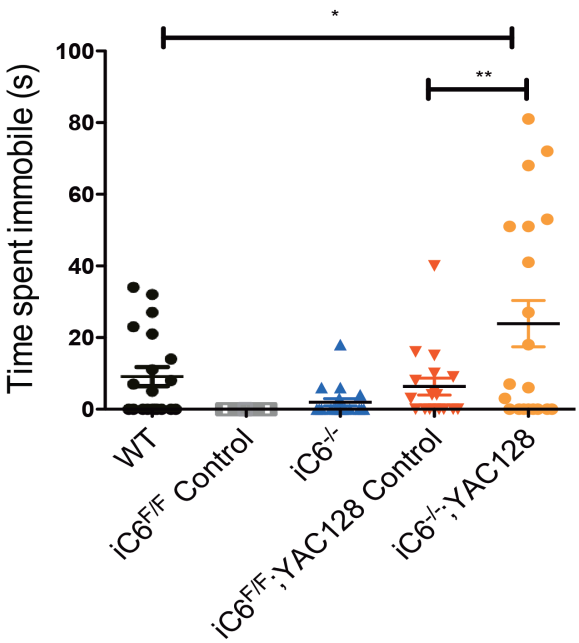

Figure S3: *iC6$^{-/-}$;YAC128* mice display depressive-like behaviour. Inducible C6 deficient mice were tested for depressive-like behaviour using the Porsolt

forced swim test. Partial loss of C6 in YAC128 mice results in increased immobility time (1-way ANOVA: $F(4,88)=7.31$, $p<0.0001$; N=18-20). * p<0.05, ** p<0.01, *** p<0.001, compared to WT unless otherwise indicated.

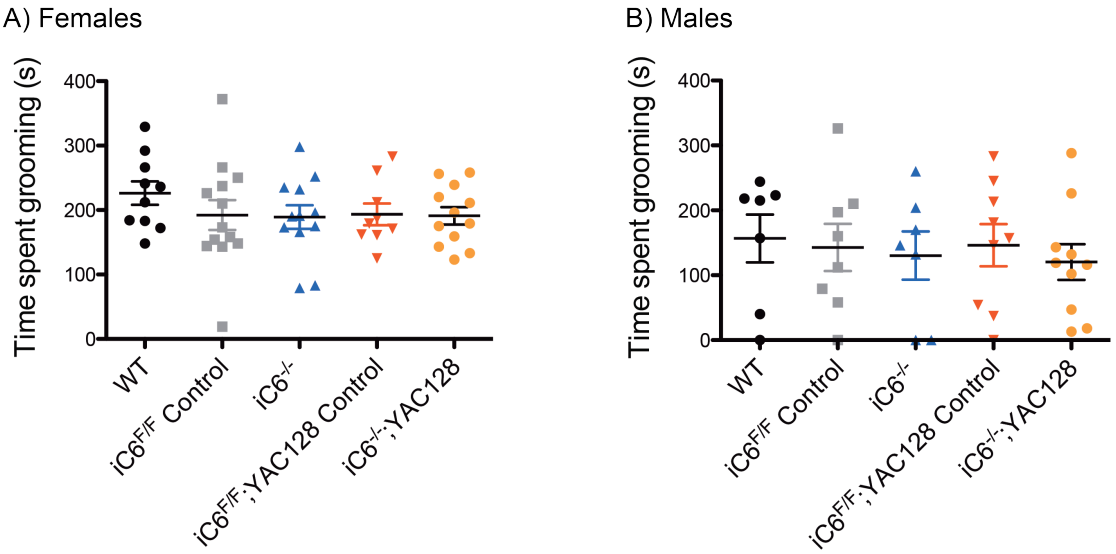

Figure S4: No genotypic differences observed in grooming behaviour. Inducible C6 deficient mice were tested for motivation to groom using the splash test. No genotypic differences were observed in time spent grooming in females (1-way ANOVA: $F(4,51)=0.638$, $p=0.6379$; N=10-13) or males (1-way ANOVA: $F(4,36)=0.182$, $p=0.9460$; N=7-10). * p<0.05, ** p<0.01, *** p<0.001, compared to WT unless otherwise indicated.

A) Latency to Climb

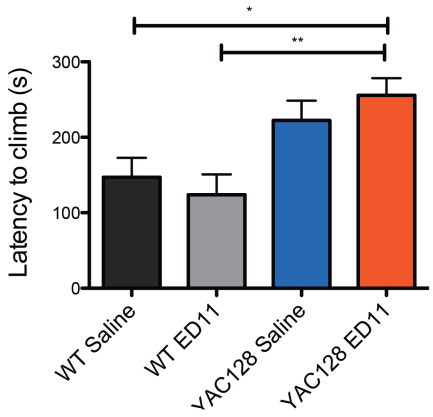

B) Total Time Spent Climbing

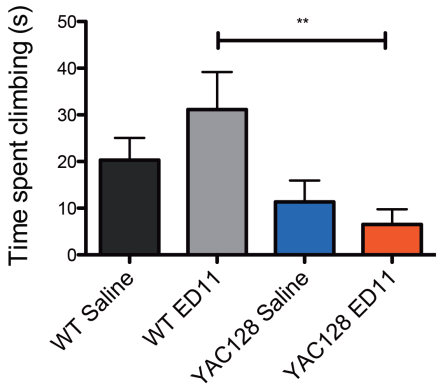

C) Climbing Events

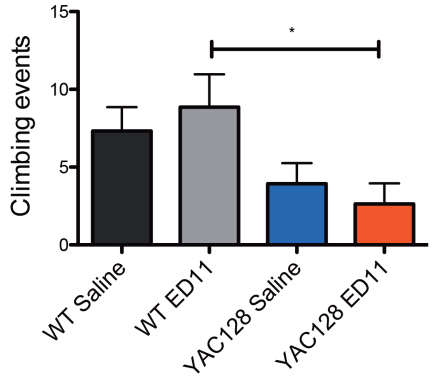

Figure S5: ED11-treated YAC128 mice are not protected from climbing deficits. Saline- and ED11-treated WT and YAC128 mice were tested for motor function using the climbing apparatus at 4 months. ED11-treated YAC128 mice had comparable latencies to climb (A, 1-way ANOVA: $F(3,56)=5.98$, $p=0.0013$; N=14-16), total time spent climbing (B, 1-way ANOVA: $F(3,56)=3.28$, $p=0.0274$; N=14-16), and climbing events (C, 1-way ANOVA: $F(3,56)=4.12$, $p=0.0104$; N=14-16) as saline-treated YAC128 mice. * p<0.05, ** p<0.01, *** p<0.001, compared to WT unless otherwise indicated.

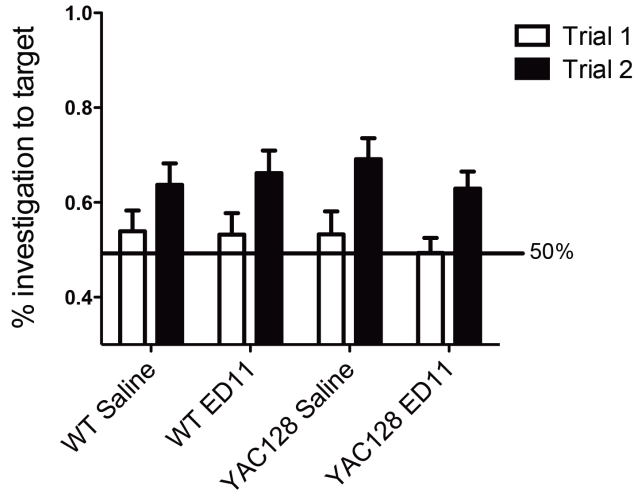

Figure S6: No genotypic differences observed in the novel object preference test between WT and YAC128 mice at 6 months of age. Saline- and ED11-treated WT and YAC128 mice were tested for cognitive function using the novel object preference test at 6 months but no genotypic differences were observed at this time point between WT and YAC128 mice.

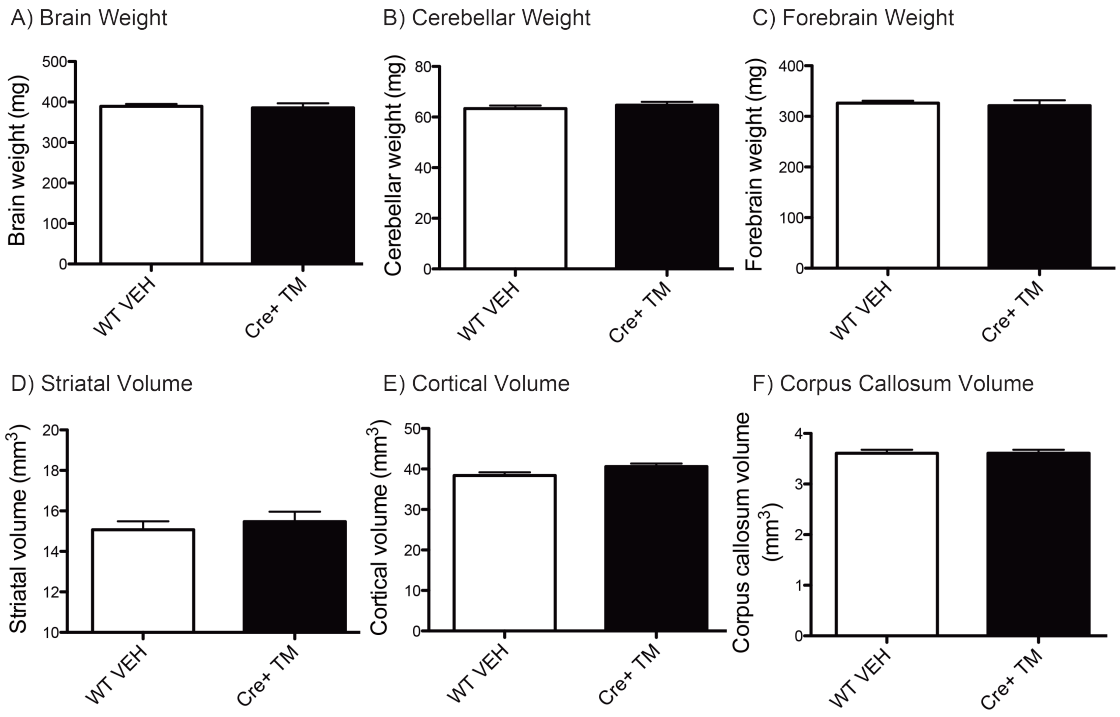

Figure S7: No neuropathological differences observed in Cre control mice. Vehicle-treated WT and tamoxifen-treated Cre-positive mice were perfused and assessed for brain structure changes at 3 months of age. No differences were observed in whole brain weight (A; unpaired two-tailed t-test: $t(28)=0.299$, $p=0.7674$; N=6-8), cerebellar weight (B; unpaired two-tailed t-test: $t(28)=0.789$, $p=0.4368$; N=6-8), forebrain weight (C; unpaired two-tailed t-test: $t(28)=0.453$, $p=0.6542$; N=6-8), or striatal volume (D; unpaired two-tailed t-test: $t(30)=0.620$, $p=0.5390$; N=6-8). Data from cortical volume is just statistically significant but unlikely to be a biologically relevant difference (E; unpaired two-tailed t-test: $t(28)=2.049$, $p=0.0499$; N=6-8). No statistical differences were observed for corpus callosum volume (F; unpaired two-tailed t-test: $t(28)=0.00645$, $p=0.9949$; N=6-8).